MULTI-RATING ELECTRONIC BALLAST FOR FLUORESCENT LAMPS BASED ON OPERATING FREQUENCY DETERMINATION

MR. PIYASAWAT NAVARATANA NA AYUDHYA

A THESIS SUBMITTED IN PARTIAL FULFILLMENT
OF THE REQUIREMENTS FOR
THE DEGREE OF DOCTOR OF PHILOSOPHY
(ELECTRICAL AND COMPUTER ENGINEERING)
FACULTY OF ENGINEERING
KING MONGKUT'S UNIVERSITY OF TECHNOLOGY THONBURI
2011

Multi-rating Electronic Ballast for Fluorescent Lamps based on Operating Frequency Determination

Mr. Piyasawat Navaratana Na Ayudhya M.Eng. (Electrical Engineering)

A Thesis Submitted in Partial Fulfillment
of the Requirement for
the Degree of Doctor of Philosophy (Electrical and Computer Engineering)
Faculty of Engineering
King Mongkut's University of Technology Thonburi
2011

Thesis Committee

.... (Asst. Prof. Mongkol Konghirun, Ph.D.)	Chairman of Thesis Committee
.... (Asst. Prof. Anawach Sangswang, Ph.D.)	Member and Thesis Advisor
.... (Asst. Prof. Sumate Naetiladdanon, Ph.D.)	Member and Thesis Co-Advisor
.... (Lect. Kamon Jirasereeamornkul, Ph.D.)	Member
.... (Asst. Prof. Jensak Eakburanawat, Ph.D.)	Member
.... (Asst. Prof. Adisorn Leelasantitham, Ph.D.)	Member

Thesis Title	Multi-rating Electronic Ballast for Fluorescent Lamps based on Operating Frequency Determination
Thesis Credits	36
Candidate	Mr. Piyasawat Navaratana Na Ayudhya
Thesis Advisors	Asst. Prof. Dr. Anawach Sangswang
	Asst. Prof. Dr. Sumate Naetiladdanon
Program	Doctor of Philosophy
Field of Study	Electrical and Computer Engineering
Department	Computer Engineering
Faculty	Engineering
B.E.	2554

Abstract

This thesis presents a multi-rating electronic ballast system with lamp rating detection capability. The proposed electronic ballast can help simplify the task of choosing appropriate ballasts for lamps with different ratings. This allows inexperienced users to select and buy ballasts with minimal damage. In addition, it will reduce unnecessary stocks of electronic ballasts with different ratings to only one model of ballast. The proposed electronic ballast shares the same basic hardware as typical electronic ballasts, namely a PFC boost converter, a power controlled resonant inverter and protection circuitry. The only difference is the developed algorithms that consist of the multi-step power regulation, possibility weight calculation and decision making procedure. This software fits the capability of a general 8-bits microcontroller. This thesis provides a hardware designing procedure in order to operates the full range of T8 fluorescents power rating. From the experimentally obtained operating frequency of the lamps, a possibility weight is constructed to help facilitate the lamp classification. The proposed detection algorithm employs a multi-step lamp power regulation algorithm where decision making is based on the possibility weight that is calculated from the sensed frequency. Simulation and experimental results show that the proposed detection method can successfully detect the targeted lamp power rating and deliver the desired power to the lamp.

Keywords : electronic ballast / fluorescent lamp / multi-rating / automatic detection / frequency determination / multi-step power regulation / possibility weight

หัวข้อวิทยานิพนธ์	บัลลาสต์อิเล็กทรอนิกส์แบบหลายพิกัด
หน่วยกิต	36
ผู้เขียน	นายปิยสวัสดิ์ นวรัตน์ ณ อยุธยา
อาจารย์ที่ปรึกษา	ผศ.ดร.อนวัช แสงสว่าง
	ผศ.ดร.สุเมธ เนติลัดดานนท์
หลักสูตร	ปรัชญาดุษฎีบัณฑิต
สาขาวิชา	วิศวกรรมไฟฟ้าและคอมพิวเตอร์
ภาควิชา	วิศวกรรมคอมพิวเตอร์
คณะ	วิศวกรรมศาสตร์
พ.ศ.	2554

บทคัดย่อ

วิทยานิพนธ์นี้นำเสนอระบบบัลลาสต์อิเล็กทรอนิกส์แบบหลายพิกัดกำลังที่ความสามารถในการตรวจสอบพิกัดหลอดไฟ บัลลาสต์อิเล็กทรอนิกส์ที่นำเสนอสามารถช่วยลดความซับซ้อนของการเลือกบัลลาสต์ที่เหมาะสมสำหรับพิกัดของหลอดที่แตกต่างกัน บัลลาสต์นี้จะช่วยผู้ใช้มือใหม่ที่จะเลือกและซื้อบัลลาสต์โดยลดความเสี่ยงต่อความเสียหายที่อาจเกิดขึ้นได้ นอกจากนี้มันยังลดจำนวนรุ่นของบัลลาสต์อิเล็กทรอนิกส์สำหรับหลอดที่มีพิกัดต่างกันให้เหลือเพียงรุ่นเดียว บัลลาสต์อิเล็กทรอนิกส์ที่นำเสนอมีฮาร์ดแวร์พื้นฐานเช่นเดียวกับบัลลาสต์อิเล็กทรอนิกส์โดยทั่วไปคือ วงจรแปลงผันบูสที่มีการแก้ตัวประกอบกำลัง อินเวอร์เตอร์เรโซแนน และ วงจรป้องกัน จุดแตกต่างอยู่ที่อัลกอริทึมที่ประกอบด้วยการควบคุมกำลังขับแบบหลายขั้นตอน การคำนวณน้ำหนักความเป็นไปได้ และกระบวนการตัดสินใจ ซอฟต์แวร์นี้ยังเหมาะกับความสามารถของไมโครคอนโทรลเลอร์ขนาด 8 บิตโดยทั่วไป วิทยานิพนธ์นี้ประกอบด้วย ขั้นตอนการออกแบบฮาร์ดแวร์เพื่อที่จะขับหลอดฟลูออเรสเซนต์ T8 ได้ทุกพิกัดกำลัง ฟังก์ชันของน้ำหนักความเป็นไปได้ถูกสร้างขึ้นจากการทดลองเก็บความถี่ทำงานของหลอดไฟพิกัดต่างๆ เพื่อช่วยอำนวยความสะดวกในการจำแนกประเภทของหลอดไฟ กระบวนการตรวจสอบนี้อาศัยการควบคุมกำลังไฟฟ้าแบบหลายขั้นโดยการตัดสินใจขึ้นอยู่กับน้ำหนักความเป็นไปได้ที่คำนวณจากความถี่ทำงาน ผลของการจำลองและการทดลองแสดงให้เห็นว่าวิธีการตรวจสอบที่นำเสนอประสบความสำเร็จ โดยสามารถตรวจสอบพิกัดกำลังไฟฟ้าของหลอดฟลูออเรสเซนต์และขับหลอดด้วยกำลังไฟฟ้าที่หลอดต้องการ

คำสำคัญ : อิเล็กทรอนิกส์บัลลาสต์ / หลอดฟลูออเรสเซนต์ / หลายพิกัดกำลัง / ตรวจจับอัตโนมัติ / ตรวจจับความถี่ / การควบคุมกำลังไฟฟ้าแบบขั้นบันได / น้ำหนักของความเป็นไปได้

ACKNOWLEDGEMENTS

The financial support given by the Higher Education Research Promotion and National Research University Project of Thailand, Office of the Higher Education Commission is gratefully acknowledged. A special thank is directed to Mr. Lee Atthawetchakul, the Managing Director of Dyno Electric Co., Ltd. who initiated the project and provided special equipments. Also, thanks to Dr. Kamon Jirasereeamornkul and Mr. Charnyut Karnjanapiboon who supported me when starting this work.

At the department I would like to thank my advisor Asst. Prof. Dr. Anawach Sangswang and Asst. Prof. Dr. Sumate Naetiladdanon who always find some extra time for discussions, no matter the time and reason.

Thanks to the thesis committee, Asst. Prof. Dr. Mongkol Konghirun, Dr. Kamol Jirasereeamornkul, Asst. Prof. Dr. Jensak Eakburanawat and Asst. Prof. Dr. Adisorn Leelasantitham.

Last but not least, the most important support, my family and my friend. Without you this would not have been possible.

Piyasawat Navaratana Na Ayudhya

CONTENTS

PAGE

LIST OF TABLES

LIST OF FIGURES

PAGE

FIGURE

PAGE

PAGE

LIST OF SYMBOLS

ADC	=	Analog to Digital Converter
AC	=	Alternating Current
C	=	Capacitance (F) or Capacitor
CCM	=	Continuous Conduction Mode
CriCM	=	Critical Conduction Mode
D	=	Diode
DC	=	Direct Current
DCM	=	Discontinuous Conduction Mode
e	=	Exponential Constant (2.71828182845904)
f	=	Frequency (Hz)
I	=	Current (A)
ign	=	Ignition
inv	=	Inverter
j	=	Imagine Value ($\sqrt{-1}$)
L	=	Inductance (H) or Inductor
ln	=	Natural Logarithm
LPF	=	Low Pass Filter
MCU	=	Microcontroller Unit
P	=	Power (W)
PFC	=	Power Factor Corrector
ph	=	Pre-heat
PWM	=	Pulse Width Modulator
Q	=	Transistor or Quality Factor
R	=	Resistance (Ohm) or Resistor
r	=	Resonant
Re	=	Real Part
ref	=	Reference
sys	=	System
T	=	Temperature (˚C)
THD	=	Total Harmonic Distortion
V	=	Voltage (V)
W_P	=	Possibility Weight
Δ	=	Delta
η	=	Efficiency
ω	=	Frequency (radian)
π	=	Pi constant (3.14159265358979)

CHAPTER 1 INTRODUCTION

A fluorescent lamp is a gas-discharge lamp that uses electricity to excite mercury vapor. The excited mercury atoms cause a phosphor to fluoresce, producing visible light. Compared with conventional incandescent lamps, a fluorescent lamp converts electrical power into light more efficiently. Thus, they are commonly used in lighting applications. However, the fluorescent lamps always require a ballast to stabilize the lamp at the required operating point by limiting the discharge current [1], [2]. Simple magnetic ballasts, like ones used in typical fluorescent sets, operated at the line frequency, have many drawbacks, such as low efficiency, low input power factor and bulky size. Recently, electronic ballasts that employ transistors to boost line-frequency to high-frequency become increasingly popular because of the improved lamp efficacy and system efficiency [3].

1.1 Background

Fluorescent lamps are negative differential resistance devices, so as more current flows through them, the electrical resistance of the fluorescent lamp drops, allowing even more current to flow. When connected directly to a constant-voltage power supply, the fluorescent lamp would rapidly be damaged from the uncontrolled current flow. To prevent this, fluorescent lamps must be used with an auxiliary device, a ballast, for the purpose of current regulation.

1.1.1 Magnetic Ballast and Starter

Ballasts are used to stabilize the current through an electrical load. They are often found when an electrical circuit or device presents a negative differential resistance to the supply. If such a device is connected to a constant-voltage power supply, it would draw an increasing amount of current until it is destroyed or has caused the power supply to fail. The ballast provides a positive resistance or reactance that limits the current to a proper level. This means that the ballast is provided for the proper operation of the negative-resistance device by appearing to be a legitimate, stable resistance in the circuit.

Because of the power dissipation, resistors are not used as ballasts for lamps of more than about two watts. Instead, a reactance is used. However, losses in the ballast due to its resistance and magnetic core are not negligible, about 5 to 25% of the lamp input wattage.

An inductor is very common in line-frequency ballasts to provide the proper starting and operating electrical condition to power a fluorescent lamp, neon lamp, or high intensity discharge (HID) lamp. Because of the use of the inductor, such ballasts are usually called magnetic ballasts as shown in figure 1.1.

Figure 1.1 Magnetic ballast

The magnetic ballast alone is not sufficient to operate the mentioned types of lamps. To start it, the mercury atoms in the fluorescent tube must be ionized before the arc can "strike" within the tube. A high voltage, in an order of a thousand of volts, is needed. The automatic glow starter, shown in Figure 1.2, consists of a small gas-discharge tube, containing neon or argon and fitted with a bimetallic electrode. When power is first applied to the lamp circuit, a glow discharge occurs over the electrodes of the starter. This glow discharge will heat the gas in the starter and causes the bimetallic electrode to bend to the other electrode. When the electrodes touch, the two filaments of the fluorescent lamp and the ballast will effectively be switched in series to the supply voltage. This causes the filaments to glow and emit electrons into the gas column. The touching electrodes in the starter then stops the glow discharge, causing the gas to cool down again. The bimetallic electrode also cools down and starts to move back. When the electrodes separate, the discharged current from the ballast provides the high voltage to start the lamp. Figures 1.3 and 1.4 show the wiring diagram and operating sequence of such a fluorescent lamp with magnetic ballast and starter.

Figure 1.2 Starter

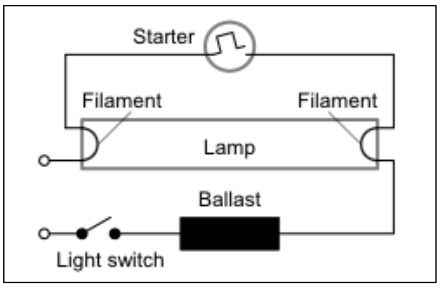

Figure 1.3 Wiring diagram of the fluorescent, ballast and starter

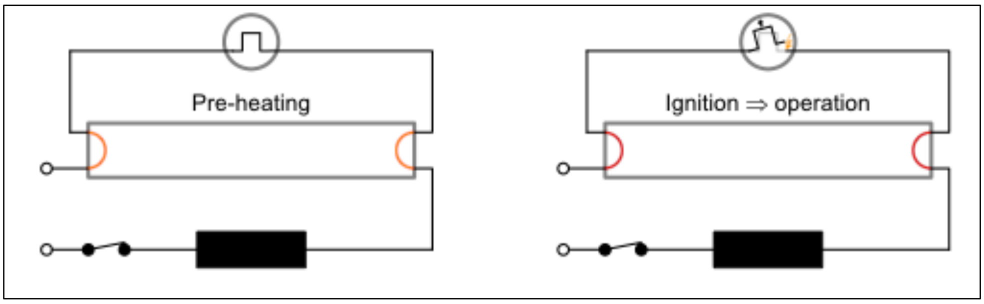

Figure 1.4 The preheating and ignition are operated by the starter

An inductor is very common in line-frequency ballasts to provide the proper starting and operating electrical condition to power a fluorescent lamp, neon lamp, or high intensity discharge (HID) lamp. An advantage of the magnetic ballast is that it is the easiest circuit to operate the fluorescent lamp.

A major disadvantage of the inductor is that the current phase angle is shifted from the voltage phase angle, resulting in a poor power factor. Due to the low frequency driving, the light from the lamp operated by this type of ballast suffers light flickering. For large lamps, line voltage may not be sufficient to start the lamp, so an autotransformer winding must be included in the ballast to step up the voltage. The autotransformer is designed with enough leakage inductance so that the current is appropriately limited. Because of the required large inductors and capacitors, reactive ballasts operated at line frequency tend to be large and heavy. They commonly also produce acoustic noise (line-frequency hum) [36]

1.1.2 Electronic Ballast

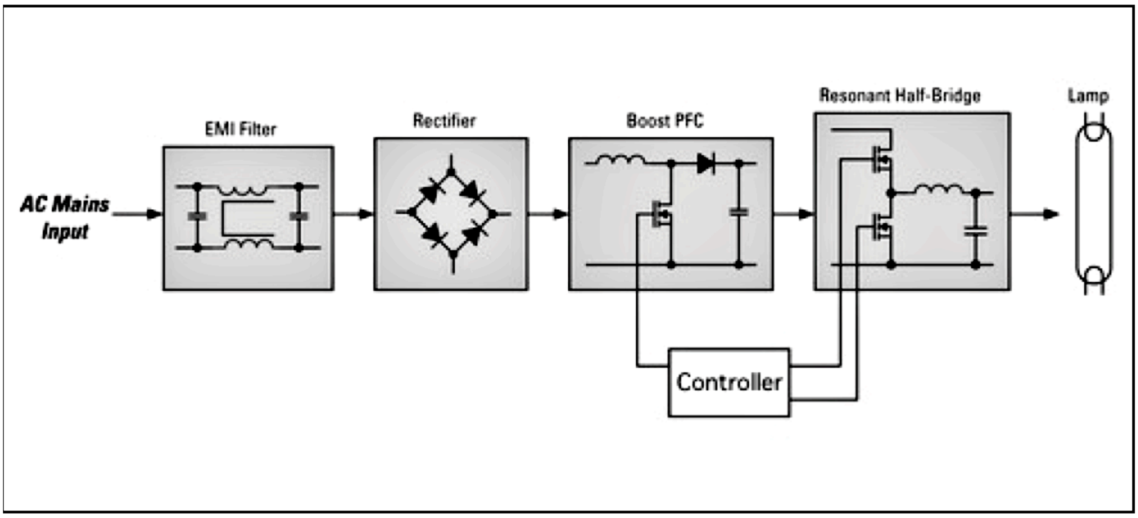

Figure 1.5 The block diagram of an electronic ballast

An electronic ballast uses a solid state electronic circuit to provide proper starting and operating condition to power fluorescent lamps. The ballast's operating frequency can be varied from the standard 50 Hz frequency to 20 kHz or higher, substantially eliminating the stroboscopic effect of flicker associated with fluorescent lighting. In addition, under operating frequency higher than 10 kHz, the internal discharge causes the gas to remain ionized in the arc stream. This means more continuum of light emission resulting in roughly 10-20% higher efficacy than an operation at the line frequency of 50 Hz. The lamp efficacy increases at 10 kHz and continues to improve until approximately the frequency of 20 kHz [4] -[6]. As shown in figure 1.5, electronic ballasts (EB) usually consist of a front-stage power factor corrector (PFC) for input current shaping and a second stage of resonant inverter for ballasting the lamp. The two stages are interconnected by a DC link of fixed voltage. A dimming function may be achieved by adjusting the switching frequency of the half bridge switches in the inverter, so that the reactances of resonant inductor and capacitor are varied. Thus, the lamp power is controlled. Because the availability of the frequency variation, the starter is not needed since the high voltage can be produced by reducing the frequency to the resonant position. The states of operation are illustrated in figure 1.6 consisting of preheat, ignition and run. Each operation is achieved by changing the half bridge driving frequency. Initially, the resonant tank exhibits a high-Q resonant load curve, the ballast starts with 100 kHz operating frequency and goes down to 63 kHz preheating frequency to heat up the filaments, indicating with small arrows on the top curve. At this frequency, the lamp voltage is not high enough to make the lamp ignited. The frequency is continually decreased to the ignition point at the frequency of 58.2kHz. At this point, the lamp voltage is high enough so that the lamp is ignited. After ignition, the frequency response curve changes into the low-Q, indicating by the bottom curve, since the current can flow through the lamp. Then the operating frequency is decreased to 40 kHz to drive the lamp at its power rating.

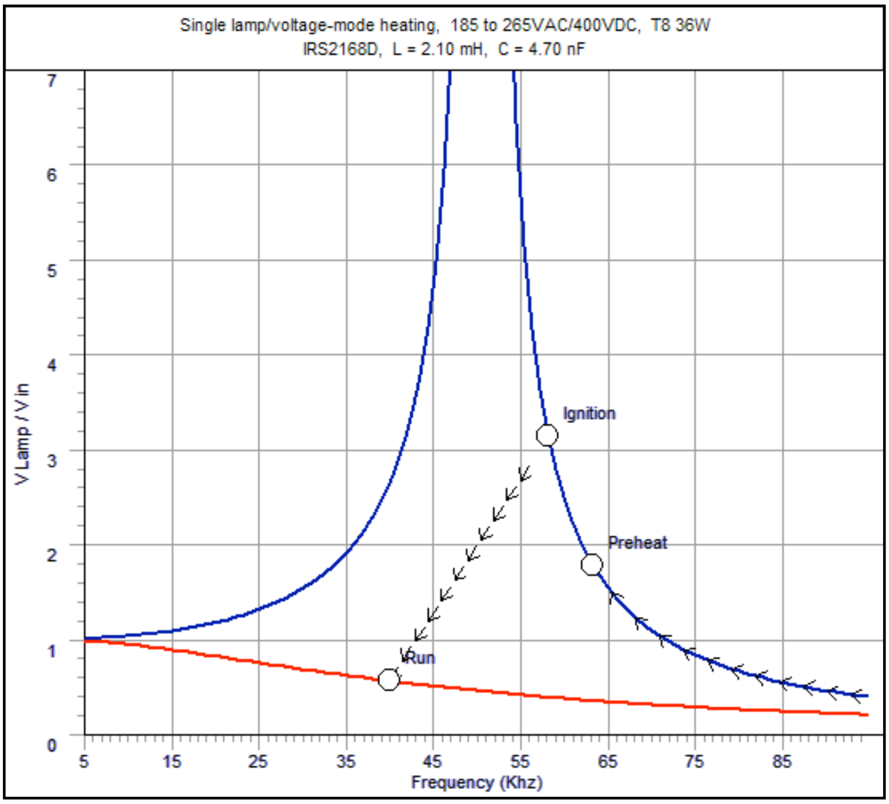

Figure 1.6 The operating point graph of the electronic ballast (voltage and frequency)

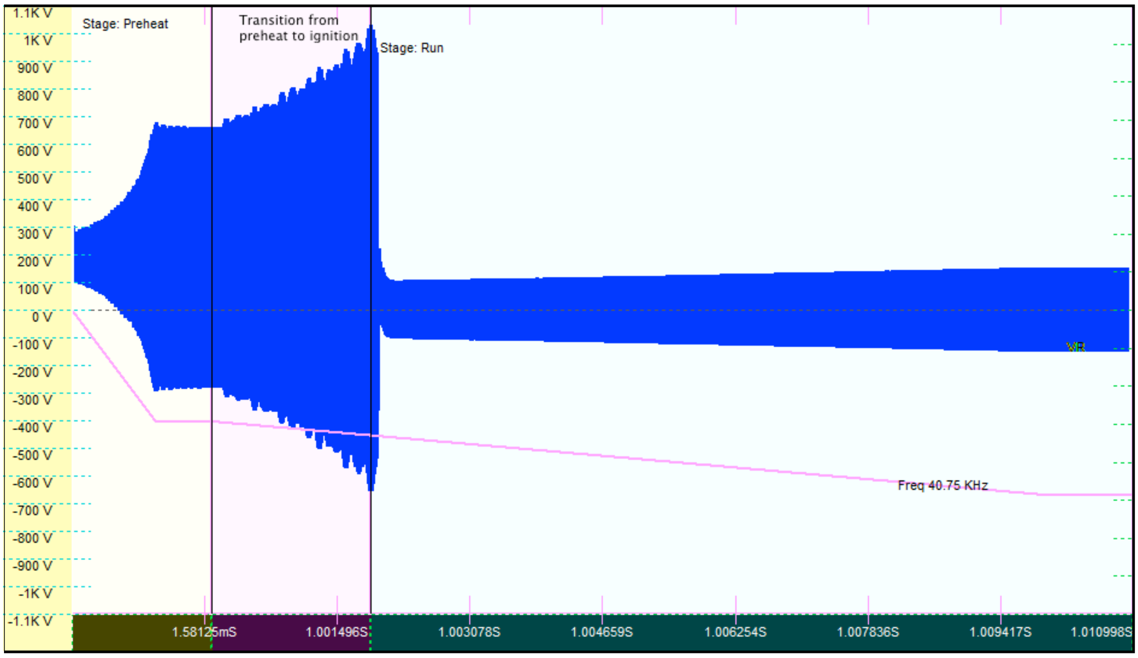

Figure 1.7 The lamp voltage at each state vs. time (the preheat time is compressed by 600:1 for clarity)

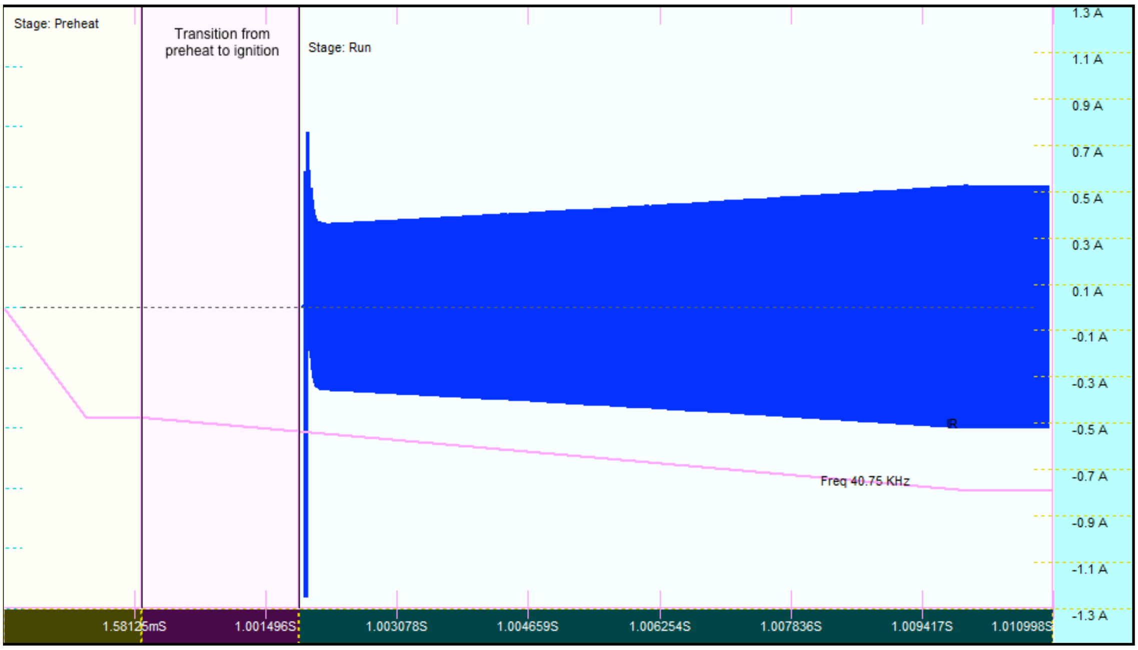

Figure 1.8 The lamp current at each state vs. time (the preheat time is compressed by 600:1 for clarity)

Figures 1.7 and 1.8 show the lamp voltage and current at each state of operation. At preheat state, the lamp initially has infinite resistance so that there is no lamp current. When the voltage is high enough, the lamp is ignited and current begin to flow through the lamp. This makes the lamp operate in low-Q condition i.e. the running state.

Because of the higher efficiency of the ballast itself and the improvement of lamp efficacy by operating the lamp at a higher frequency, the electronic ballasts offer higher lamp efficacy, as shown in figure 1.9. It is seen that light efficacy of the electronic ballast is rather constant compared with the magnetic ballasts. The PFC boost converter equipped in the electronic ballast plays an important role in maintaining a constant DC voltage at the input of the half-bridge inverter, no matter what the AC input voltage is. Since the lamp frequency is kept constant, the output power to the lamp remains constant. This results in a steady efficacy under an input voltage variation. The magnetic ballasts, however, do not contain a voltage regulation capability. The lamp power is therefore changed with the input voltage. Since the light efficacy of the fluorescent lamps is inversely proportional with the lamp power [6], the increase in the input voltage causes lower light efficacy as shown in figure 1.9. The higher electrical efficiency and light efficacy are the key advantages over the conventional magnetic ballasts.

The use of a PFC on the AC-DC stage, specifically a boost rectifier operating in discontinuous conduction mode (DCM) with constant frequency and constant duty cycle, enables an operation with an input power factor close to unity and a constant output power over the wide range of input voltage. Moreover, modern electronic ballasts can be easily implemented with microprocessor circuits, allowing control strategy fulfillment for energy savings and lamp protection features [7].

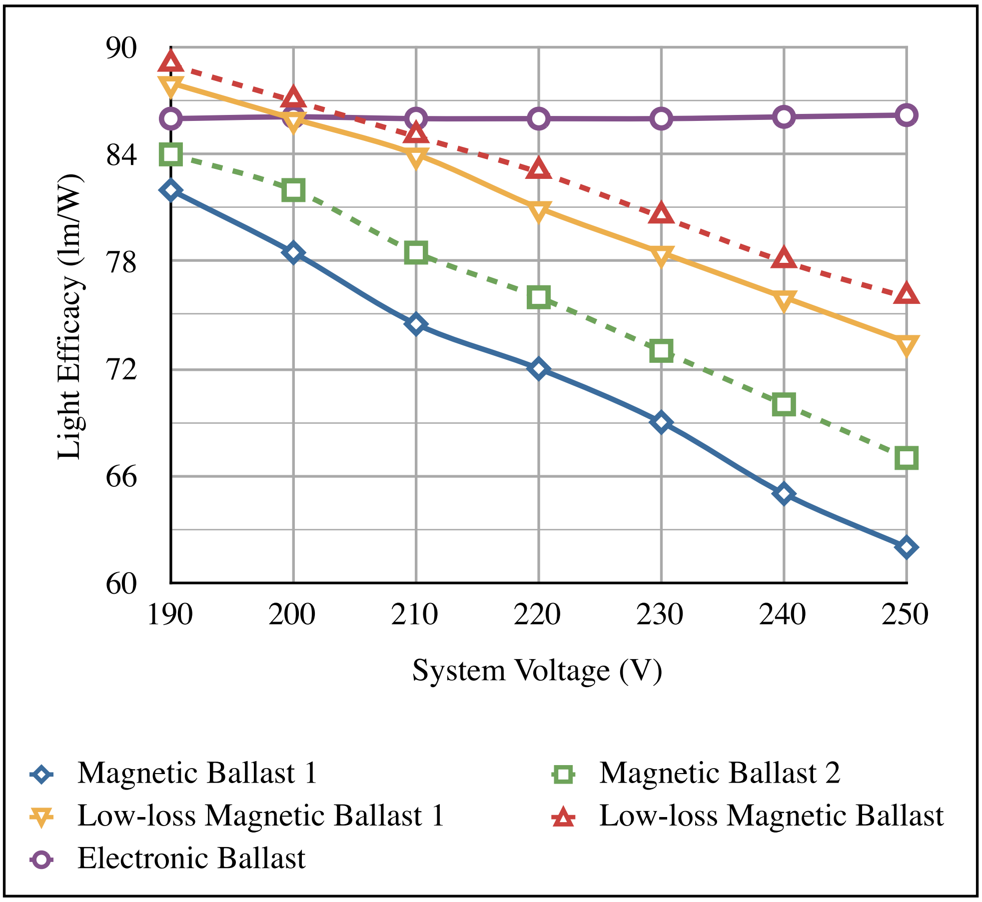

Figure 1.9 The light efficacy VS system voltage of 58 W T8 lamp operating with magnetic ballast, low-lost magnetic ballast and electronic ballast [6]

1.2 The Literature Review

Commercially available lamps, such as 18 W, 32 W and 36 W T8 lamps, must be used with electronic ballasts specifically designed for each lamp power rating. A mismatch between ballast and lamp ratings usually results in damage to both the lamp and the ballast circuit, caused by over-current or hard switching [8], [9]. With many different ratings of fluorescent lamps, an equally large stock of specifically rated electronic ballasts is required. The multi-rating fluorescent ballast is an effective solution to eliminate this problem. Because the controller of the multi-rating ballast must regulate and deliver correct amount of power to the lamp with unknown rating, the lamp rating must be accurately detected where the detection process must be executed sufficiently fast.

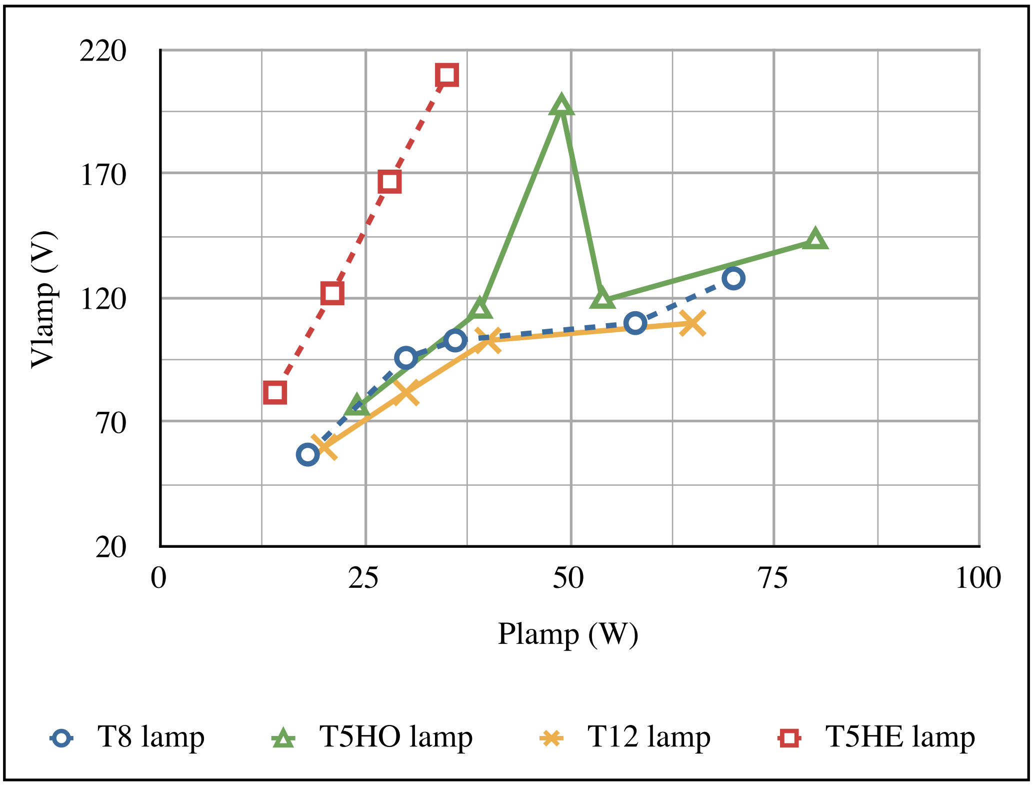

Figure 1.10 The relation of voltage and power rating of the T8, T5HE, T5HO and T12 fluorescent lamp [11]

Fluorescent lamp detection techniques earlier mainly focused on end-of-life detection [29], [30], lamp power [31], fault detection [32], and lamp open detection [33], [34]. The only literature technique that can automatically detect and operate the fluorescent lamps at the rated power based on lamp voltage was reported in [10]. This technique was standing on the assumption that if the lamp is not dimmed, this lamp voltage will remain constant under steady-state conditions. Because the lamp behaves almost like a resistance at high frequency operation (>20 kHz), it is evident that the actual power drawn by the lamp is approximately equal to the product of RMS values of lamp voltage and current. This method presents the lamp rating detection technique by using lamp voltage. It yields great recognition results when the lamp voltage is significantly different. The algorithm is simple and easy to implement. Figure 1.10 shows the relation of the lamp voltage and the power rating of T5HE, T5HO, T8 and T12 fluorescent lamp series. From this figure, the T5HE lamp series is appropriate for the voltage detection method since the lamp voltage of the different rating lamps in this series are very distinguishable.

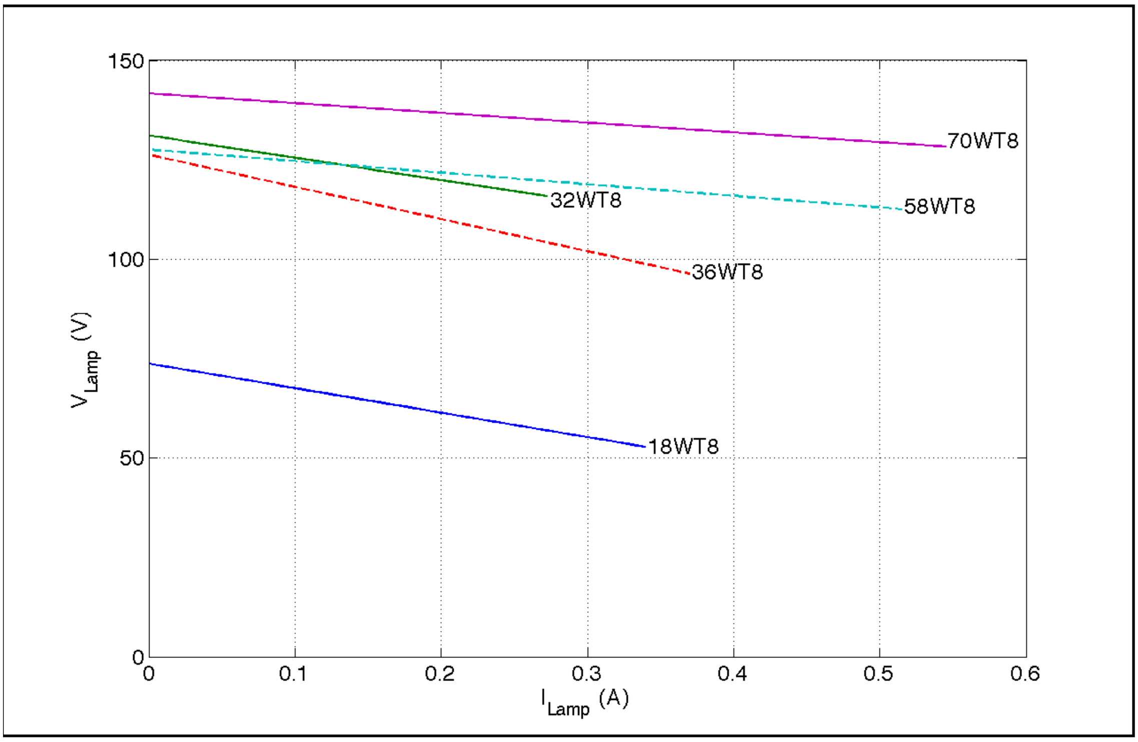

Figure 1.11 The V-I characteristic of the T8 fluorescent lamp

However, a proper operating frequency cannot be assigned to an unknown lamp without damaging the lamp. A detection process must be executed to determine the lamp wattage. The voltage detection method relies on the lamp voltage after striking (ignition) which is varied with surrounding conditions such as, the lamp temperature, age, and manufacturer. Therefore, different lamp ratings might have overlapped voltage ranges. For example, 32WT8 and 58WT8 lamps operate at the same voltage, ranging from 117 V to 127 V, which can lead to misidentification of the lamp. In addition, noise can interfere with the sensing voltage, and adding a filter may increase the cost of the system. As shown in figure 1.12, noise signals can be coupled to the reference voltage source and the output voltage from the attenuator by several means. For example, switching signals from the switching power supply can be coupled through the stray capacitance between the conductor track to the reference voltage source.

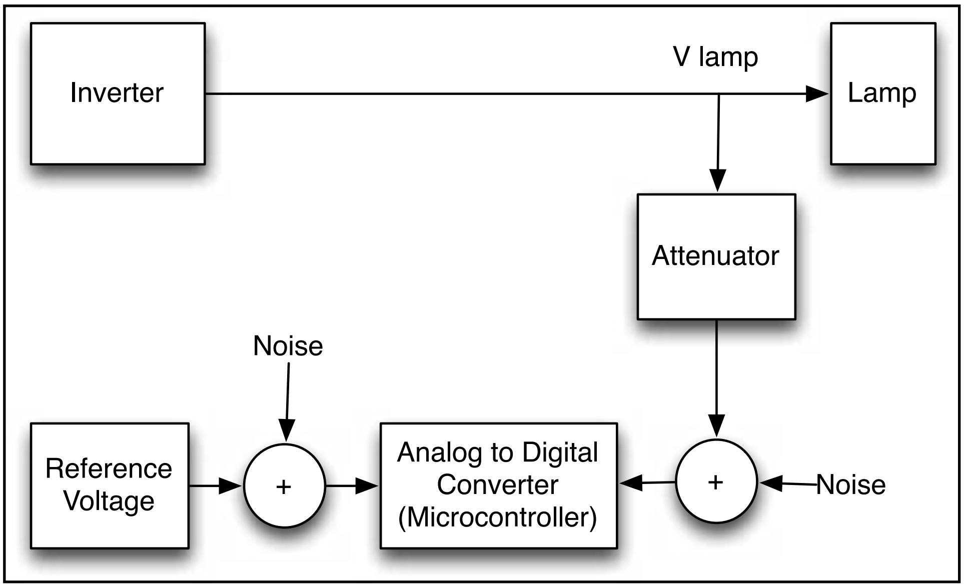

Figure 1.12 Noise signals coupled to the reference voltage and the attenuator circuit

The filament resistance detection was introduced in [11] to differentiate the lamp with close discharge voltages. This method is based on the assumption that the lamp ratings can be put in categories through the lamp filament resistances. For example, the 18-36W T8 lamp resistances are approximately 2 ohms and the 58-70W T8 lamp resistances are 2.5 ohms. With this method, the 32 W and 58 W lamp can be distinguished. However, the filament resistance may be varied with temperature. Moreover, the resistance of each type of lamps is very close. Thus, the accuracy of this method highly depends on the temperature of the filament. Finally, the noise from the switching power supply in the ballast can easily interfere with the measured signals and results in an error in resistant measurement.

1.3 Motivation

Although the voltage detection method can differentiate the lamp rating by interfacing the controller with high precision measurement device such as high frequency true RMS digital voltmeter, the implementation by using simple sensing circuit and the commonly used micro-controllers is a difficult task because of the interference from the power supply and the complication of RMS calculation (multiplication and division of the floating point variables). An approach that is highly immune to the noise and easy to measure is desirable. The frequency detection is introduced in this thesis. The frequency based information systems (FIS.), such as frequency modulation radio signal (FM.), are far better at rejecting noise than amplitude based information systems (AIS.) such as amplitude modulation radio signal (AM.). Noise generally is spread uniformly across the spectrum. The amplitude of the noise varies randomly at these frequencies. The change in amplitude can actually modulate the signal and be picked up in the amplitude based information systems. As a result, amplitude based information systems are very sensitive to random noise. Special filters need to be installed to keep the interference out of your car radio. Frequency based information systems are inherently immune to random noise. In order for the noise to interfere, it would have to modulate the frequency somehow. But the noise is distributed uniformly in frequency and varies mostly in amplitude. As a result, there is virtually no interference picked up in the frequency based information systems. Therefore, its superior immunity to random noise is achieved [37].

1.4 Objective and Approach

By using the same assumption, that the lamp behaves almost like a resistance at high frequency operation. If the same rating fluorescent lamps are operated at the same frequency, these lamps will draw the same electrical power as illustrated in figure 1.10. This is the basic operating method of the simple fixed frequency electronic ballast [1].

This thesis presents a multi-rating electronic ballast for fluorescent lamps based on operating frequency determination. The thesis includes the configuration and the controller design of a multi-rating electronic ballast. We propose a lamp rating detection algorithm, composed of multi-step lamp power regulation and the trapezoidal possibility weight decision based on a given set of lamp operating frequency data. The potential benefits of the proposed method include:

- The operating frequency determination technique reduces the opportunity of the lamp information being interfered by noise. This benefit arises from choosing of the frequency modulation over the amplitude modulation data communication method.
- The power regulation technique help constraining the lamp operating state to a specific point right after it is ignited. The lamps will consume the same power every time they are started. Then the power regulation command will be changed among the predetermined operating points. The trend of operating frequencies (frequency characteristics) for identifying the lamp is then achieved.
- The trapezoidal possibility weight decision [12] is a simple data recognition method. Because of the variation between lamp manufacturers, bulb age, and temperature, the running frequency is not necessarily constant. We experimentally verified that the operating frequency varies during our lamp power regulation experiment. The simplified version of the Gaussian distribution of these operating frequencies, the trapezoidal possibility weight, is introduced. This method decreases the unnecessary CPU processing time to calculate the complex exponential equation while the identification rate is about the same.

A hardware prototype of the electronic ballast is carried out on an 8 bits micro-controller. The widely used fluorescent lamp series, T8, is considered as an objective of this thesis.

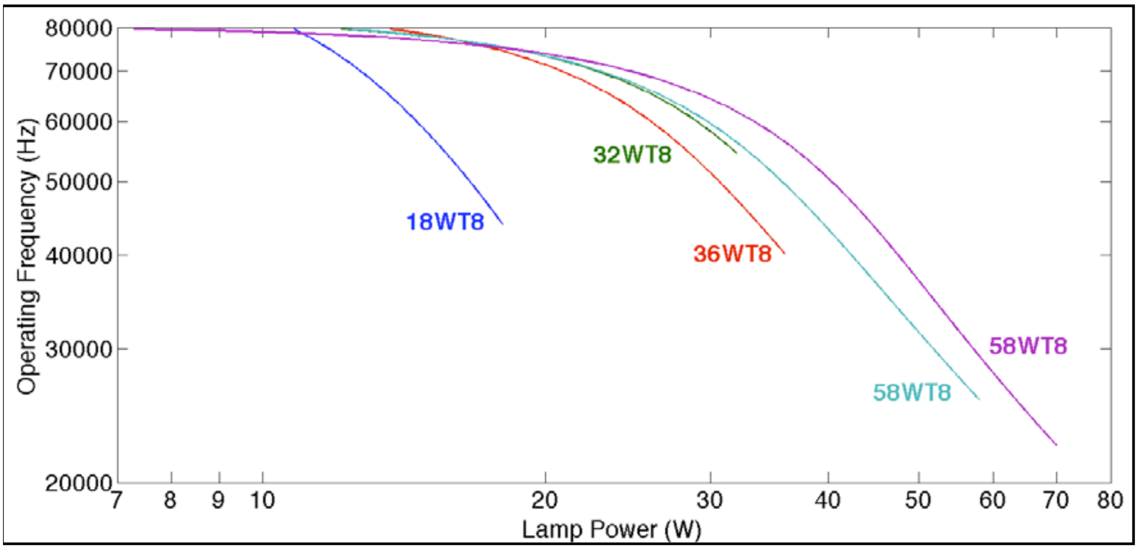

Figure 1.11 The operating frequency VS Lamp power of the T8 series

1.5 Contribution

The proposed multi-rating electronic ballast reduces the complicated task of choosing the ballast to match up the lamp. This benefit allows inexperience users, such as householder, to use it without accidentally damaging the lamps. In addition, the large organizations that have plenty of lamp with more than one rating can stock only one model of ballast. This thesis mentions on the T8 lamp series that is widely used in Thailand. The fluorescent lamps, regardless of the series, have the same behavior. Therefore, this method can be used with another type of fluorescent lamps by changing the software parameters. With non-complicate algorithm, the low-cost microcontroller is adequate. In addition, this microcontroller controls both PFC boost converter and half-bridge inverter, the dedicate IC for PFC or half-bridge controller is not needed. Therefore, it reasonably reduces the ballast price.

1.6 Thesis Organization

This thesis consist of 5 chapters. The details of each chapter are provided as follows.

1.6.1 The Introduction to the Proposed Method

This chapter describes the behavior of a fluorescent lamp, how to use them and the operation of magnetic ballast and starter. Then the basic configuration of an electronic ballast and its benefits over a magnetic ballast are shown. The literature review motivation, objective and contribution are.

1.6.2 Electronic Ballast Design

The electronic ballast design procedure is presented. This procedure includes the components selection and the software model. Moreover, this chapter shows the calculation method of ballast with dynamic model of a fluorescent lamp.

1.6.3 Multi-rating Electronic Ballast

This chapter includes the ideas of how to detect the lamp rating. It describes the pattern classification methods and introduces the trapezoidal weight function for lamp power rating detection. It also describes the hardware configuration and the software function.

1.6.4 Experimental results

This chapter includes the experimental results of the PFC boost converter, preheat condition, running frequency, electrical efficiency, light efficacy and lamp detection result.

1.6.5 Conclusions

This chapter shows the summary of contributions and future work.

CHAPTER 2 ELECTRONIC BALLAST DESIGN

This chapter consists of the configuration of electronic ballast, mode of operation, components selection, software model, the fluorescent lamp dynamic model and numerical calculation. The configuration of electronic ballast describes how does each part of ballast work. Then the 3 modes of ballast operation include preheat, ignition and run are described. These modes lead to the components selection and software model. Finally, the numerical calculation with a dynamic lamp model is described.

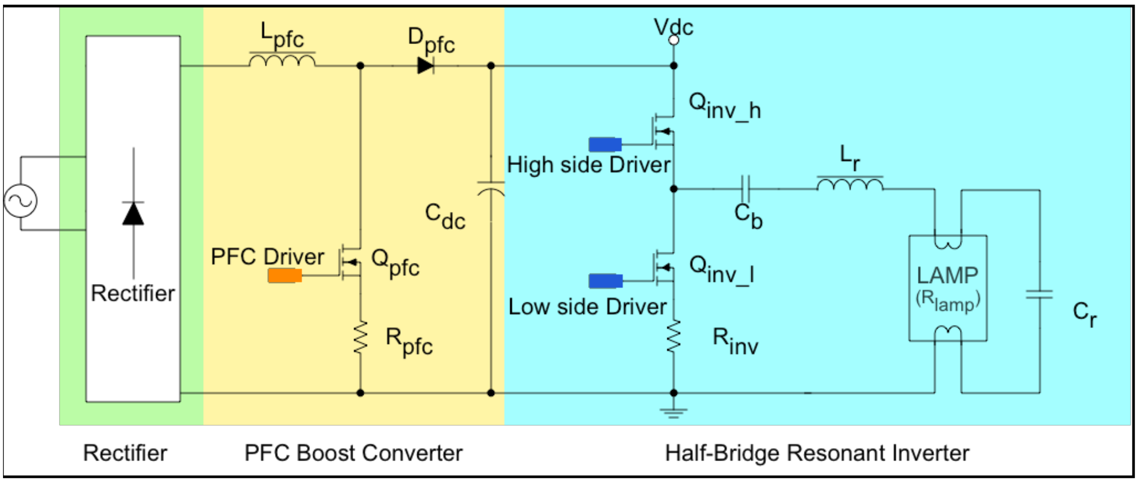

Figure 2.1 Schematic of the general electronic ballast

2.1 Configuration of Electronic Ballast

The electronic ballasts usually consist of a front-stage power factor corrector (PFC) for input current shaping and a second stage of resonant inverter for ballasting the lamp as shown in figure 2.1. The two stages are interconnected by a DC link of fixed voltage. he inductor used in the front-stage power factor corrector is integrated with the resonant inductor in the output-stage of the ballast inverter, so that the usage of the magnetic core material, and thus the cost, can be reduced. Preheating, igniting and dimming functions are achieved by adjusting the switching frequency of and in the inverter, so that the reactances of L_r and C_r are varied and thus the lamp power is controlled. For preheat and ignition, the lamp is not conducting and the circuit is a series L_r–C_r. During running, the lamp is conducting, and the circuit is an L_r in series with a parallel R_{lamp}–C_r. Where R_{lamp} is the equivalent resistance of the lamp.

2.1.1 Rectifier

A rectifier is an electrical device that converts alternating current (AC), which periodically reverses direction, to direct current (DC) which flows in only one direction. The process is known as rectification. The rectifier in the typical electronic ballast always be full-wave rectifier circuit using four diodes as shown in figure 2.2. The DC output of this rectifier will be the input of the next PFC boost converter.

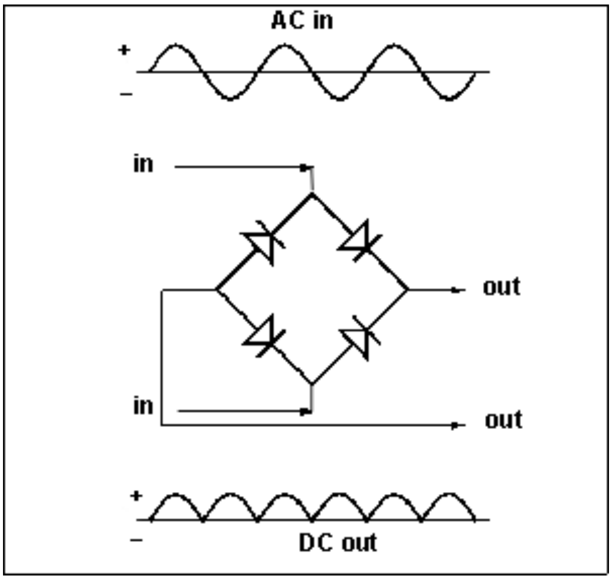

Figure 2.2 Schematic of the full-wave rectifier, input waveform and output waveform

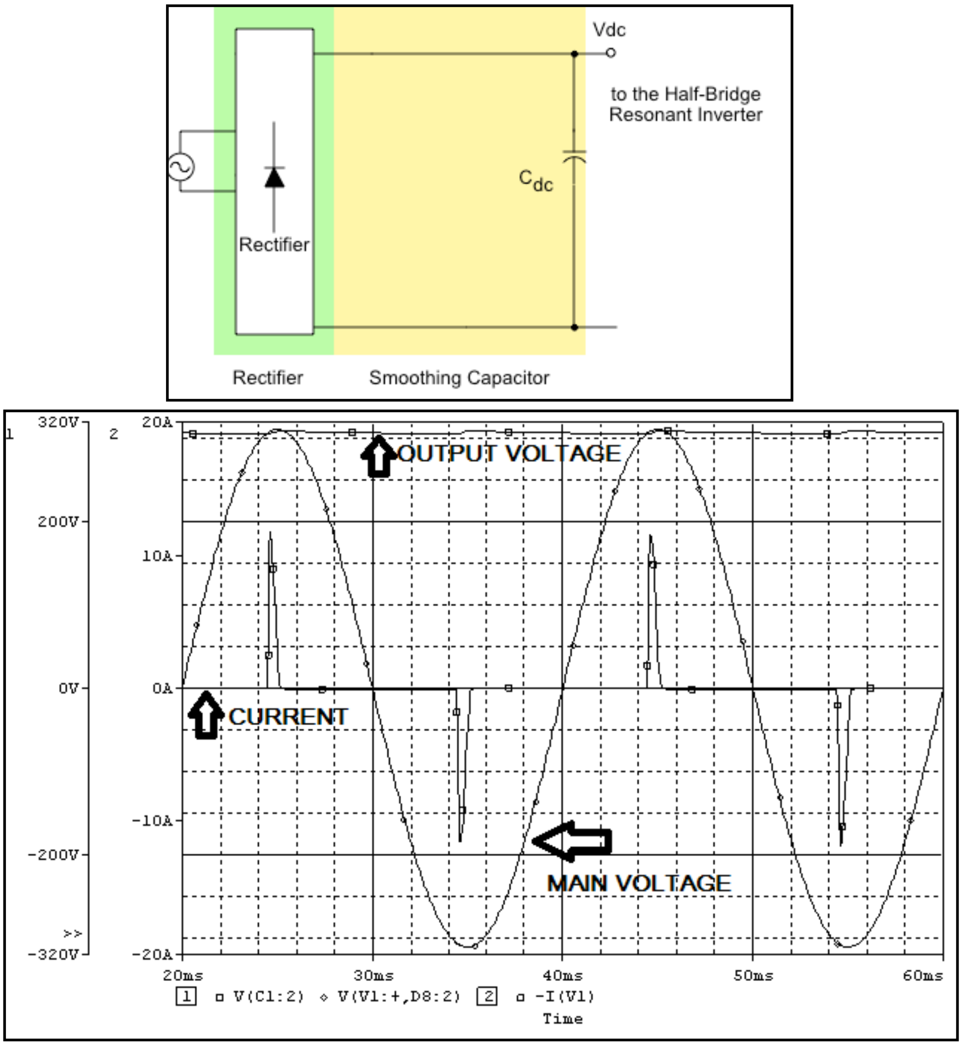

Figure 2.3 Schematic of the full-wave rectifier with bulk smoothing capacitor, input waveform and output waveform

2.1.2 PFC Boost Converter

Adding the large capacitor at the output of rectifier circuit is the easiest way to smooth the DC voltage. The capacitor charging current only flows when the input voltage (less the voltage drops across the rectifiers) is greater than the voltage on the capacitor. When it is less, the rectifiers are off and little or no current flows. Therefore, the current is highly non-sinusoidal, as shown in figure 2.3. The low power factor caused by the high harmonic content of the currents causes similar problems for the power company to those caused by sinusoidal reactive power, only worse. The harmonics cause distortion in the voltage waveform, and can even cause destructive resonances in the power grid.

To correct the power factor, the active power factor correction circuit was introduced. Active power factor correction can achieve very high power factors 0.98 and above. For power factor correction (PFC) converters, two main approaches are followed for the converter and control design. For low power applications, PFC converters are often operated in the discontinuous conduction mode (DCM) as they behave approximately as voltage followers. Hence, no input current controller is required. However, higher power applications ask for operation in the continuous conduction mode (CCM), since in DCM the device stresses and the conducted emissions become too high. An input current controller is now required, since the input current does not inherently track the input voltage. However, there is an operation mode between CCM and DCM that the switch is immediately turned on when the inductor current goes down to zero. This mode is called critical conduction mode (CriCM). The CriCM boost converter that compromises the advantage and disadvantage of CCM and DCM, is as easy as DCM to be applied with less conducted emission. This mode is widely used with low power application such as an electronic ballast. The inductor current of CriCM and CCM converter are illustrated in figure 2.4 and 2.5.

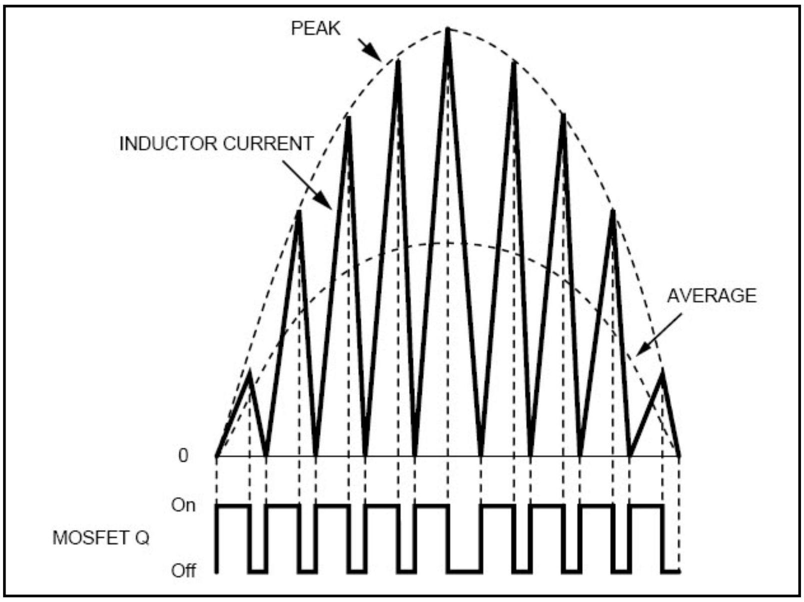

Figure 2.4 Inductor current waveform and MOSFET driving Signal of critical mode CriCM converter

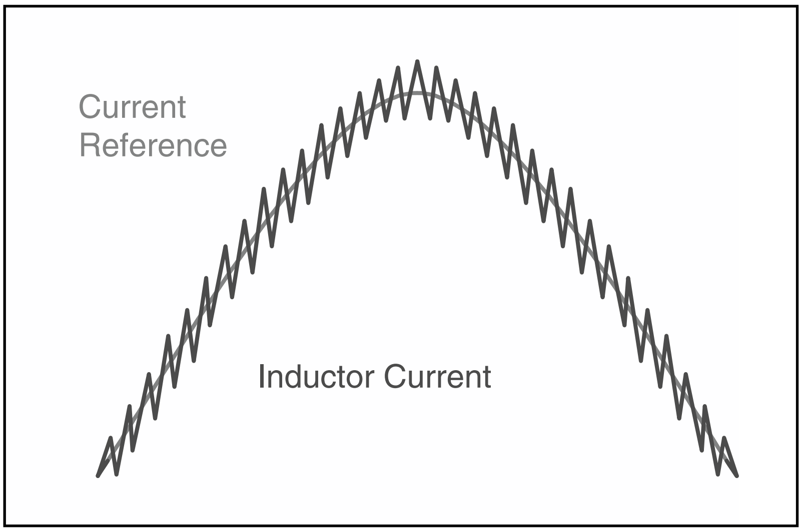

Figure 2.5 Inductor current waveform of average current mode CCM converter

However, the circuit of those converter types shares the same configuration except some of the sensing circuit. In one of the simplest architectures, an inductor, a MOSFET switch, and a diode are added between the rectifier bridge and the bulk capacitor, in a boost switch-mode power supply configuration. This is what we call PFC boost converter. The intermediate DC bus voltage is chosen to be higher than the peak voltage of the rectifier bridge, so the switch-mode controller will be working in boost mode. From figure 2.6, the controller driving the switch (Q_{pfc}) will adjust the duty cycle of the switch control signal so that the desired current and voltage targets are maintained. The switching frequency is chosen to be much higher than the AC mains frequency (20-100 kHz). The small current ripple at the switching frequency and its harmonics can be filtered using a passive filter on the AC mains input, similar to passive PFC, but much easier because of the lower amplitude and higher frequency of the ripple current.

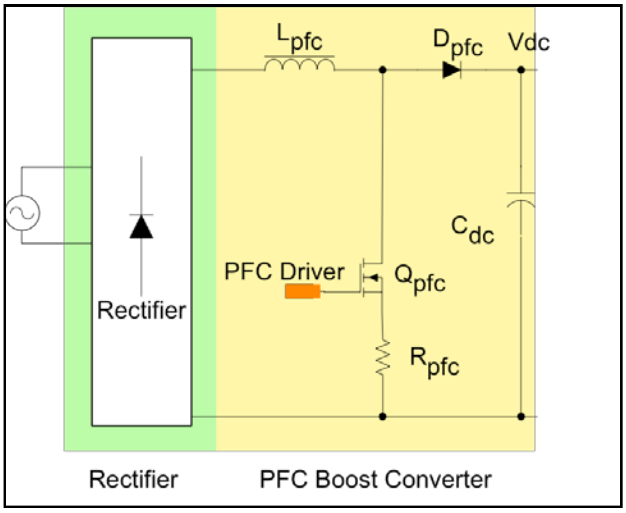

Figure 2.6 The schematic diagram of the PFC boost converter

During phase one the switch is closed, shorting one end of the inductor (L_{pfc}) to ground. Current is drawn through the inductor by the rectifier bridge, energizing the inductor's magnetic field. During phase two, the switch is opened. Since the current on the inductor cannot change instantaneously, the voltage on the inductor increases almost instantaneously until it is above the DC bus voltage by enough to turn on the diode (D_{pfc}). The current going through the inductor charges the bulk capacitor (C_{dc}) as the magnetic field collapses slightly and simultaneously raises the DC bus voltage slightly. All the while, the inverter is drawing current from the DC bus to power the lamp, using the charge stored on the bulk capacitor and thus reducing the DC bus voltage.

The amount of current drawn out of the AC mains is controlled in a manner such that the short-term average current is in phase with the mains voltage sine wave. Thus, the current through the inductor is controlled so that it approximates a full-wave rectified sine wave, plus and minus the switching frequency components as illustrated in figure 2.5. The average amplitude of the full-wave rectified current is controlled over the long term so that the DC bus voltage is regulated to the target voltage. This means the average current flowing into the capacitor from the rectifier and inductor (when the transistor switch is off) must match the average current going out to the inverter and lamp.

2.1.3 Half-Bridge Inverter and Resonant Circuit

In this part of circuit, the half-bridge inverter generates the square wave with peak voltage equal to the DC bus voltage (V_{dc}) provided by the boost converter. With the blocking capacitance (C_{dc}), the DC component of this square is eliminated. Therefore, the input voltage of the resonant circuit is a square wave with voltage toggle between $\pm V_{dc}/2$ volt. This inverter is connected with a resonant circuit and lamp. The simplify circuit of this inverter is shown in figure 2.7.

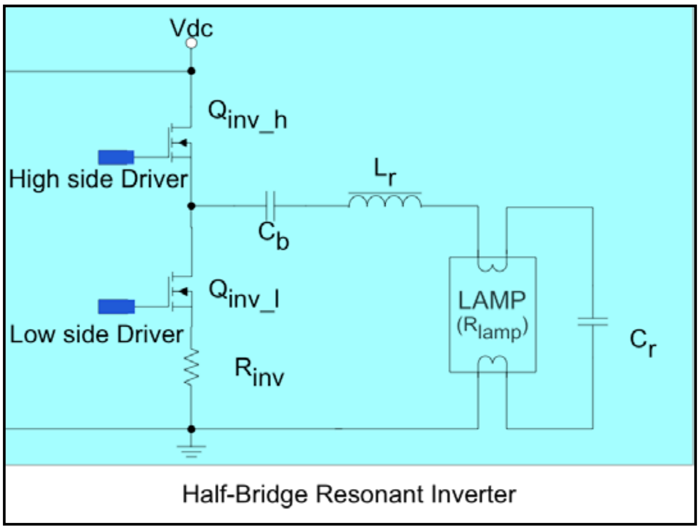

Figure 2.7 The half-bridge inverter and resonant circuit

With the resonant circuit, the magnitude of the transfer function (lamp voltage divided by input voltage) for the two circuit configurations, illustrates the operating characteristics for this design approach (see figure 2.8). The currents and voltages corresponding to the resulting operating frequencies determine the maximum current and voltage ratings for the inductor, capacitor, and the switches, which, in turn, directly determine the size and cost of the ballast. The frequency response of lamp voltage is divided into 2 modes that are before ignition (high-Q) and after ignition (low-Q). The high-Q frequency response occurs when the lamp is not yet ignited because of the infinite resistance of lamp. In this condition, the response of lamp voltage is the response of L_r - C_r circuit. The relation between inverter output voltage and lamp voltage is shown in figure 2.9. Because of lamp infinite resistance, there is no current in figure 2.9. The voltage slowly increase because the inverter frequency is decreased. After ignition, the lamp acts as a resistance so that the frequency response changes into low-Q RCL circuit. The current that flow through the lamp after ignition causes the decreasing in lamp voltage. The relation between inverter output voltage, lamp voltage and lamp current after ignition are shown in figure 2.10.

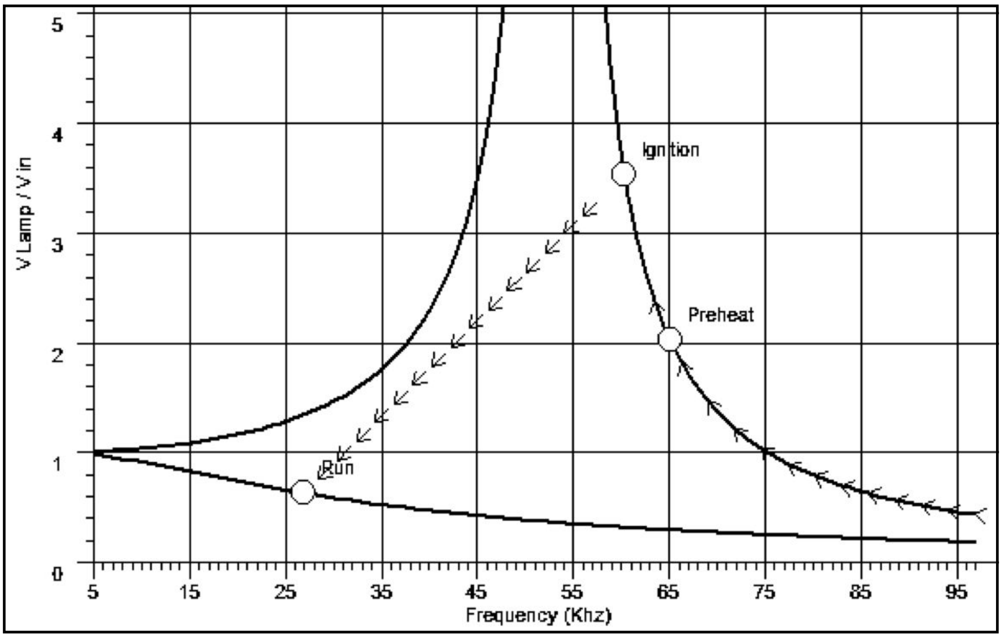

Figure 2.8 Operating frequency VS voltage gain (before and after ignition)

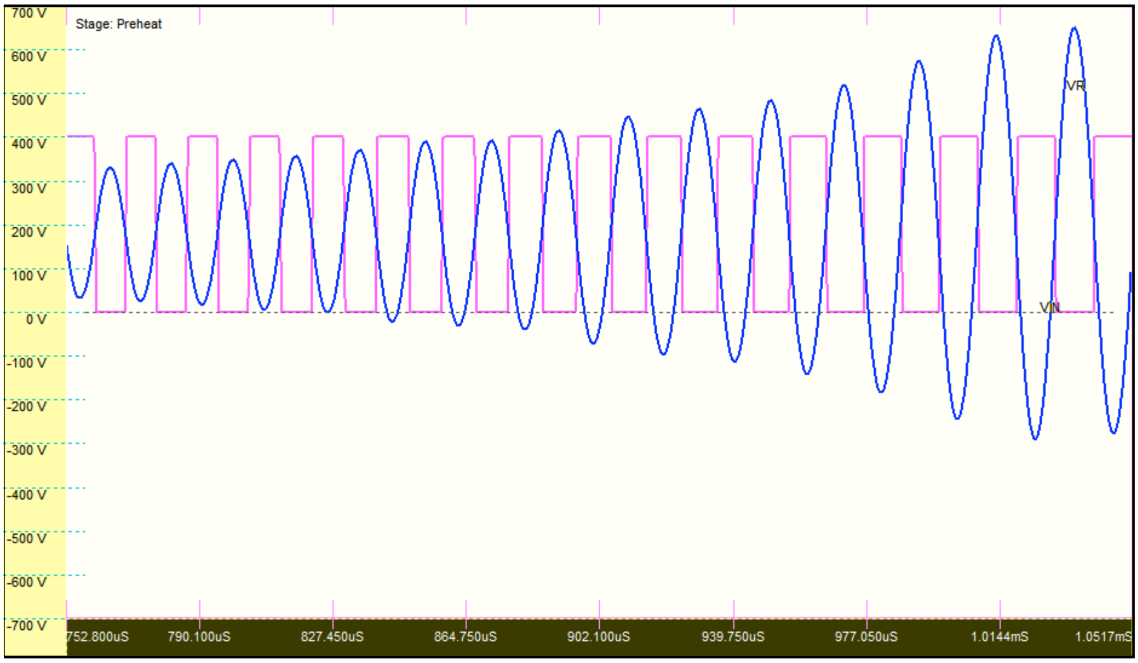

Figure 2.9 Inverter output voltage and lamp voltage in time domain when the lamp is not ignited

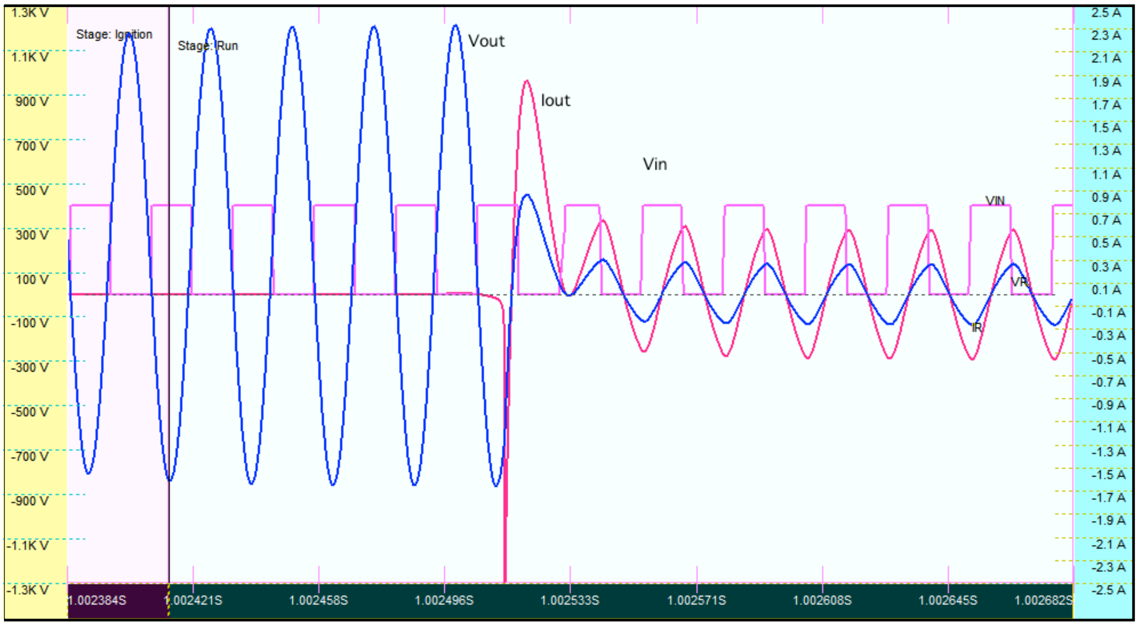

Figure 2.10 Inverter output voltage, lamp voltage and lamp current in time domain before and after ignition

To determine the operating condition of ballast and lamp, the model that consists of a set of equations for each operating frequency and the corresponding lamp voltage and circuit current are considered. These operating frequencies are a function of inductance, capacitance, input voltage, filaments preheating current, ignition voltage, lamp running voltage, and power. The analysis of each state of operation and resonant circuit component selection is described below.

2.2 Mode of Operation

The operation modes of the general electronic ballast consist of preheat, ignition and run. The low price electronic ballast may ignore the preheat state and go directly to the ignition state when it is starting.

2.2.1 Preheat

During preheat, the resistance of the lamp is assumed to be infinite and the filament resistance negligible, resulting in an L_r–C_r series circuit. Using the impedance across the capacitor, the preheat frequency is:

$$f_{ph} = \frac{I_{ph}}{2\pi C_r V_{ph}} \tag{2.1}$$

And the transfer function is:

$$\frac{V_{ph}}{4V_{dc}/\pi} = \frac{1}{\left|1 - 4LC_r\pi^2 f_{ph}^2\right|} \tag{2.2}$$

Solving (1) and (2) simultaneously yields:

$$V_{ph} = -\frac{V_{dc}}{\pi} + \sqrt{\left(\frac{V_{dc}}{\pi}\right)^2 + \frac{I_{ph}^2 L_r}{C_r}} \tag{2.3}$$

Where V_{in} is input square-wave voltage amplitude (V),
V_{ph} is lamp preheat voltage amplitude (V),
I_{ph} is filament preheat current amplitude (A),
L is output stage inductor (H),
C is output stage capacitor (F).

Note that the linear analysis uses the fundamental frequency of the square-wave produced by the half-bridge switches. Square-wave harmonics are assumed negligible.

2.2.2 Ignition

During ignition, the frequency for a given ignition voltage can be found using (2.2). Since the lamp is still an open circuit, the ignition frequency is:

$$f_{ign} = \frac{1}{2\pi\sqrt{L_r C_r}}\sqrt{1 + \frac{4V_{in}/\pi}{V_{ign}}} \tag{2.4}$$

Where V_{ign} is the lamp ignition voltage amplitude (V).

The associated ignition current amplitude flowing in the circuit that determines the maximum current ratings for the inductor and half-bridge switches, becomes:

$$I_{ign} = 2\pi f_{ign} C_r V_{ign} \tag{2.5}$$

2.2.3 Run

Once the lamp has ignited, the resistance of the lamp is no longer negligible, and the system becomes a low-Q RCL series-parallel circuit with a transfer function as:

$$V_{run} = \frac{4V_{dc}/\pi}{\sqrt{\left(1 - L_r C_r \omega^2\right)^2 + L_r^2 \omega^2 / R_{lamp}^2}} \tag{2.6}$$

The running frequency (hertz) becomes:

$$f_{run} = \frac{1}{2\pi}\sqrt{\frac{1}{L_r C_r} - \frac{1}{2R_{lamp}^2 C_r^2} + \sqrt{\left(\frac{1}{L_r C_r} - \frac{1}{2R_{lamp}^2 C_r^2}\right)^2 - 4\frac{1-\left(4V_{dc}/V_{lamp}\pi\right)^2}{L_r^2 C_r^2}}} \tag{2.7}$$

Where R_{lamp} is assumed to be the linearized lamp resistance determined from the running lamp power and voltage at a single operating point.

$$R_{lamp} = \frac{V_{lamp}^2}{2P_{lamp}} \tag{2.8}$$

Where P_{lamp} is the lamp running power (W), and V_{lamp} is the lamp running voltage amplitude (V).

2.3 Components Selection

The main components that have to be selected are the PFC inductor, the resonant inductor and the resonant capacitor.

2.3.1 Inductor Selection for PFC Boost Converter

General electronic ballast drives the lamp with fixed frequency method. From figure 2.2, the ballast starts by driving the lamp with fixed 85 kHz for 0.5 to 1 second to preheat the lamp filaments. After that, it decreases the frequency down to the running frequency. By this method, the DC voltage should be constant in which to maintain the lamp running power. Increase or decrease this voltage leads to the variation of the lamp running power. The easiest way to sustain the lamp power is to regulate the DC voltage. Thus, the PFC boost converter handles this important role with an additional benefit of the unity power factor. As discussed in [18], this converter operates in the critical conduction mode; the PFC inductor (L_{pfc}) is determined by:

$$L_{pfc} = \frac{8\times 10^{-6}\eta V_{ac(rms)}\left(V_{dc} - \sqrt{2}V_{ac(rms)}\right)}{2\sqrt{2}P_{OUT}} \tag{2.9}$$

Where η is the target efficiency of the converter; $V_{ac(rms)}$ is the minimum input RMS voltage and P_{OUT} is output power. Using the minimum universal line voltage (85 V), P_{OUT} is 34 W and assuming an efficiency of 0.95. The L_{pfc}, calculating by (2.9), is 1.8 mH.

2.3.2 Resonant Inductor and Capacitor selection

Since both L_r and C_r involve in three modes of operating, it is difficult to calculate the exact values of those L_r and C_r. The calculation process can be simplified by neglecting C_r when running mode is considered. By assume that lamp resistance is far higher than capacitor reactance, the calculation process for this mode of operation focuses on an L_r. Therefore, there are two steps of calculation. The first step is to calculate an L_r based on the power in the lamp during running. Assuming the maximum power transfer, the output stage input power is:

$$\frac{P_{lamp}}{\eta} = V_{in}I_{Lr} = \frac{\sqrt{2}V_{dc}}{\pi}I_{Lr} = \frac{\sqrt{2}V_{dc}}{\pi}\frac{V_{dc}}{4\omega L_r} = \frac{V_{dc}^2}{4\sqrt{2}\pi^2 f_{run}L_r} \tag{2.10}$$

Where P_{lamp} is the lamp power (W), η is an expected efficiency, Vin, the input voltage, is the fundamental component of the square wave produced by the inverter, V_{dc} is DC bus voltage (V), f_{run} is running frequency and I_{Lr} is Inductor current (A). Therefore, the resonant inductor is:

$$L_r = \frac{V_{dc}^2\eta}{4f_{run}\sqrt{2}\pi^2 P_{lamp}} \tag{2.11}$$

During preheat, the resistance of the lamp is infinite and the filament resistance is negligible. This results in an L_r-C_r series circuit. Using the impedance across the capacitor, the peak preheat voltage V_{ph} is given as:

$$V_{ph} = \frac{I_{ph}}{2\pi f C_r} \tag{2.12}$$

Where I_{ph} is the preheat lamp current and f is the preheat frequency. The transfer function is:

$$V_{ph} = \frac{2V_{in}}{\pi\left(\left|1 - 4\pi^2 f^2 LC\right|\right)} \tag{2.13}$$

To preheat the lamp filament with the desired current while the lamp voltage is kept below V_{ph} , the resonant capacitance can be calculated from (2.13) as:

$$C_e = \frac{I_{ph}^2 L_r}{(V_{ph} + V_{dc} / \pi)^2 - (V_{dc} / \pi)^2} \tag{2.14}$$

From (2.11) and (2.14) the different lamp power rating results different L_r and C_r. According to the lamp power rating, the ballast should be individually designed in which to achieve the proper operating condition. For example, the 36 W T8 lamp running at 32 W power with 40 kHz frequency can illuminate at full specific illumination. The DC voltage is 400 V and assuming an efficiency of 0.95. The L_r, calculating by (2.11), is 2 mH. From (2.14), by using the applicable preheating voltage at 300 V and current at 600 mA, this C_r should be 4.33nF. By using the same condition and 18WT8 ballast, the L_r and C_r should be 4.3mH and 9.2 nF in sequence.

2.4 Software Model

The model consists of a set of procedures for each mode of operation. These modes of operation include preheat, ignition and run. Software model normally has 3 states according to those modes of operation. These states are preheat state, ignition state and running state. Beside these states, an advance software model always includes 2 more states that are initial state and stop state to fulfill the ballast operation. Therefore, the software model for an electronic ballast usually has 5 states of operation include initial state, preheat state, ignition state, running state and stop state as illustrate in figure 2.11 (the stop state is not in the time frame of figure 2.11 since it will be activated by an abnormal condition of ballast).

2.4.1 Initial State

During the initial state, the controller sets the operating frequency at 100 kHz and keeps it steady for a time to charge up the blocking capacitor (C_b). However, the non-microcontroller ballasts skip this state and start with the preheat state.

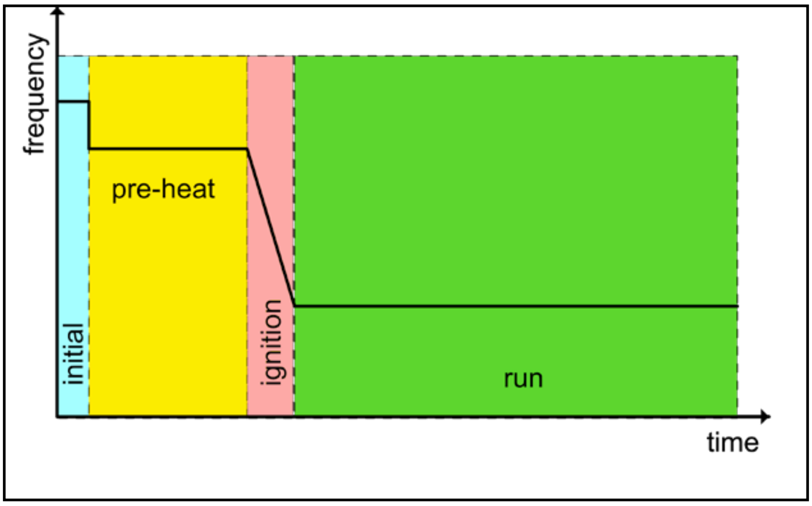

Figure 2.11 Operating frequency timing diagram

2.4.2 Preheat State

Normally, the electronic ballasts with preheat start feature operate the inverter with high operating frequency to warm up the filaments as described in 2.2.1. This frequency is depending on the required preheat current, resonant inductor (L_r) and resonant capacitor (C_r). Thus, one preheating frequency does not fit all fluorescent type and power rating.

2.4.3 Ignition State

The software decrease the frequency (increases the voltage) to ignite the lamp. The ignition speed depends on the time between each frequency step. To detect the moment when the lamp ignites, a simple assumption is used that the voltage across the lamp will significantly decrease after ignition. After the ignition, the software moves to the next running state. Note that, many electronic ballasts simply decrease the operating frequency to the desired running frequency by assume that the lamp is ignited.

2.4.4 Running State

After the ignition of the lamp, a constant frequency is set. This method basis on the assumption that the DC supply is presumed to be constant and the lamps discharge characteristic are unique for the same type and rating. According to the 2.2.3, this running frequency depends on the lamp and resonant circuit configuration. Thus, this frequency should be preselected as an expected frequency value for the lamp used. In this state, the variation of operating frequency directly affects the lamp power.

2.4.5 Stop State

If any abnormal conditions occur, the software should automatically switch itself into this state to prevent the ballast and lamp from unexpected damage. This state turns off the inverter driving signal and latch until the reset command occurs. This reset command is the lamp reinserting or the restarting of power supply. In this state, the power consumption can be reduced by putting the micro-controller into HALT mode.

2.5 The Fluorescent Lamp Dynamic Model and Numerical Calculation

The simplified resonant inverter is used in the simulation [24]. The controllable AC voltage source is connected through the resonant inductor and capacitor as a low-pass filter, with the fluorescent lamp as a resistive load (R_{lamp}) as shown in figure 2.12.

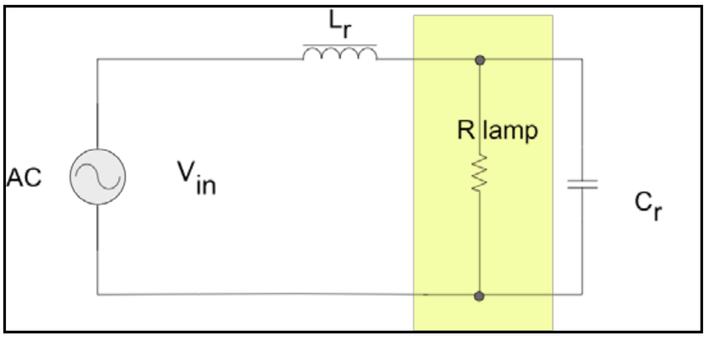

Figure 2.12 Simplified resonant inverter for electronic ballast

During the running stage, the lamp acts as a negative differential resistor [27], [28]. The characteristic graph, that is shown in figure 2.13, can be approximated by using the simple straight line. This line can be calculated as:

$$V_0 = R_S I_0 + V_{I=0} \tag{2.15}$$

$$R_{lamp} = \frac{V_0}{I_0} = \frac{V_0 R_S}{V_0 - V_H} \tag{2.15}$$

Where V_0 is the voltage at present condition, I_0 is the current at present condition and R_S and V_H are defined as:

$$R_S = \frac{V_{Max} - V_{min}}{I_{Max} - I_{min}} \tag{2.16}$$

$$V_H = V_{min} - I_{min} R_S \tag{2.17}$$

where V_{max} is the lamp voltage at the highest power, V_{min} is the lamp voltage at the lowest power, I_{max} is the lamp current at the highest power, and I_{min} is the lamp current at the lowest power. Specifications for V_{max} , V_{min} , I_{max} and I_{min} can be obtained from the lamp manufacturers.

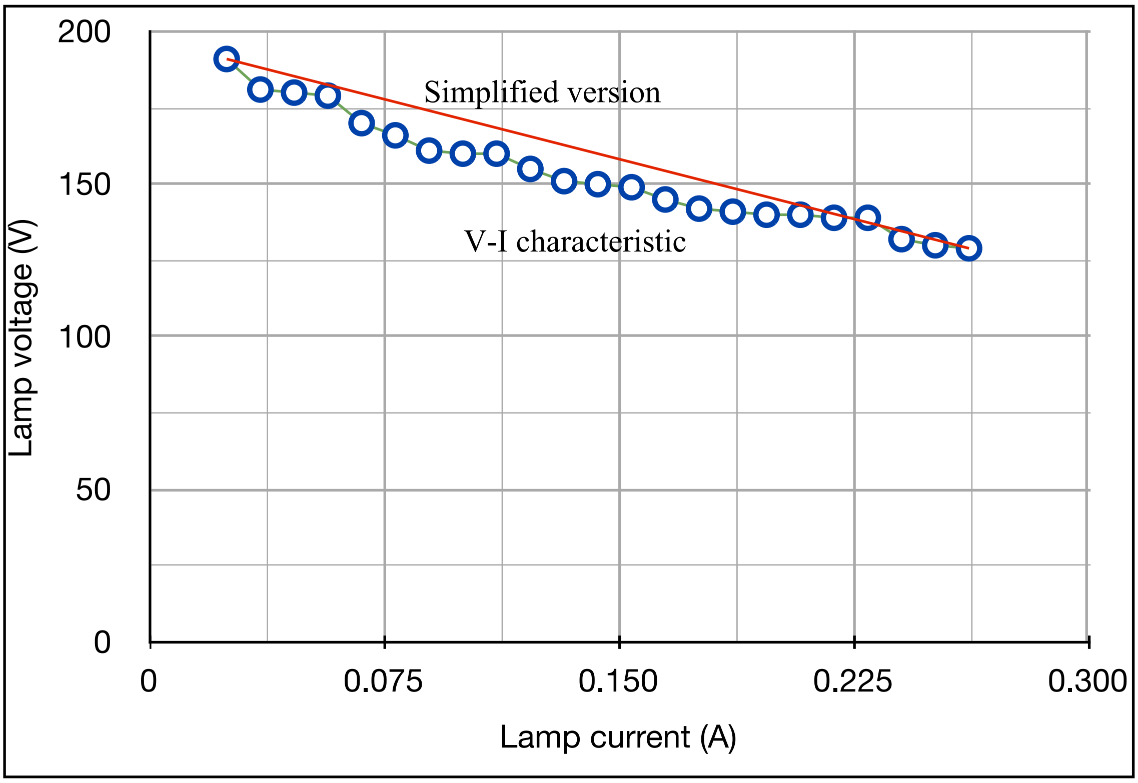

Figure 2.13 The V-I characteristic of a fluorescent lamp and its simplified

Because the higher-order harmonics account only for a small percentage of the input, the voltage and current waveforms appearing at the lamp are assumed to be sinusoidal. Considering only the fundamental component, lamp power (P_{lamp}) can be calculated as:

$$P_{lamp} = \left| \frac{-\dfrac{jV_{in}}{\omega CR_{lamp}}}{\left(j\omega L_r\right)\left(R_{lamp} - \dfrac{j}{\omega C_r}\right) - \dfrac{jR_{lamp}}{\omega C_r}} \right|^2 \tag{2.18}$$

Starting with an initial operating frequency, the lamp power is calculated. If P_{lamp} is less than the power command, the frequency is decreased and the lamp voltage, current, and resistance are recalculated at the new power level. The calculation is then iteratively repeated until the P_{lamp} is sufficiently close to the power command and the running frequency is obtained. The simulation results are shown in figure 2.14.

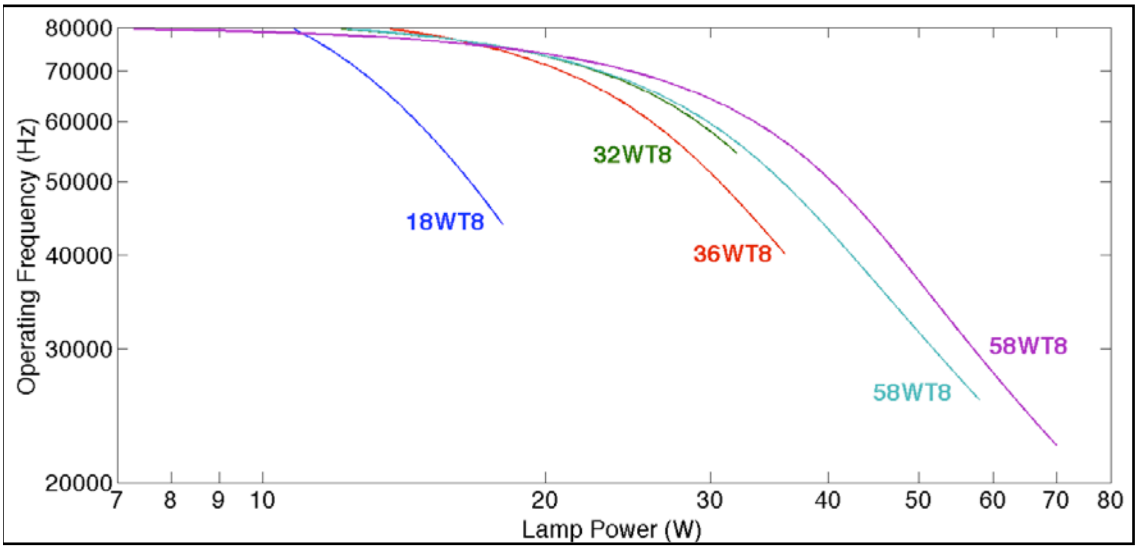

Figure 2.14 Operating frequency VS Lamp power by using the numerical calculation

CHAPTER 3 MULTI-RATING ELECTRONIC BALLAST

Fluorescent lamp detection techniques that can automatically detect and operate the fluorescent lamps at the rated power based on lamp voltage were reported in 2005 [10]. This technique is standing on the assumption that if the lamp is not dimmed, the lamp voltage will remain constant under steady-state conditions. However, a proper operating frequency cannot be determined unless the wattage of the lamp is known a priori. Thus, the constant voltage cannot be achieved. The lamp voltage after striking (ignition) varies with the lamp temperature, age, and manufacturer. Therefore, different lamp ratings might have overlapped voltage ranges. For example, 32WT8 and 58WT8 lamps operate at the same voltage, ranging from 117 V to 127 V, which can lead to misidentification of the lamp [11]. In addition, noise can interfere with the voltage, and adding a filter may increase the cost of the system.

Using the assumption that the lamp behaves as a resistance, at high frequency operation. This thesis presents a multi-rating electronic ballast for fluorescent lamps, based on operating frequency determination. The thesis includes the configuration and the controller design of the multi-rating electronic ballast. The proposed lamp rating detection algorithm, composed of multi-step lamp power regulation and the trapezoidal possibility weight decision based on a given set of lamp operating frequency data. The trapezoidal possibility weight provides a range of lamp operating frequency that can be considered as one power rating. This chapter describes of the relationship between the operating frequency and lamp power rating. The theory and background of the trapezoidal weight function are laid out. The design procedure, the multi-step power regulation and software algorithm are then discussed.

3.1 Lamp Power Rating Determination

The fluorescent lamps are manufactured in series for which they are divided by their shapes. The fluorescent lamps are typically identified by a code such as F##T##, where the letter F stands for "fluorescent." The next digits indicate the power in watts. The letter T indicates that the shape of the bulb is tubular, and the digits after indicate the diameter in eighths of an inch. Typical diameters are T12 (12/8") for residential bulbs with old magnetic ballasts, T8 (8/8") for commercial energy-saving lamps with electronic ballasts, and T5 (5/8") for very small lamps. A series of lamp contains a number of lamp rating. This number depends on the main manufacturer that dominates the market. We often can speculate the difference of lamp rating from the length of lamp tube and its diameter. For example, the 13WT5 lamp is 21" long while 8WT8 lamp is 12" long. Nonetheless, there are lamps with different ratings that share the same size such as 36WT8 and 32WT8.

The fluorescent lamp is the gas-discharge lamp. Thus, it appears to the source as a resistant load with the value that is specific to the lamp series and rating. It is assumed that if the resistance is known, the rating can be determined correctly. There are plenty of methods to measure the resistance. From the Ohm Law's, if a voltage is applied to a resistor and the current is measured, the resistance can be obtained. Applying the current and measuring the voltage is another way to calculate the resistance. Although this assumption is suitable to measure the resistance of a fixed resistor, the fluorescent resistance is not fixed. The resistance of the fluorescent lamp is a negative differential resistance. This means that the lamp has a fixed resistance when the current is fixed. Any change of current will lead to the resistance variation. For example, if the current is decreased, the resistance will be increased. This results in the increment of the voltage as shown in figure 3.1. However, if the lamp current is fixed, the lamp resistance is also fixed. This allows the use of the ordinary resistance measuring method.

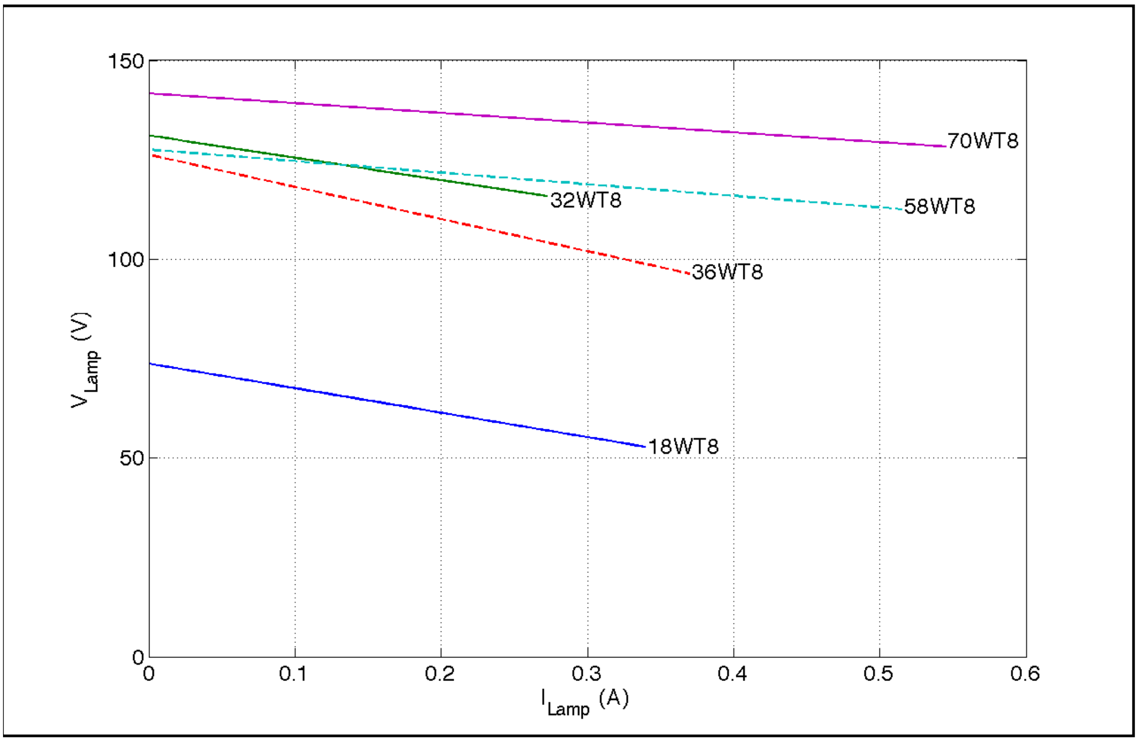

Figure 3.1 The V-I characteristic of the fluorescent lamp

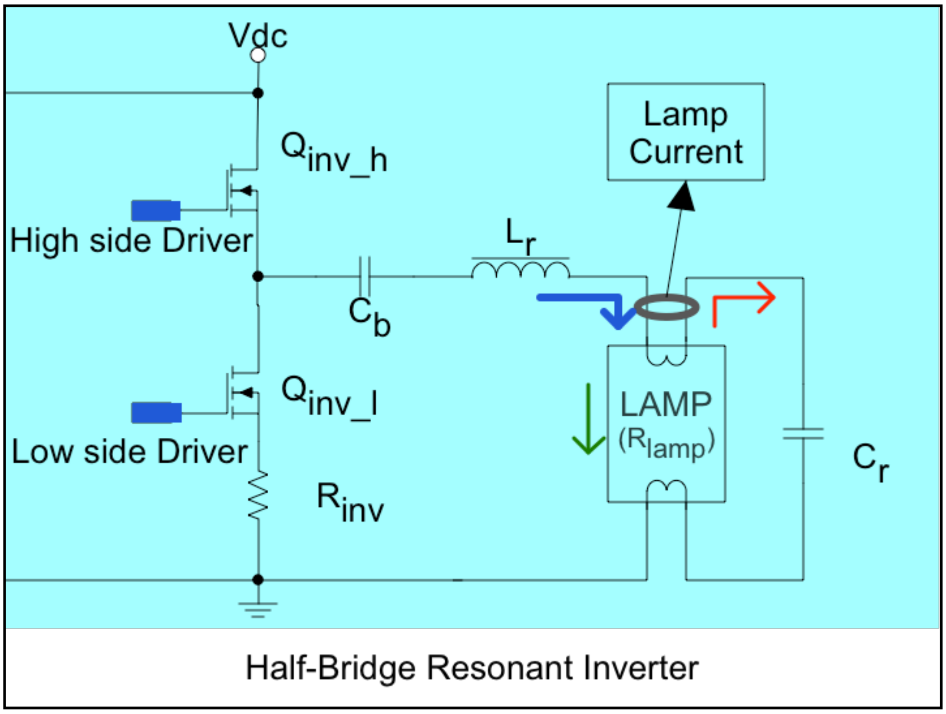

Figure 3.2 The current sensor placement for lamp discharge current measurement

Since the lamp current can be obtained by subtracting the capacitor current from the inductor current, the current sensor is placed by combining both current in opposite directions, as illustrated in figure 3.2, to alleviate the controller computing task. In addition, the AC current measuring is a difficult task for a low-cost microcontroller. Therefore, the power regulation method is introduced. Note that the input voltage of the inverter is DC and the current is also DC. This allows the use of a simple shunt resister together with a low-pass filter and a microcontroller. However, using only one state of power regulation is not enough since several lamps share the same resistance value when driving with the same power. The trend of lamp resistance versus lamp power should be included to determine the lamp characteristic. The multi-step power regulation method is introduced in this thesis. This method is suitable for acquiring the lamp characteristics with less processing time compared with the method of continuously measure the resistance throughout the characteristic line.

Instead of using voltage or current for lamp detection, this thesis introduces the use of operating frequency to determine the lamp rating. From equations 2.7 and 2.8, the lamp resistance depends on the operating frequency and the lamp power. Therefore, by keeping the supplied power fixed, the lamp resistance can be achieved by measuring the operating frequency. The benefit of using frequency information over voltage information is that the frequency itself is less vulnerable to the interference than the voltage.

3.2 Trapezoidal Weight Function

The pattern classification method is the method that enables the system to automatically classify the object into the group of the same pattern. Figure 3.3 shows two patterns including ‘o’ and ‘x’. The easiest way to differentiate the patterns is to draw the boundary between the two patterns. If the new pattern is located in the left area, it will be classified as ‘x’. The right area is for the ‘o’ pattern.

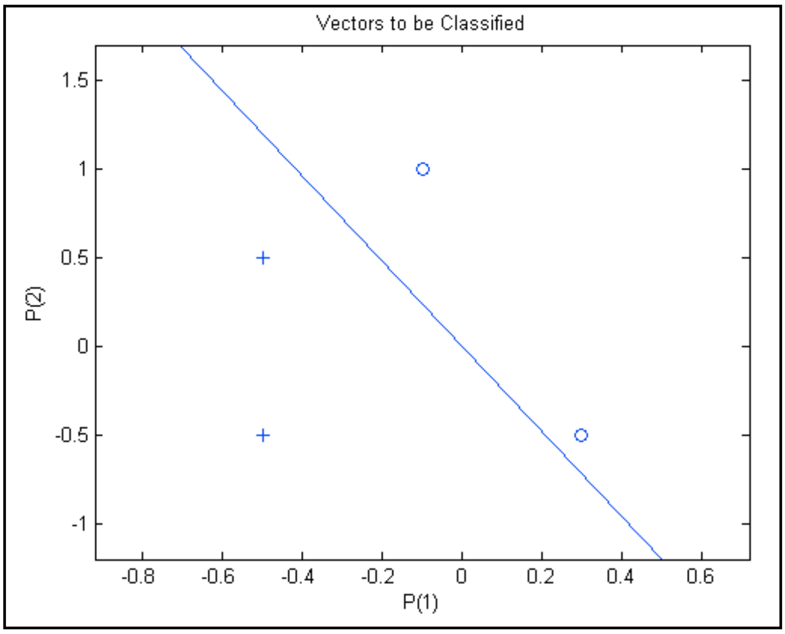

Figure 3.3 The pattern classification method by using the boundary line

Only two samples per pattern are not enough to draw the boundary. There are many ways to set the boundary line since the two patterns are easily separated. If more samples are acquired, the boundary line will be of less degree of freedom because the occupied area of the samples have increased. A depiction of the mentioned pattern is depicted in figure 3.4.

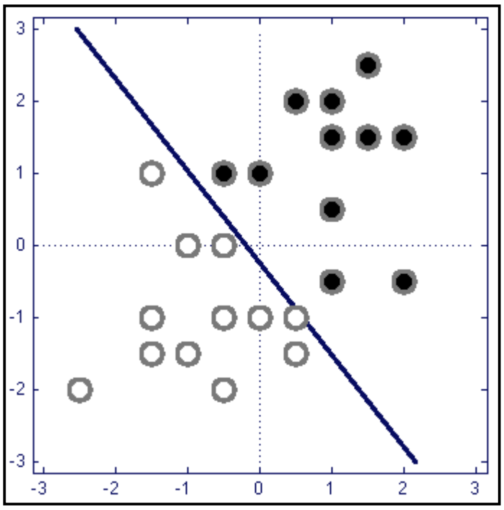

Figure 3.4 The pattern classification method by using the boundary line with more acquiring samples

For the system with more than two patterns such as the power rating of fluorescent lamp, there are 2 ways to assign the boundary line. If the number of members of all patterns are equal to the members of the universe set, the boundary is more evident. As shown in figure 3.5, the BL1 lines is the boundary line separating the R, G and B patterns. The area of each pattern is large so that the accuracy of data has little to no effect to the classification result. If the universe contains an unknown pattern, the tight boundary area should be set. This allows the unknown pattern to be rejected. Figure 3.4 shows the boundary areas of BL2R for pattern R, BL2G for pattern G and BL2B for pattern B. Data outside this area will be determined as the unknown pattern.

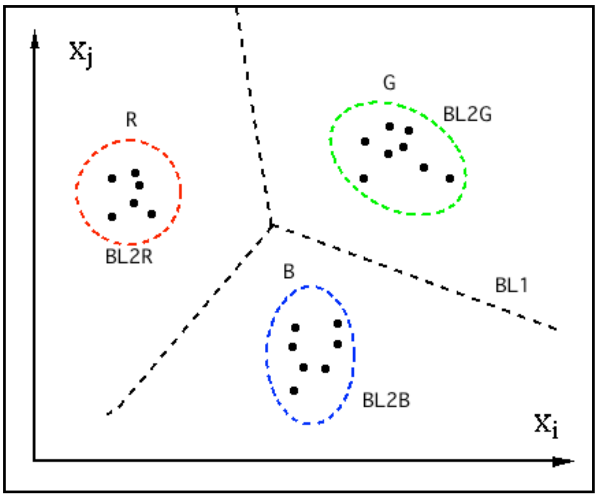

Figure 3.5 The pattern classification method by using the boundary line (BL1) and boundary area (BL2)

This hard threshold decision method is based on the uniform distribution function. For the application that the member of different patterns cannot absolutely be separated, another distribution function should be used. In figure 3.6, assuming that the boundary is drawn using the uniform distribution function indicating by the red line. A suspect black circle data will be classified as not a black circle pattern. By using figure 3.7 with this suspect black circle data, it should have 0 possibility of being black circle pattern. However, by using the flip version of figure 3.7 to classify the white pattern, the suspect black circle data, it should have 1 possibility of being white circle pattern. Therefore, the decision result is wrong for this suspect black circle data.

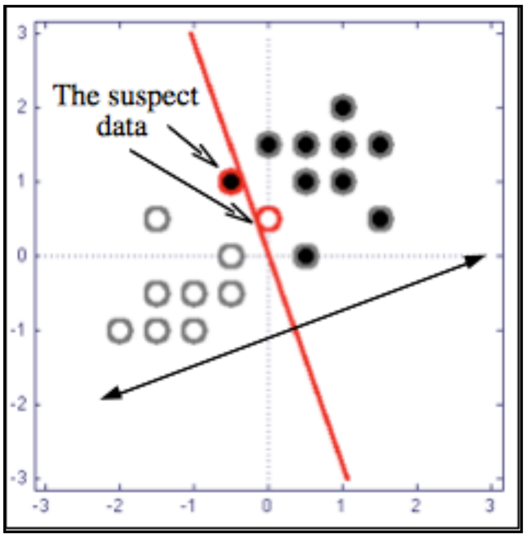

Figure 3.6 An example of data classification using hard threshold with wrong decision

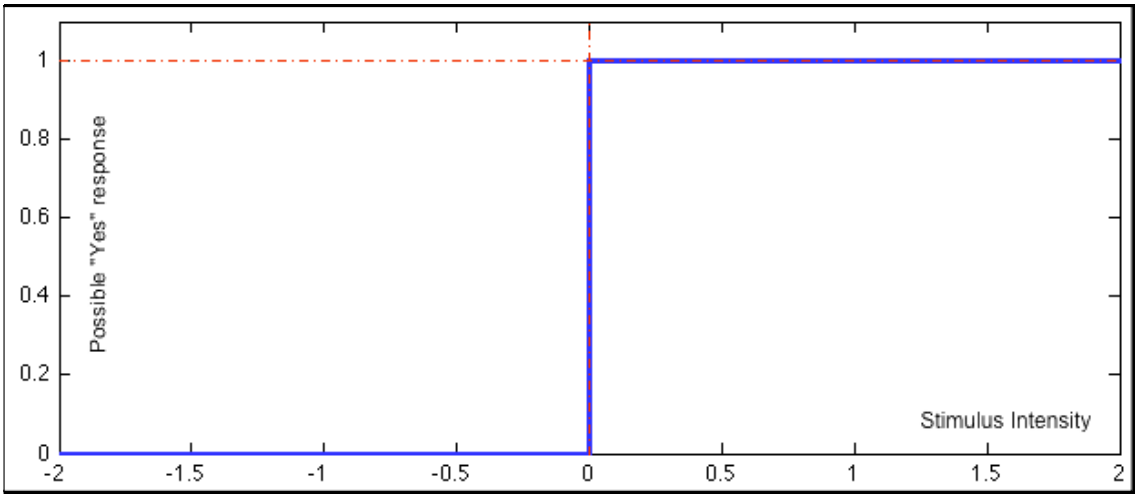

Figure 3.7 A hard threshold by using one side uniform distribution function

For the above situation, a soft threshold may be used to soften the classification result. It does not result in definite decision but a fuzzy decision like a possibility of being a white pattern is 0.2 whereas the possibility of being a black pattern is 0.5. There are many distribution functions that can be used for the pattern classification such as uniform, T, normal, F, rayleigh and trapezoidal distributions. In probability theory, the normal (or Gaussian) distribution is a continuous probability distribution that is often used as a first approximation to describe real-valued random variables that tend to cluster around a single mean value. The graph of the associated probability density function is bell-shaped, and is known as the Gaussian function or bell curve. Therefore, this distribution function is widely used in the pattern classification purpose. A soft threshold using the normal distribution as shown in figure 3.8 is described by an exponential function which will consume a considerable amount of controller computing time if implemented.

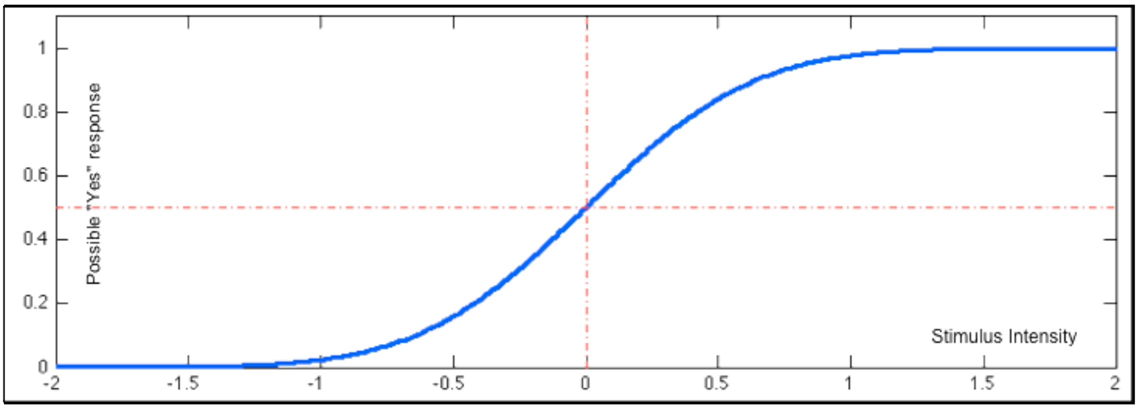

Figure 3.8 A soft threshold by using one side normal distribution function

Another widely used distribution function is the trapezoidal or linear distribution function because it simplifies the normal distribution to reduce the complication of algorithm. This function is popular and widely used in the fuzzy logic decision method [12].

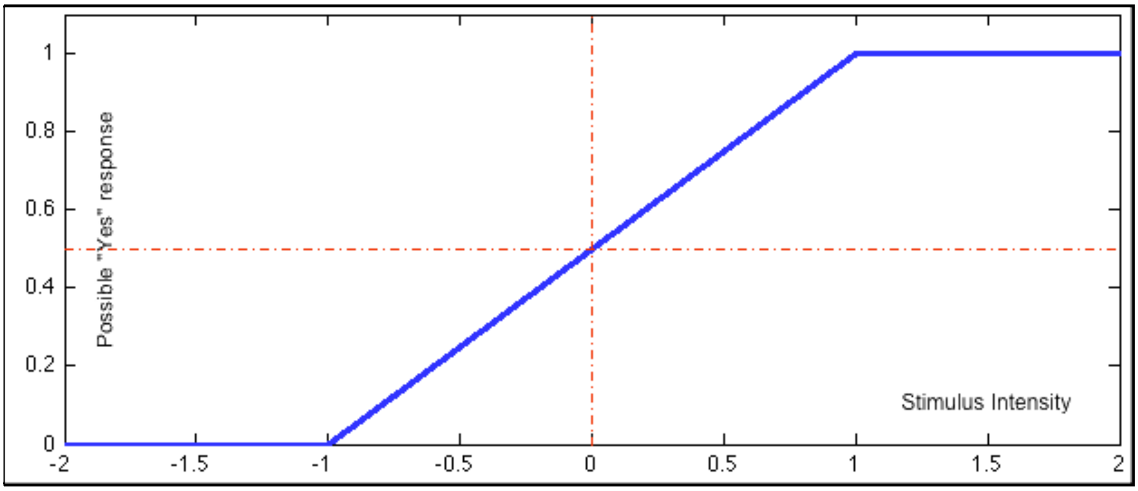

Figure 3.9 A soft threshold by using one side trapezoidal distribution function

Again with the figure 3.6, by using soft threshold trapezoidal distribution function illustrated in figure 3.9, the suspected black data results in 0.6 of the possibility of being white pattern and 0.4 for the possibility of being black pattern. With this result, if more evidences are introduced, another data vector and decision region may result in a new possibility value. Combining with the previous results will give better decision. These results can be used as the second opinion. If more opinions can be introduced, the decision output will be narrowed down to the right decision. This algorithm is called voting scheme.

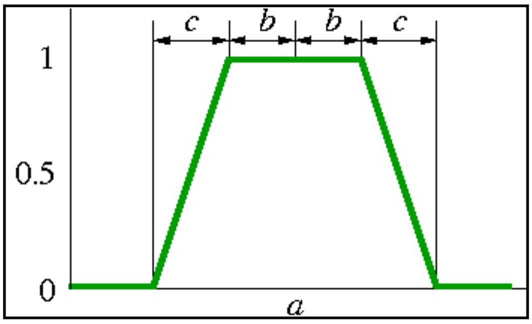

Figure 3.10 The region of pattern classification by using trapezoid distribution

In applications where there exist unknow patterns, the tight boundary area and the distribution function with soft threshold on both sides of the decision making as shown in figure 3.10 are proposed. The length of c and b in figure 3.10 can be varied to fit the intended distribution curve. The unknown pattern outside the region would be rejected. Thus, this trapezoidal function is used in this thesis as the decision making method as trapezoidal possibility weight function. The voting scheme is used in the manner of multi-step power command.

3.3 Design Procedure

Like general electronic ballast, the hardware model of multi-rating electronic ballast consists of the PFC boost converter and the inverter as shown in figure 3.11. Therefore, a set of equations for each operating frequency and the corresponding lamp voltage and circuit currents are alike. The challenge is that is all interested lamp ratings are to be supplied by a single hardware.

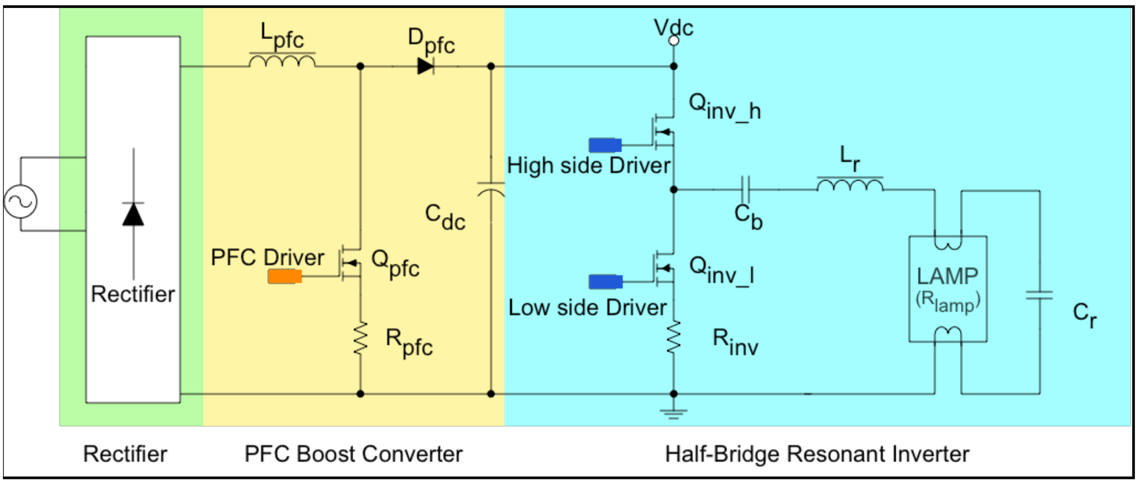

Figure 3.11 Schematic of the multi-rating electronic ballast

3.3.1 Resonant Inductor and Capacitor Selection

Since the running frequency has effects on the light efficacy, the lowest running frequency should not be set to the value below 20 kHz. On the other hand, the preheating can be much higher. If the switching frequency had been higher than 100 kHz, the switching devices would have had more switching loss. Moreover, the microcontroller generates the PWM signal by using the main oscillator generating the frequency range of 8-16 MHz for which the step of PWM period is constant. It makes the wide step of frequency in the high frequency region and narrow step of frequency in the low frequency region (the step is 0.6 kHz at 100 kHz region and 0.006 kHz at 10 kHz region). With wide step of frequency changing, it is difficult to stabilize the operating power of the lamp and may cause the light flickering. To accommodate for the power regulation in case that the lamp temperature is still very high (i.e. it had just been turned off or reheated), the preheating frequency should be around 80 kHz because the lamp resistance is around 4-6 times higher than normal. The operating frequency is empirically set 60 kHz to avoid unnecessarily large steps in frequency changing. By substitution of the frequency range of 20 kHz to 60 kHz in (2.11) with $\eta = 0.95$ and $V_{dc} = 400$ V, the inductances of each lamp wattage are shown in table 3.1.

Table 3.1 Resonance inductor calculated results for T8

Power rating (W)	L for f=20kHz(mH)	L for f=60kHz(mH)
18	7.56	2.52
32	4.25	1.42
36	3.78	1.26
58	2.35	0.78
70	1.94	0.68

Notice that, for the lamp wattage of 32 W to 70 W, the overlapped inductance is between 1.42 mH to 1.94 mH while the lamp wattage of 18 W to 36 W gives the inductance of 2.52 mH to 3.78 mH. The middle value of the inductance between the two ranges is chosen at 2.23 mH and used in the design procedure to determine the operating frequency. This may cause the running frequency of the 18 W lamp to be higher while the running frequency of 70 W lamps to be lower than expected. The calculation is based on the assumption that the lamp resistance is much higher than the capacitor reactance. Even with the inclusion of the capacitor, the running frequency will still be in the desired region by using (2.14). Thus, the selection of inductance and capacitance is done by a quick substitution of L in (2.14) where the resonant capacitance is obtained as 4.83 nF. A capacitance of 4.7 nF is chosen due to availability. Once the inductance and capacitance are obtained, they are used in computer simulation to validate the operating frequency as shown in table 3.2. The operating frequency is located in the range of 22 kHz to 50 kHz where the lowest frequency is slightly higher than the originally selected frequency of 20 kHz.

Table 3.2 Numerical calculation of the running frequency of the electronic ballast using L = 2.2 mH and C = 4.7 nF

Power rating	Running frequency (Calculate)
18 W	49.9 kHz
32 W	53 kHz
36 W	39 kHz
58 W	24.1 kHz
70 W	20.8 kHz

3.3.2 Inductor Selection for PFC Boost Converter

From 2.14, L_{pfc} is selected by applying the maximum possible output power so that the ballast is capable of handling the highest power rating of the T8 series. Using the minimum universal line voltage (85 V), P_{OUT} is 70 W and assuming an efficiency of 0.95. The , using (2.14), L_{pfc} is obtained as

$$L_{pfc} = \frac{8 \times 10^{-6} \times 0.95 \times 85\left(400 - 85\sqrt{2}\right)}{2\sqrt{2} \times 70} = 913\mu H \qquad (3.1)$$

The above calculated inductance guarantees that with 70W lamp, the lowest operating frequency is 25 kHz with a regulated 400 V at the dc bus where the power factor and %THD are 0.9 and 15%, respectively. The overall efficiency is at 0.85. Had the inductance been higher, the frequency would have been reduced which may cause the PFC to operate in the continuous-conduction mode. As a consequence, the power factor and the THD will be deteriorated. On the other hand, if the inductance is lower, the operating frequency will be increased. The electromagnetic interference will be unavoidably present in the ballast circuitry.

3.4 Ballast Controller Design

The operation of the electronic ballast system can be divided into two parts, the PFC boost converter and the half-bridge inverter. The operation of boost converter can be described as two stages: operate and stop. The operation of the inverter are divided into five stages namely, initialization, preheat, lamp detection, run, and stop. The block diagram of the ballast controller is shown in figure 3.12. The controller operates both the boost converter and the inverter. For the boost converter, the controller controls the Vdc by sensing the voltage from Vdc and the timing from current zero crossing and sends out the driving signal to the boost converter. For the inverter, the lamp power is regulated by sensing the voltage from V_{Rinv} and sends out the driving signal to the inverter. The V_{lamp} is the lamp voltage that is used for the protection purpose. The fault procedure is programmed as interrupt service routine to immediately stop the ballast if an abnormal condition occurs. The initial state has been added to the beginning for the purpose of charging the blocking capacitor and waiting for the steady state of the PFC boost converter.

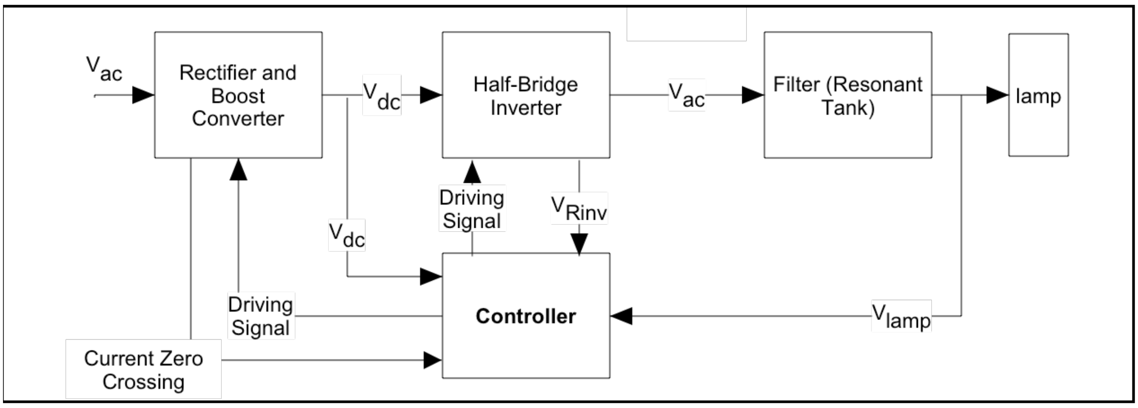

Figure 3.12 Controller block diagram

3.4.1 PFC Boost Converter Operating State

The microcontroller controls the PFC boost converter in critical conduction mode by using a monostable multivibrator (one-shot) circuit. The multivibrator generates a pulse with constant width for a single period of 20 ms to PFC Driver shown in figure 3.11. After the falling edge of this pulse, the current from the PFC inductor (L_{pfc}) start reducing. When the inductor current reaches zero value, the voltage from the auxiliary winding of L_{pfc} trigs the microcontroller to generate another pulse. This pulse width is related to the PFC output voltage (V_{dc}). The control loop regulates the V_{dc} at 400 V along with power factor close to unity. The input voltage from the rectifier is used to determine the AC period. This method uses less microcontroller processing time so that it still has enough capability to process other tasks such as output power control and lamp rating detection.

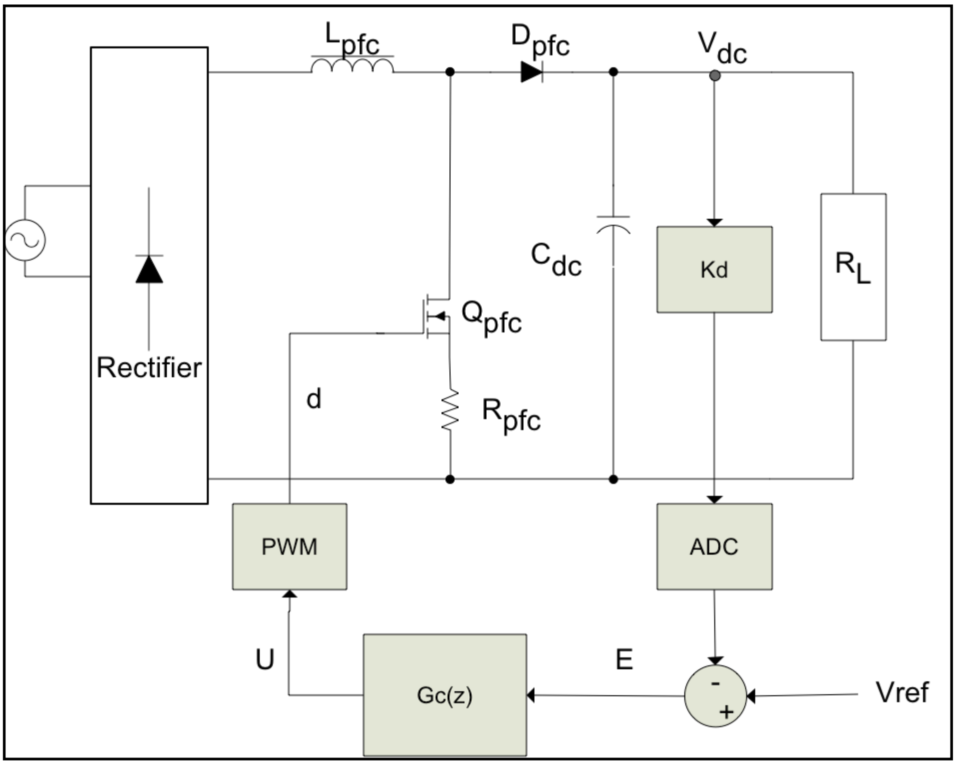

Figure 3.13 PFC boost converter block diagram

Figure 3.13 shows the block diagram of the PFC boost converter where k_d is the factor of the output loop voltage and $G_c(Z)$ is the transfer function of the PI controller. The block diagram of the boost PFC converter control loop is shown in figure 3.13 where each block can be derived as:

$$k_d = \frac{1}{V_{dc(\max)}} = \frac{1}{V_{ref(ADC)} \times ratio} = \frac{1}{5 \times 157} = 1.27 \times 10^{-3} \qquad (3.2)$$

Where $V_{ref(ADC)}$ is the analog-to-digital reference voltage. "ratio" is the voltage attenuation ratio of the sensed signal before feeding to the controller (i.e. the gain of the signal conditioner). In figure 3.14, $G_p(s)$ is the transfer function of the power converter stage in figure 3.13.

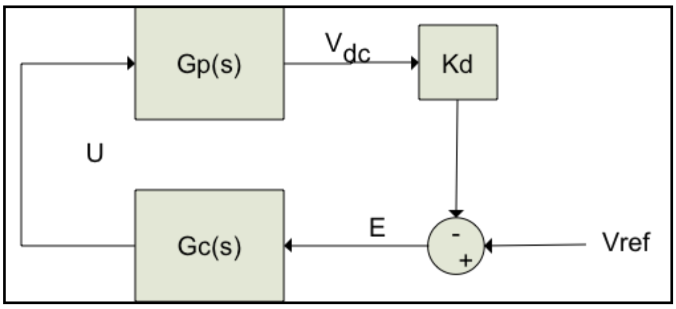

Figure 3.14 PFC boost converter and controller transfer function block diagram

The transfer function of PI controller ($G_c(Z)$) is:

$$k_p + \frac{k_I}{s} \tag{3.3}$$

where k_P and k_I are the gains for proportional and integral portions of the PI controller.

The transfer function of the boost converter ($G_P(s)$) is given by:

$$G_P(s) = \frac{\hat{V}_{dc}}{\hat{d}} = \frac{G_{d0}}{1 + {s}/{\omega_P}} \tag{3.4}$$

Where:

$$G_{d0} = \frac{2V_{dc}}{D}\frac{M-1}{2M-1} \tag{3.5}$$

$$M = \frac{V_{dc}}{\sqrt{2}V_{AC}} \tag{3.6}$$

V_{dc} is output DC voltage. V_{AC} is input AC voltage. D is duty cycle that is given by:

$$D = \sqrt{\frac{2L_{pfc}}{R_e T_S}} \tag{3.7}$$

where R_e is the effective resistance of the boost converter seen by the controller.

$$R_e = \frac{V_M^2}{I_{o(\max)}(V_O - \sqrt{2}V_{AC})} \tag{3.8}$$

$$\omega_P = \frac{2M-1}{(M-1)C_{pfc}R_L} \tag{3.9}$$

By using (3.4) to (3.9), the boost converter transfer function is:

$$G_P = \frac{1980}{0.05468s + 1} \tag{3.10}$$

The bode diagram of the loop control of the boost PFC converter K_d *G_C (s)*G_P (s) is shown in figure 3.15.

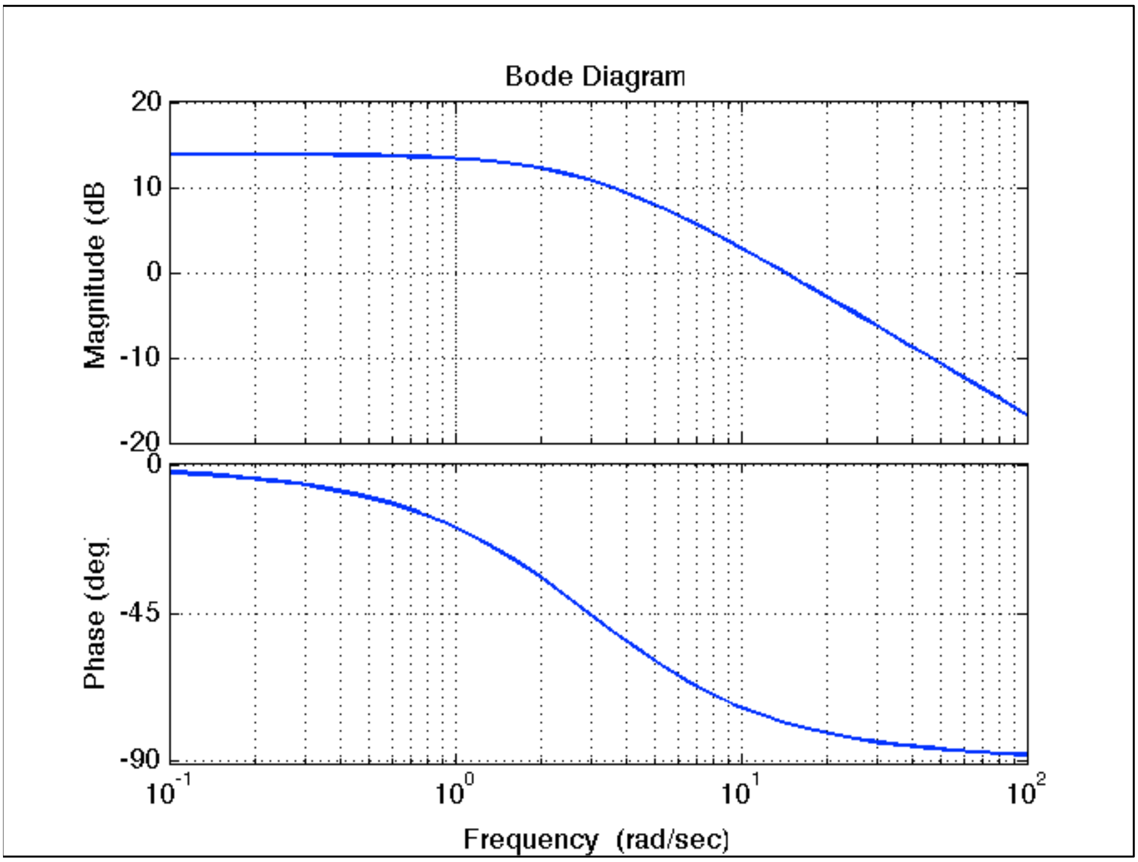

Figure 3.15 Bode diagram of control loop of PFC boost converter

Figure 3.15 shows the bode diagram of control loop of PFC boost converter. Since the idea of this controller is to avoid the use of the complicate command like multiplier, converter must operate at constant duty cycle over an AC input line frequency cycle. This is achieved by designing the microcontroller to change the PWM command when the AC voltage crosses zero. The controller voltage loop crossover frequency is also placed at 100 Hz. Therefore, the k_P and k_I are set to 2 and 92, respectively.

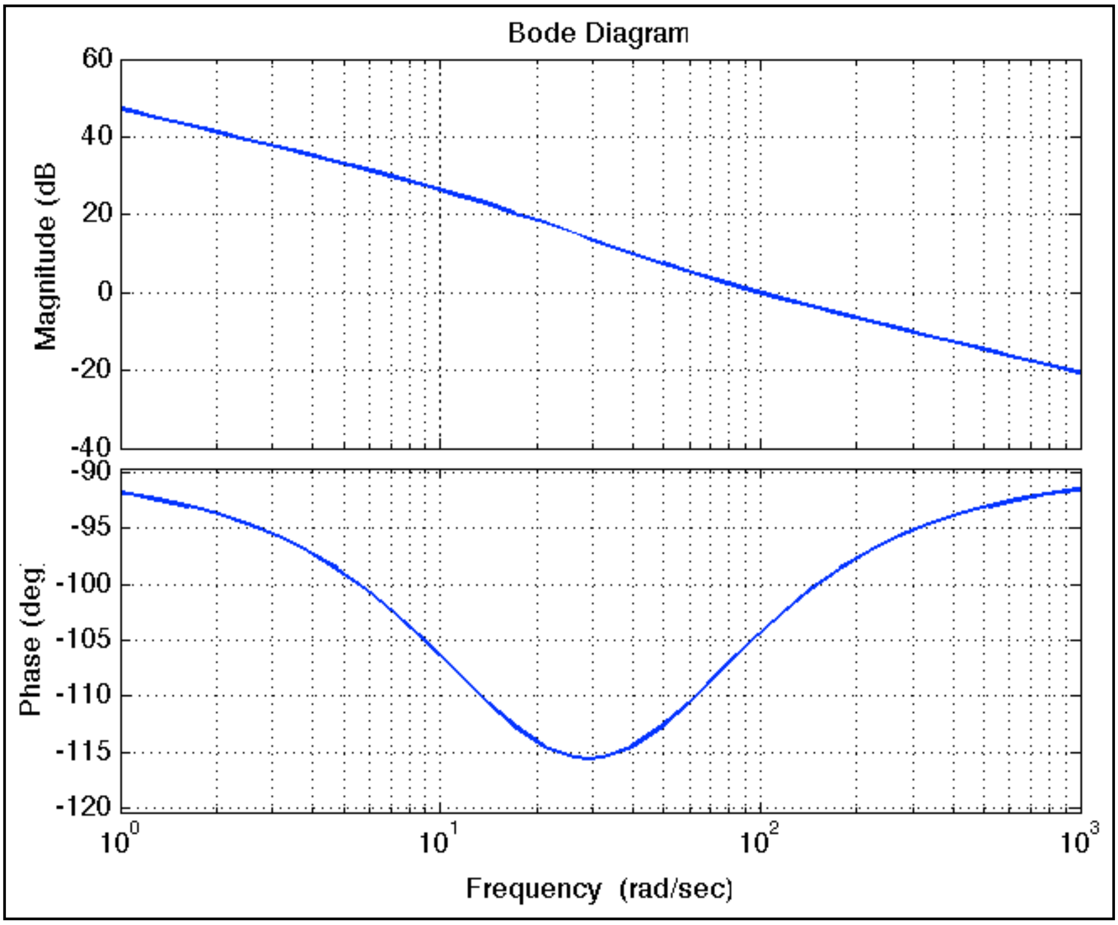

Figure 3.16 Bode diagram of control loop of PFC boost converter

With PI controller, figure 3.16 shows that the crossover frequency of the voltage loop is 100 Hz and the phase margin is of 76 degrees that is higher than 45 degrees.

Knowing the analog version of the controller transfer function G_C (s), we can apply the method of discretization "ZOH"[35] to obtain the digital controller G_C (z) :

$$G_C(z) = \frac{2z - 1.999}{z - 1} \approx 2\frac{z-1}{z-1} = 2\frac{1 - z^{-1}}{1 - z^{-1}} \tag{3.11}$$

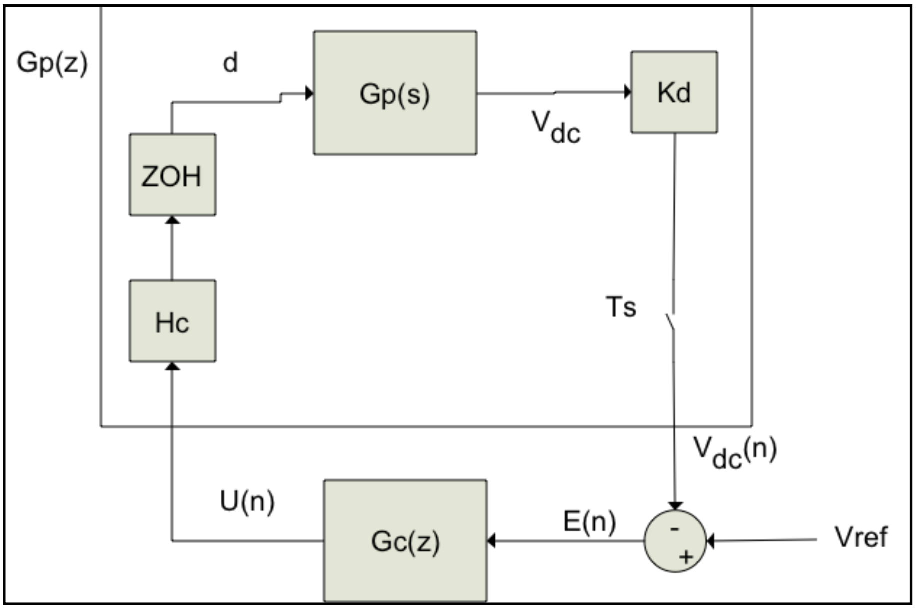

Figure 3.17 PFC boost converter and controller block diagram in z-domain

In Figure 3.17, the process of sampling and hold is represented by an ideal switch operating with the period of Ts. The PWM module is represented by ZOH. The controller of the voltage loop is represented by $G_C(z)$. The power circuit of the boost PFC converter is $G_P(s)$. The conditioning circuit of the output voltage and the gain of the A/D converter is represented by Kd. The conversion time of the A/D converter converter is represented by HC. The small signal of the power circuit $G_P(s)$ is passed directly in discrete-time $G_P(z)$ by using the transfer function given by:

$$G_P(z) = \frac{0.3621}{z - 0.9998} \qquad (3.12)$$

where H_C is 1 (assuming zero conversion time) and the delay given by the A/D conversion is zero. The block diagram of the PFC boost converter and controller in z-domain is shows in figure 3.17.

Bode diagram of this digital control system is shown in figure 3.18. The gain margin is 67 dB, phase margin is 75 degrees and crossover frequency is also 100 Hz. This converter is deemed stable since phase margin is greater than 45 degrees. The step response of this converter is experimentally studied in chapter 4. By using low-cost MCU with this simple control method, the error multiplying process is not included. As a result, there is a current distortion around the zero crossing that results in the THD value higher than 10%. If the THD is below 10% is needed, the dedicated PFC controller would be necessary in exchange of cost and size for the desired power quality. The PF and THD results are also shown in chapter 4.

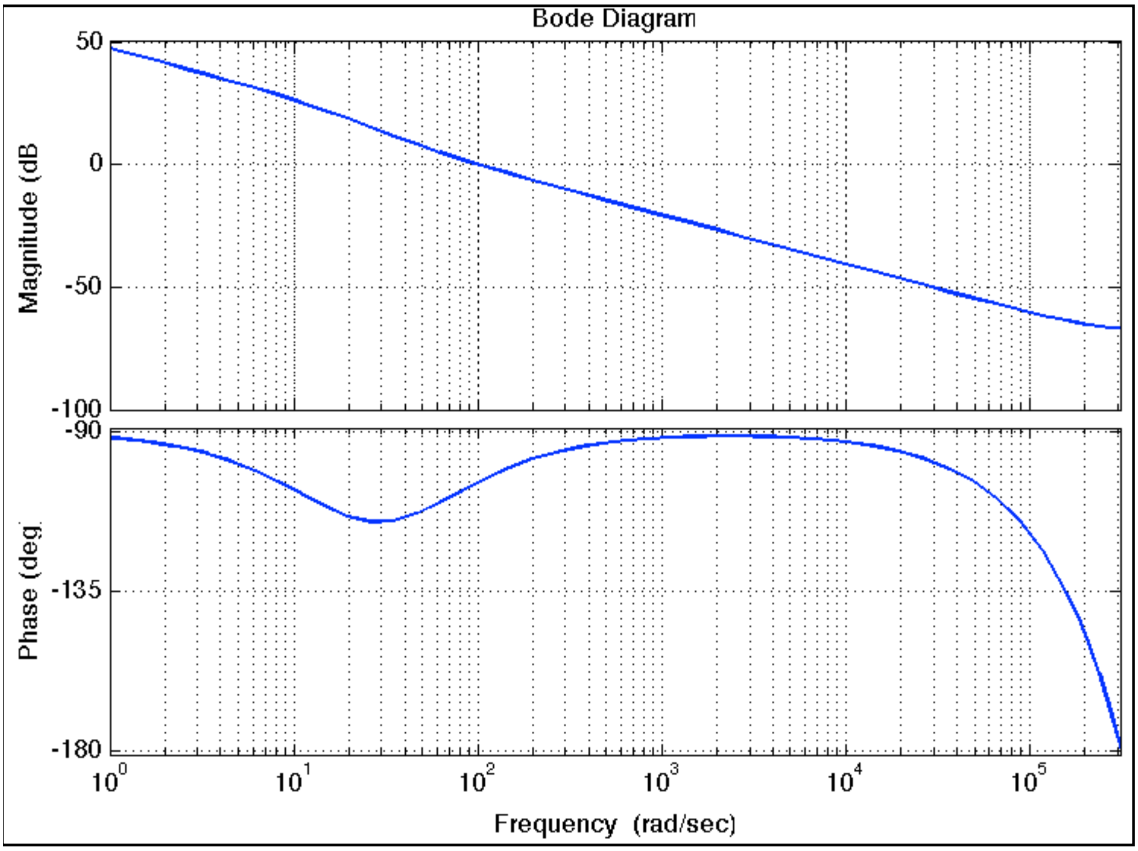

Figure 3.18 Bode diagram of digital control loop of PFC boost converter

3.4.2 PFC Boost Converter Stop State

If abnormal conditions occur, the software will automatically switch into the safety state that is designed to turn off the PFC driver. Abnormal conditions may cause by over current in the MOSFET or over- and under- voltages on the AC input. This state also stops the inverter operation to avoid unintended effects. The the maximum charging inductor current is sensed through a small resistor $RA8 = 0.33\Omega$. The threshold voltage at the digital input is set to 1.5 V and the over current threshold is set at 4.54 A.

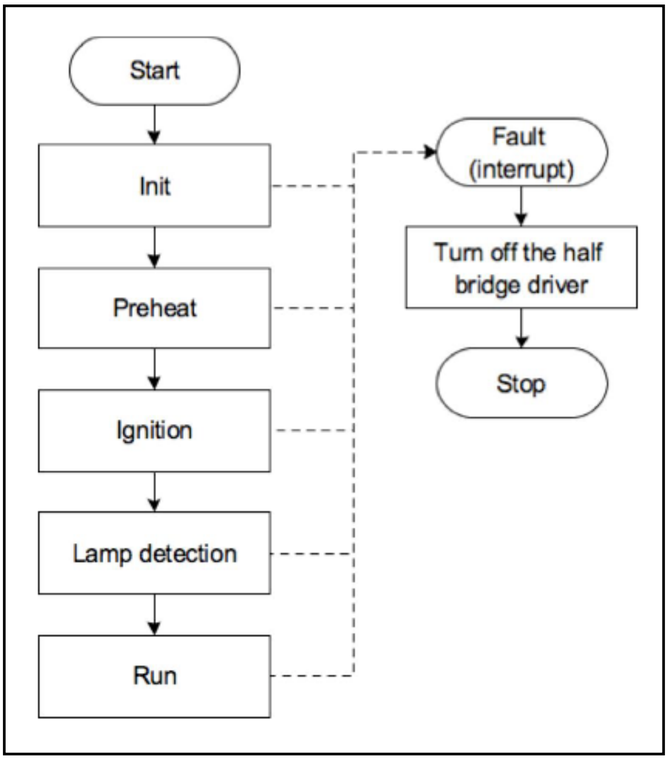

Figure 3.19 Flowchart of the multi-rating electronic ballast operation

3.4.3 Inverter Initialization State

The flowchart of inverter operations is illustrated in figure 3.19. This ballast contains the sequence of procedures including preheat, ignition, lamp detection and run as described in section 2.4. If an abnormal condition occurs, the interrupt service routine will turn the half bridge driver off to protect the system. During the initial phase, the controller sets the PWM frequency at 100 kHz and keeps it steady for 100 ms.

3.4.4 Inverter Preheat State

This state heats up the lamp filaments to the proper temperature before ignition. Electronic ballasts with preheat starting feature initially operate the inverter under high frequency to heat the filaments up. This frequency is depending on the required preheat current, resonant inductor and resonant capacitor. Thus, one preheating frequency does not fit all fluorescent types and power ratings. The preheat state warms the filaments up with a constant power to ensure the proper temperature for all T8 lamps. The controller raises the frequency by one step every time the measured current is greater than the desired value, and lowers the frequency if the current is lower than the desired value. This state takes approximately 0.5 to 1 second depending on the current command value [19].

3.4.5 Inverter Ignition State

The controller decreases the frequency (increases the voltage) to ignite the lamp. Since the voltage across the lamp will significantly decrease after ignition because the current begins to flow through the lamp then, the voltage change is used as ignition indication. After detecting the ignition, the controller moves to the next phase.

3.4.6 Inverter Stop State

If abnormal conditions occur, the software will automatically switch into the safety state that is -the half bridge driver is turned off. Abnormal conditions may arise resulting from lamp bulb removal, lamp failure to ignite, over-current or over-voltage, or a rectifying effect (end of life :EOL).

The bulb removal is detected by using the 'Lamp_present' node described in figure A.4. This node voltage is 0 V when the lamp is connected to the ballast. If there is no lamp connected, this node voltage will be 5V.

The over voltage is detected by using the 'V_lamp_PK' node. The voltage threshold is 300 V that is the maximum preheat voltage. This over voltage detection is disabled during the ignition state.

The over current is detected by using the 'CSO' node that is the peak current of the low side switch Q3. This peak current is very high if the switching frequency is lower than the resonant frequency. This phenomenon is called hard switching.

The EOL is detected by using 'EOL' node voltage. This node provides an averaged lamp voltage value of 2.5 V when the lamp is in normal condition. If EOL lamp is connected and run, this node voltage will be either higher or lower than 2.5V. The threshold voltage is 1.5 V and 3.5 V, respectively.

The lamp ignition failure is detected by using both 'V_lamp_PK' and decided by the software procedure. During the ignition process, the software detects the lamp voltage to determine the success of ignition. If the lamp ignition is successful, the current will start to flow through the lamp. As a result, the lamp voltage decreases. An unsuccessful ignition leads to the considerably high voltage at the output and will damage the ballast. If the operating frequency is decreased to the minimum available frequency and the lamp voltage does not decrease, indicating unsuccessful ignition, the controller will stop the driver.

3.4.7 Inverter Run State

During this phase, the controller measures the current required to deliver a given power to the lamp. The measured value is compared with a preset power command value, and the software corrects the resulting difference. As mentioned above, the lamp power can be controlled by varying the operating frequency. The lamp power decreases when the supplied frequency increases, as shown in figure 3.20. The proper frequency must be generated to ensure that the connected lamp is not overdriven. The current regulation method is used to control the lamp power at its rating [20]. The DC voltage (V_{dc}), the inverter current (I_{inv}) and the inverter output power (P_{inv}) are related as:

$$P_{inv} = V_{dc} . I_{inv} \tag{3.13}$$

For a constant DC voltage:

$$P_{inv} \ \alpha \ I_{inv} \tag{3.14}$$

Thus:

$$P_{inv} = P_{lamp} + P_{loss} \tag{3.15}$$

where P_{loss} is the system loss and constant related to P_{lamp}. The power relationship is found as:

$$P_{inv} \ \alpha \ P_{lamp} \ \alpha \ I_{inv} \tag{3.16}$$

The average voltage of the R_{inv} in figure 3.11 represents the current through the half-bridge driver. By adjusting the $V_{R_{inv}}$ voltage results in a control of the lamp power (P_{lamp}). Note that the required inverter power is about 2 W less than the lamp rating for the same lumen output of a traditional magnetic ballast, resulting from the high frequency of operation.

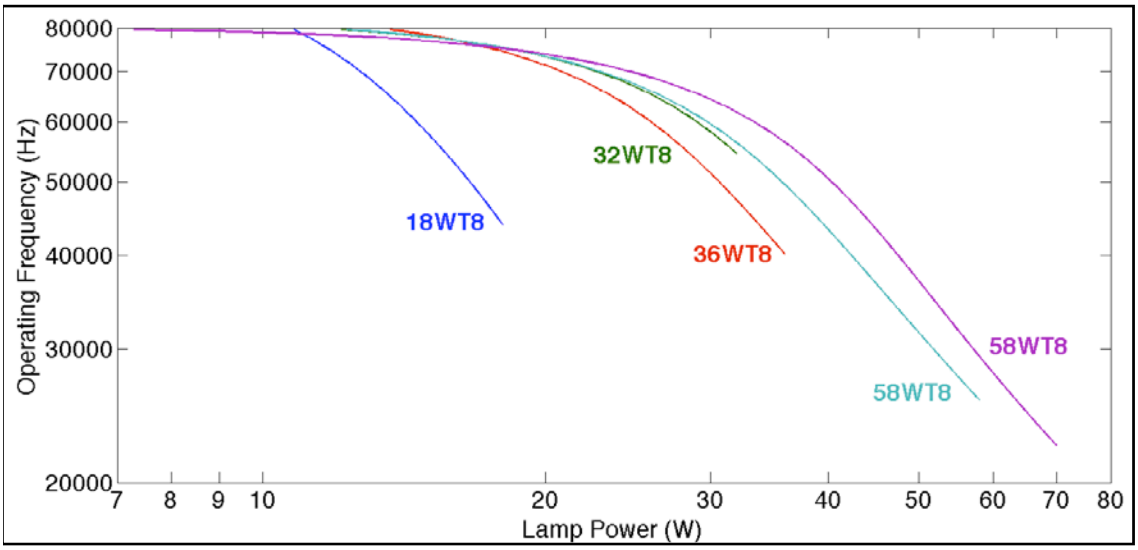

Figure 3.20 Operating frequency VS lamp power

The lamp power is regulated by varying the operating frequency. The output power is detected by using the 'I_lamp' node from figure A.4. This control loop can be as slow as 0.1 Hz since it looks smooth like an expensive dimmable lighting system. Figure 3.21 shows the block diagram of the inverter where k_d is the factor of the output loop voltage and $G_c(Z)$ is the transfer function of PI controller.

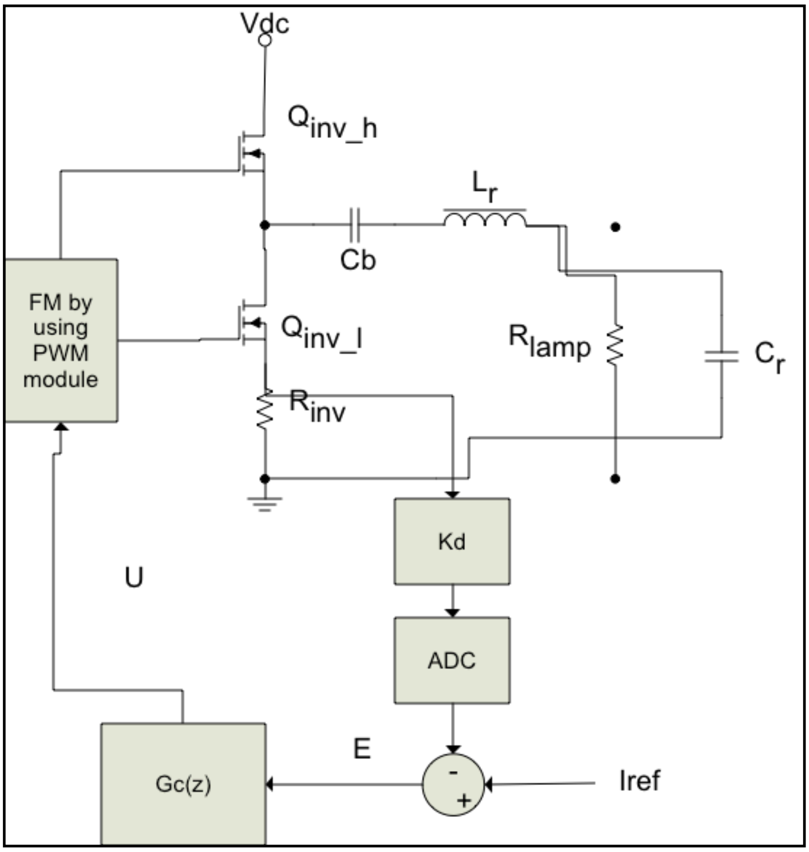

Figure 3.21 Half bridge inverter block diagram

$$k_d = \frac{1}{I_{(\max)}} = \frac{1}{0.2} = 5 \tag{3.17}$$

The transfer function of PI controller ($G_c(s)$) is:

$$k_p + \frac{k_I}{s} \tag{3.18}$$

Where k_P and k_I are gain of PI controller that is 0 and 2.

The behavior of resonant inverter is nonlinear and complex. In addition, the lamp resistance is dynamic to its current. We can make a linear transfer function by using the local linearization technique. Since the ballast is operated at a higher frequency than the resonant frequency ω0, the behavior of the inverter can be modeled by the constant, $-K_{inv}$ as:

$$\frac{\Delta P}{\Delta \omega} = \frac{P_r(\omega_1) - P_r(\omega_0)}{\omega_1 - \omega_0} = -K_{inv} \tag{3.19}$$

The local linear lamp power is given by:

$$P_r = -K_{inv}\omega + P_0 \tag{3.20}$$

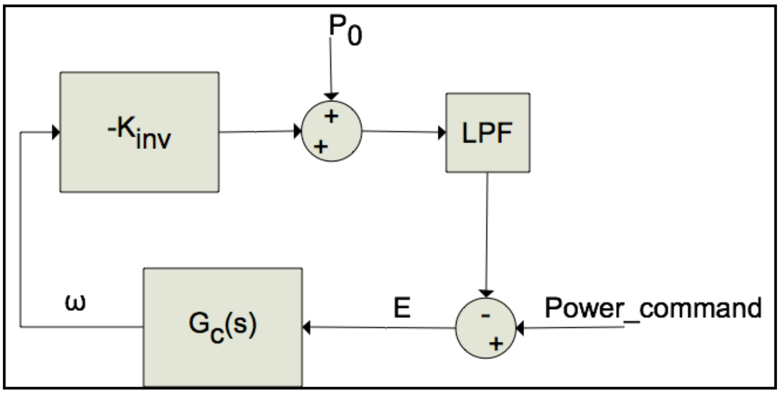

Figure 3.22 The block diagram of electronic ballast

Since the lamp resistance varies under real operation and the assumption of fixed lamp resistance may not be valid. To calculate K_{inv}, the lamp dynamic model and simplified version of inverter are used. Figure 3.22 shows the class D resonant inverter which is one of the most commonly used electronic ballast circuits. The input voltage of the resonant network is either switched to zero or V_{dc} by two half-bridge transistors. The effective input waveform is a square-wave with voltages between 0V and V_{dc}. The dc blocking capacitor, C_b, is large and can be approximated by a short circuit at high ballast's operating frequency.

At running state, the lamp acts like a negative differential resistor with its voltage and current waveforms in phase. The resonant inductor, L_r, and capacitor, C_r form a low-pass filter with the fluorescent lamp as a resistive load, R_{lamp}. In typical ballast designs, the circuit operates around the natural resonant frequency with the resonant network Q_L greater than 1/2. Under these conditions, square-wave harmonics are attenuated at 40 dB/decade. This accounts for less than 4 % of the total lamp power [35]. Since the higher-order harmonics only account for a small percentage of the input signal, the voltage and current waveforms appearing at the lamp can be assumed to be sinusoidal.

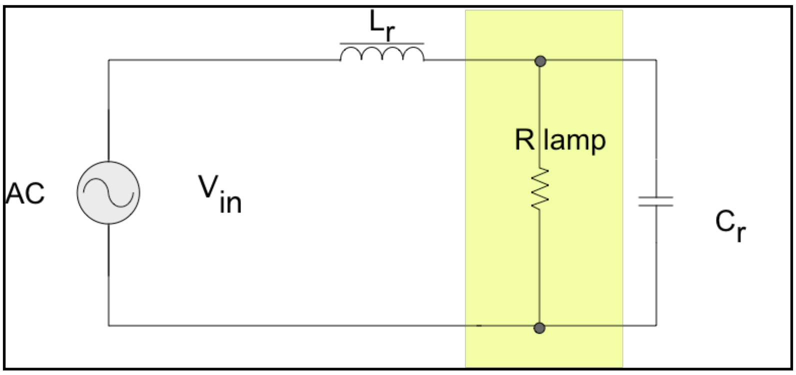

Figure 3.23 The simplified version of electronic ballast

The simplify version of inverter [24] as shown in figure 3.23 is used in simulation study. By using fundamental component of square wave output, the lamp power can be calculated as:

$$V_{lamp} = \frac{-jR_{lamp}V_{in}}{j\omega^2 C_r L_r R_{lamp} + \omega L_{lamp} - jR_{lamp}} \tag{3.21}$$

$$P_{lamp} = \mathrm{Re}\left[\frac{V_{lamp}^2}{R_{lamp}}\right] \tag{3.22}$$

Where: $L_r = 2.2mH, C_r = 4.7nF$ and V_{in} is fundamental component of square wave.

$$V_{in} = \frac{\sqrt{2}}{\pi}V_{dc} \tag{3.23}$$

From [27] the negative differential resistance of fluorescent is simplified as:

$$R_{lamp} = \frac{V_0 R_S}{V_0 - V_H} \tag{3.24}$$

where V_0 is the voltage at present condition and R_S and V_H are defined as:

$$R_S = \frac{V_{Max} - V_{min}}{I_{Max} - I_{min}} \tag{3.25}$$

$$V_H = V_{min} - I_{min}R_S \tag{3.26}$$

where V_{Max} is lamp voltage at the highest power; V_{min} is the lamp voltage at the lowest power; I_{Max} is the lamp current at the highest power and I_{min} is the lamp current at the lowest power. The R_S and V_H of the T8 fluorescent lamps series are illustrated in table 3.3.

Table 3.3 R_S and V_H of the T8 fluorescent lamps series

P.Rating	R_S	V_H
18W	-61.60	73.69
32W	-56.00	131.07
36W	-50.63	116.97
58W	-29.09	127.54
70W	-24.53	141.65

From (3.19), the calculated K_{inv} for T8 lamp series are shown in table 3.4.

Table 3.4 K_{inv} and P_0 of the T8 fluorescent lamps series

P.Rating	**K_{inv}**	**P_0**
18W	4.468×10^{-04}	123.273
32W	3.207×10^{-04}	102.100
36W	1.159×10^{-04}	60.966
58W	8.737×10^{-05}	57.801
70W	4.311×10^{-05}	28.361

From figure A.4, the transfer function of LPF of the current sensing circuit is:

$$LPF = \frac{1}{1+R_{37}C_{25}s} = \frac{1}{1+(10k)(470n)s} = \frac{1}{1+0.0047s} \qquad (3.27)$$

To achieve stable operation, the system bandwidth f_{BW} must be selected to a value lower than the crossover frequency of the low-pass filter (LPF) circuit.
By setting the desired crossover frequency to a half of the LPF crossover frequency at 17 Hz, the k_p and k_i are obtained as 0 and 76.6, respectively.

$$G_C(s) = \frac{76.6}{s} \qquad (3.28)$$

The transfer function of the control loop (sys=$G_c(s)$* K_{INV}*LPF) with 18W lamp is presented as:

$$sys = \frac{17.24}{0.0047s^2 + s + 3.449} \qquad (3.29)$$

The bode diagram is shown in figure 3.24. The phase margin is 97 degrees and bandwidth is 17 Hz. This converter seems to be stable since phase margin is above 45 degrees.

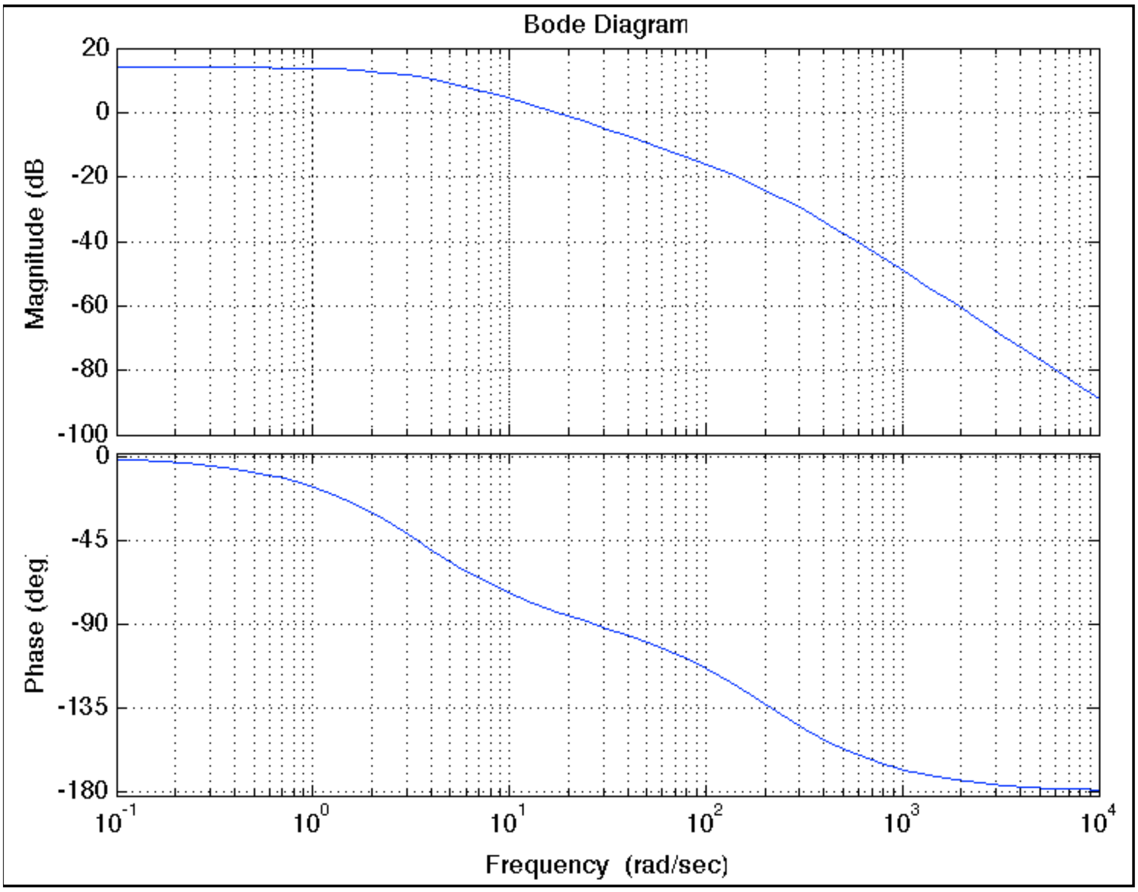

Figure 3.24 Bode diagram of control loop of electronic ballast operating with 18W lamp

3.5 Lamp Detection Procedure

The fluorescent lamp is manufacturing with precise discharge resistance characteristic. Therefore, the magnetic ballast with fixed inductance value is adequate to regulate the lamp current at rating power. A small change in lamp resistance because of the manufacturing process will lead to variation of the lamp running power. Similar to the magnetic ballast, the electronic ballast with fixed frequency method needs a consistent lamp characteristic. According to this phenomenon, the lamp resistance characteristic is unique and it reflects the lamp rating.

There are many methods to detect the lamp resistance such as detecting the voltage and current. However, the lamp resistance dynamically relates to the lamp power as shown in figure 3.23, the nonsystematic resistance detection will lead to inconsistent lamp detection results. Moreover, this characteristic must be measured when the lamp is in discharge mode or running state. The wrong running frequency will damage the lamp resulting from the over current since the proper operating frequency is not known apriori.

In this thesis, the lamp rating detection procedure is composed of multi-step lamp power regulation and the trapezoidal possibility weight decision based on the lamp operating frequency. After ignition, the multi-step lamp power regulation is started with the lowest power command. For example, the 16 W power command is used for the T8 series lamps. In the power control loop, the operating frequency is determined and recorded in the controller. This frequency is used to classify the 18 W (lowest) from the group. If the measured frequency is within the valid range, then no further decision is necessary and the controller continues to the running state. However, because of the variation between lamp manufacturers, bulb age, and temperature, the running frequency is not necessarily constant. We experimentally verified that the operating frequency varies during our lamp power regulation experiment.

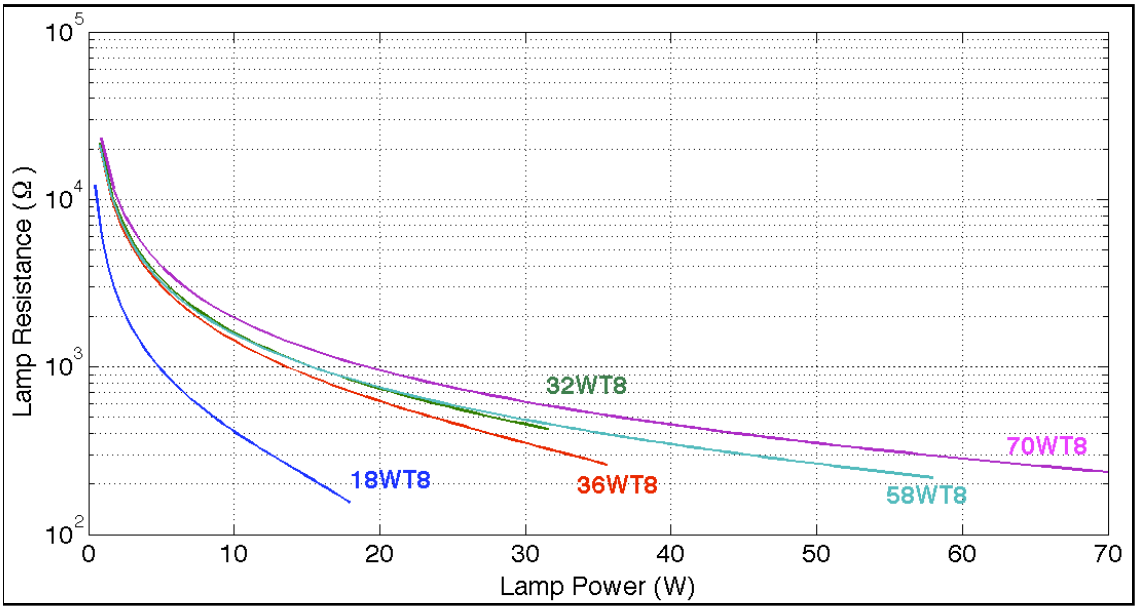

Figure 3.25 Lamp resistance VS Lamp power

A number of T8 lamps, 16 W, 30 W, 34 W, 56 W and 68 W are chosen as samples to acquire the running frequencies. These frequencies are used to define the possibility weight function.

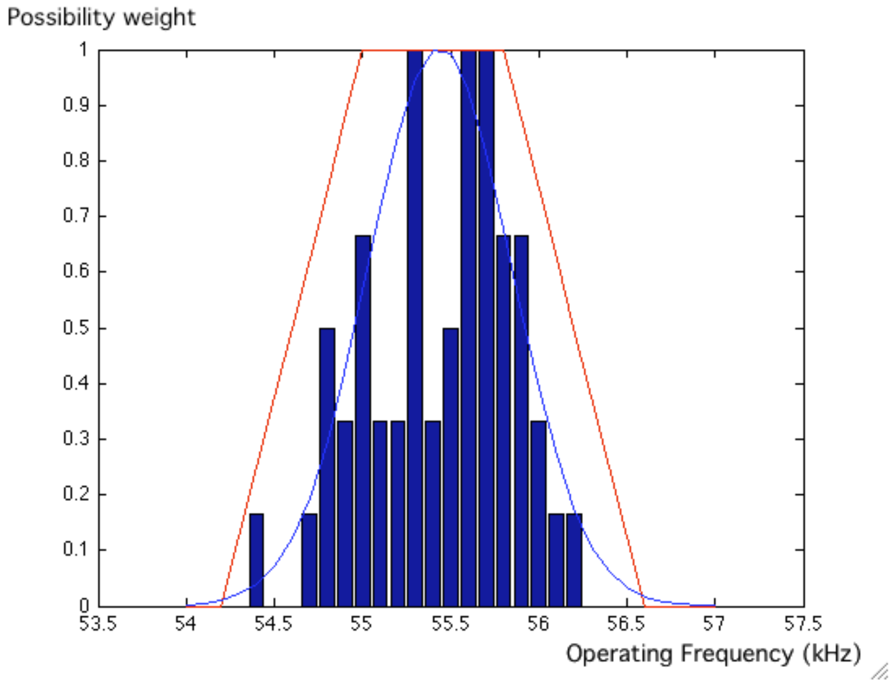

Figure 3.26 The normalized histogram of 32 W lamp running at 30 W, the normal distribution function and the trapezoidal possibility weight (W_P) that simplifies the distribution function

Figure 3.24 shows the normalized histogram of 32 W lamp running at 30 W. Assuming that the distribution is a normal distribution, the distribution function is [38]:

$$f(x) = \frac{1}{\sqrt{2\pi\sigma^2}} e^{-\frac{(x-\mu)^2}{2\sigma^2}} \tag{3.30}$$

where $\bar{x}$ as an approximation of μ and sd as an approximation of σ .

$$\bar{x} = \frac{1}{n}\sum_{i=1}^{n} x_i , sd = \sqrt{\frac{1}{n}\sum_{i=1}^{n}(x_i - \bar{x})^2} \tag{3.31}$$

Where n=number of samples, x_i = frequency of sample i.

An approximation of the normal distribution is shown in figure 3.25. To simplify this normal distribution function to the trapezoidal function, the trapezoidal possibility weight function is approximately drawn to cover the whole histogram and share the same slope as the most of normal distribution function as shown in figure 3.25. This trapezoidal possibility weight function is:

$$W_P = \begin{cases} 1 & ;\bar{x} - 0.5sd, x, \bar{x} + 0.5sd \\ \dfrac{1}{sd}x - \dfrac{\bar{x} - 1.5sd}{sd} & ;\bar{x} - 1.5sd, x, \bar{x} - 0.5sd \\ \dfrac{-1}{sd}x + \dfrac{\bar{x} + 1.5sd}{sd} & ;\bar{x} + 0.5sd, x, \bar{x} + 1.5sd \end{cases} \tag{3.32}$$

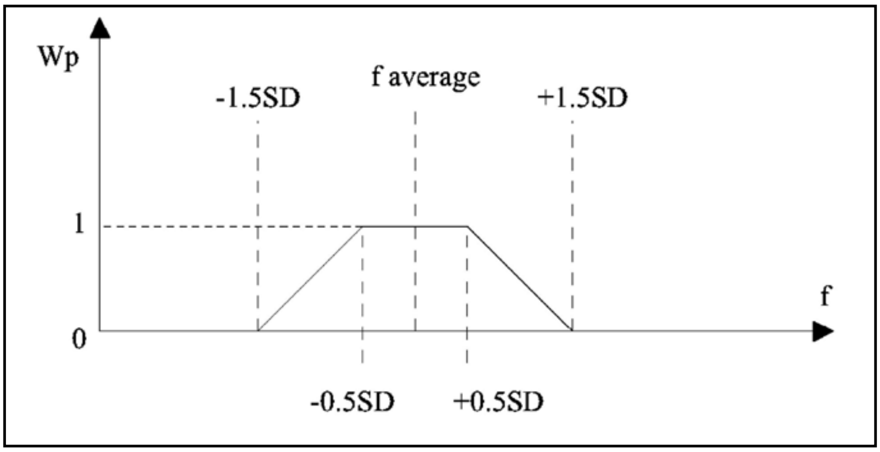

Figure 3.27 Trapezoidal possibility weight (W_P) VS running frequency

From figure 3.16, the shape of trapezoid can be adapted by changing the multiplier ($\pm 0.5\,and \pm 1.5$). The $\pm 1.5sd$ is chosen because this trapezoid should at least cover all members (i.e. lamp operating frequency). Widen this area will not improve the result since there is no operating frequency out there. The variation of the top width can be changed from $\pm 1.5sd$ (that is the rectangular shape) to 0 (that is the shape of triangle). If there is no overlapped regions of the operating frequency, the top width will not affect the decision result. In the case that there is an overlapped frequency range, the crossover frequency should be set to the middle value. From the experiment, the only overlapped region occurs with the 32W and 58W lamps operating at 16 W power level. This is not side overlapped but they share the same frequency range. Thus, the decision will not be affected by the shape of the trapezoid.

The relation between the probability weight and the running frequency is illustrated in figure 3.25. For example, if the average operating frequency of a 36 W lamp running at 16 W is 75.88 kHz, and its standard deviation is 36 Hz, then $W_{P(36Wat16W)}$ is

$$W_{P(36at16)} = \begin{cases} 1 & ;48.69kHz, f, 50.39kHz \\ 0.588f - 46.99 & ;46.99Hz, f, 48.69kHz \\ 0.588f + 50.39 & ;50.39kHz, f, 52.09kHz \end{cases} \tag{3.33}$$

where f = measured lamp operating frequency (kHz).

Table 3.5 and 3.6 provide the average value and standard deviation of running frequencies at 16 to 68 W of power regulation. A dash (-) symbol is a prohibited power command.

Table 3.5 Average running frequency of ballast at various lamp power ratings

Average of operating frequency at power command	16 W (kHz)	30 W (kHz)	34 W (kHz)	56 W (kHz)	68 W (kHz)
T8-18	49.59	-	-	-	-
T8-32	76.26	55.44	-	-	-
T8-36	75.88	48.25	40.59	-	-
T8-58	76.26	57.16	50.09	25.21	-
T8-70	75.79	62.49	56.82	28.73	21.75

Table 3.6 Standard deviation of running frequency of ballast at various lamp power ratings

S.D. of operating frequency at power command	16 W (kHz)	30 W (kHz)	34 W (kHz)	56 W (kHz)	68 W (kHz)
T8-18	1.7	-	-	-	-
T8-32	0.004	0.816	-	-	-
T8-36	0.036	1.022	1.210	-	-
T8-58	0.002	0.288	0.444	0.476	-
T8-70	0.010	0.160	0.234	0.360	0.270

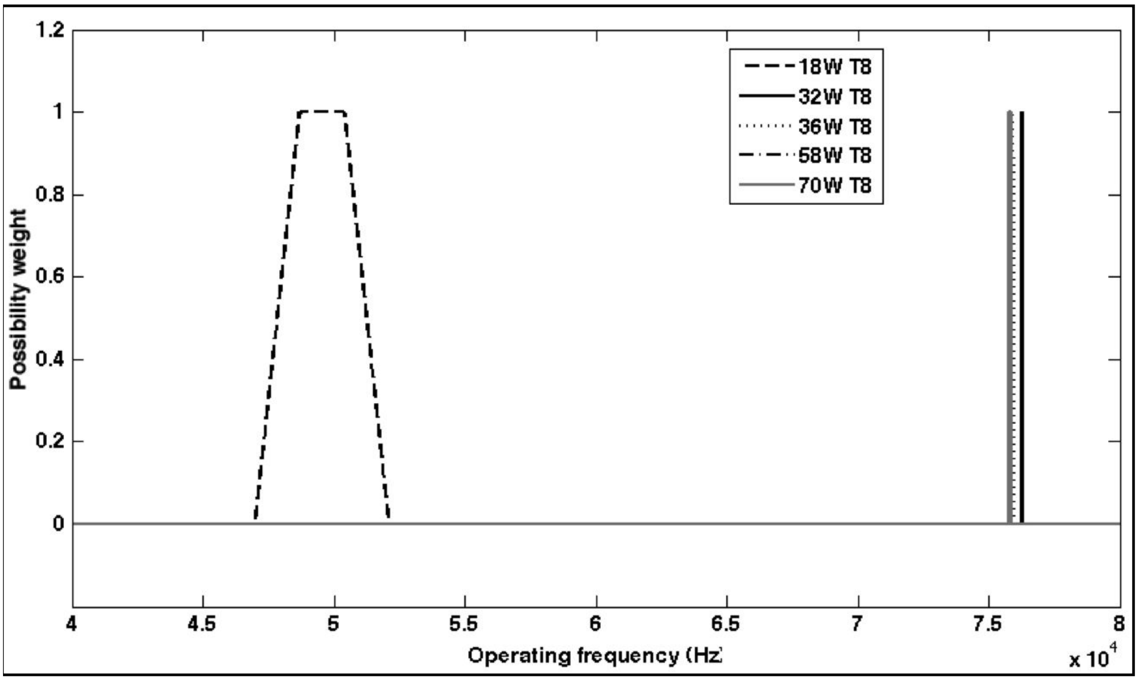

Figure 3.28 Possibility weight (W_P) VS operating frequency of T8 lamps at 16 W power regulation

Figure 3.27 and 3.28 shows the possibility weight and operating frequency of T8 series lamps at 16 W power regulation. The operating frequency of 18 W lamp is significantly far from others resulting in high accuracy of 18 W lamp detection. However, the possibility weight of 58 W lamp is overlapped with the 32 W lamp causing inaccuracy in detection at this state. When the 30 W power regulation is applied with the 32 W, 36 W, 58 W and 70 W T8 lamps, there is no overlapping in the possibility weight of T8 lamps as shown in figure 3.29 and 3.30 where the 32 W lamp can be accurately detected.

From the reason above, both the multi-step lamp power regulation and possibility weight decision are applied together and the lamp rating detection algorithm can be described as follows:

Step 1: Regulate the output power at the lowest power command such as 16 W for the T8 series.

Step 2: Calculate the probability weight for all lamp ratings. If the highest W_P is obtained at the lamp rating that equals the power command, the lamp rating equals the power regulated, then go to step 4.

Step 3: If the delivered power is still below the lamp rating, step up to the next power command (30, 34, 56 and 68 W) and repeat step 1 and 2 again until the power command reaches the highest value of the series then go to step 4.

Step 4: Summarize the total W_P of each lamp rating for each power regulation. The lamp rating is determined from the total highest W_P .

The Block diagram and the flowchart of this detection algorithm are illustrated in figure 3.32 and 3.33.

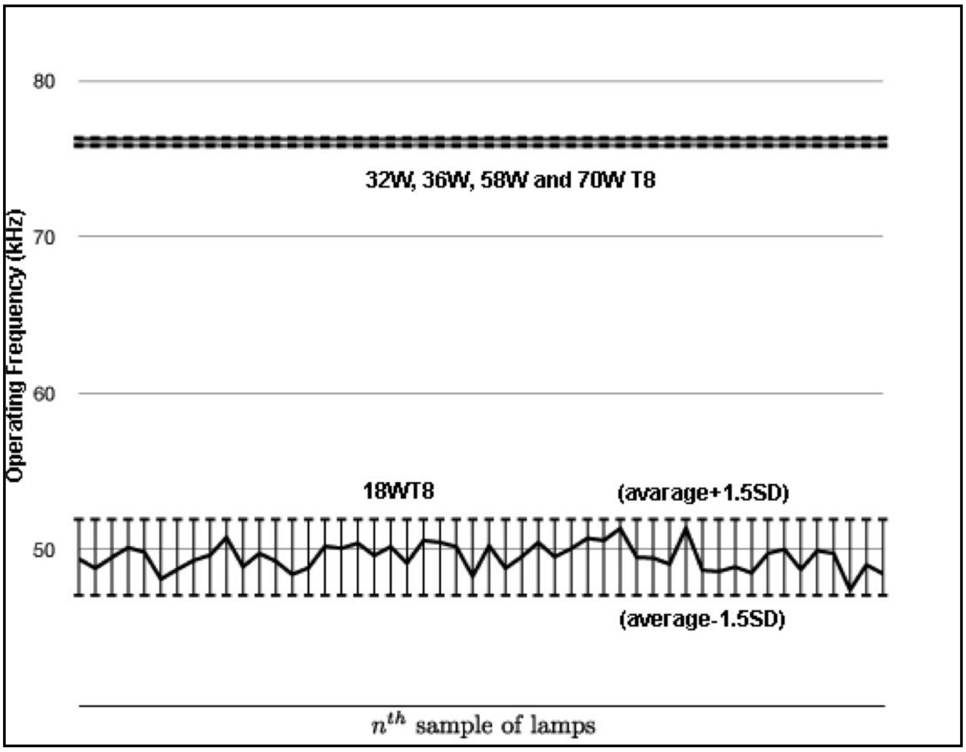

Figure 3.29 Operating frequency at 16 W power regulation of n^{th} lamp sample in the possibility weight region

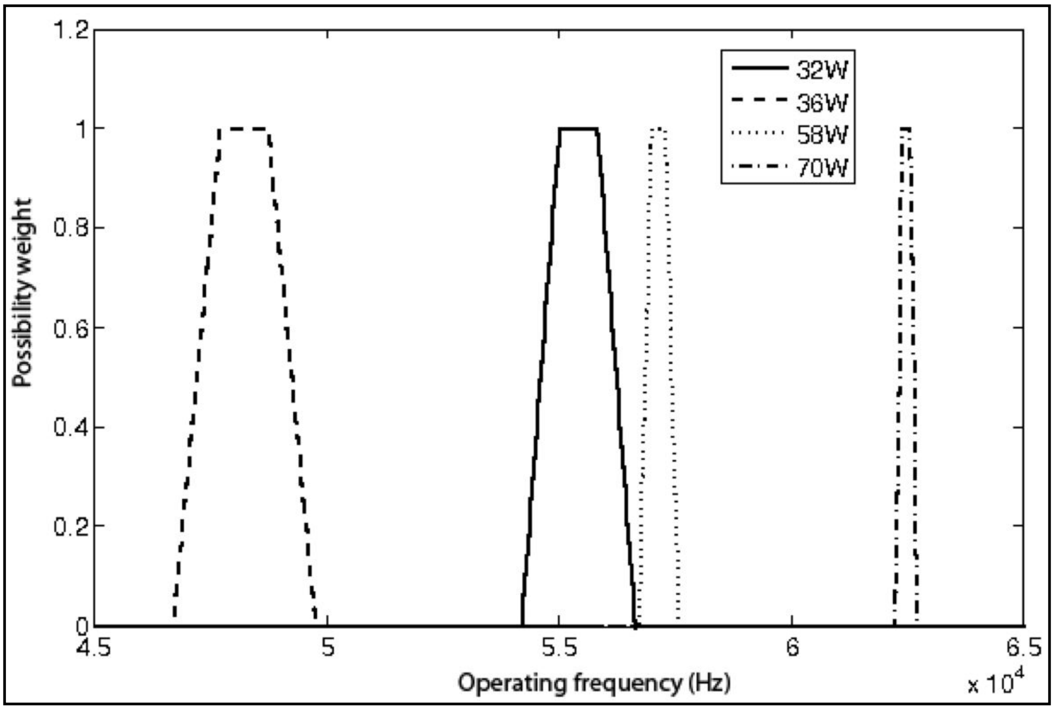

Figure 3.30 Possibility weight (W_P) VS operating frequency of T8 lamps at 30 W power regulation

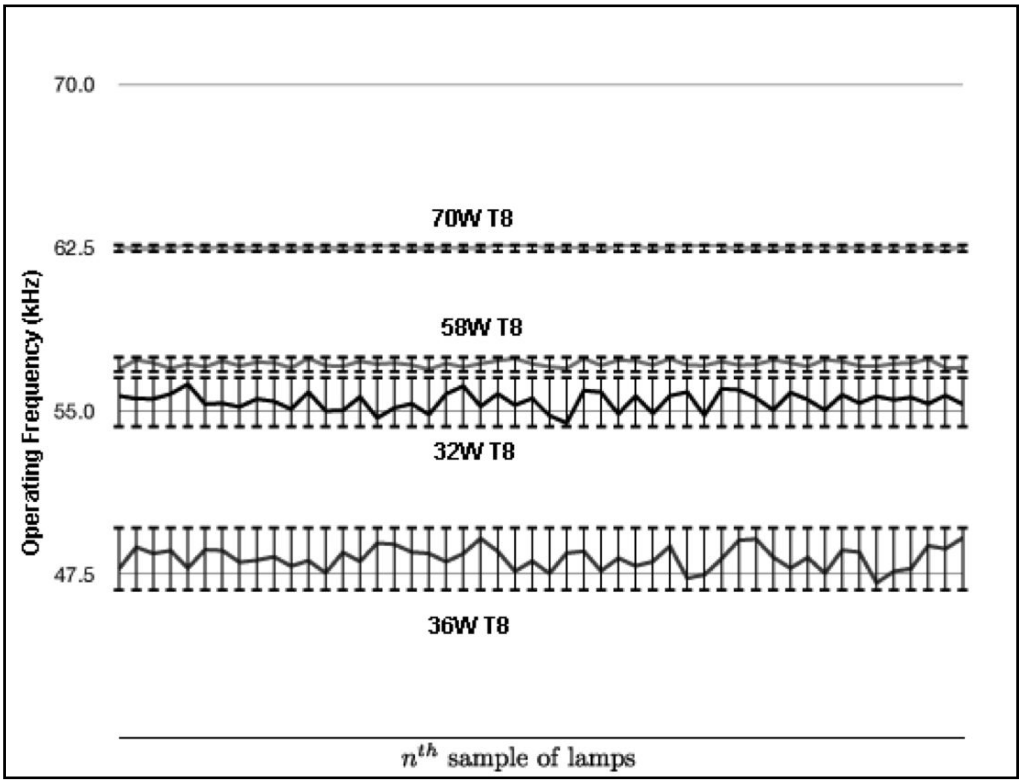

Figure 3.31 Operating frequency at 30 W power regulation of n^{th} lamp sample in the possibility weight region

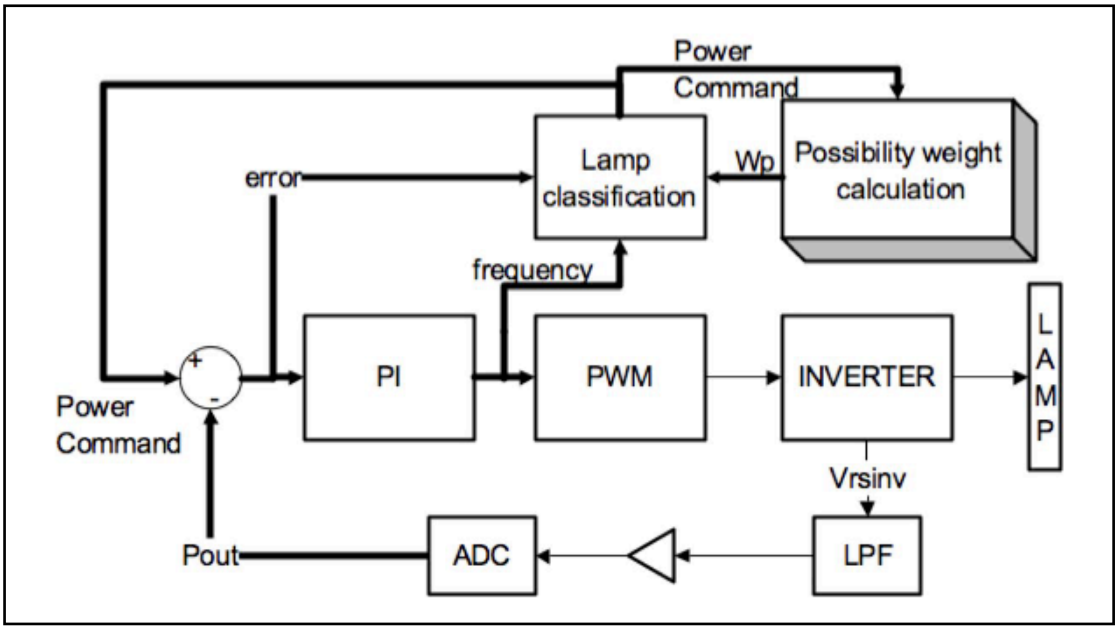

Figure 3.32 Block diagram of the lamp rating detection algorithm

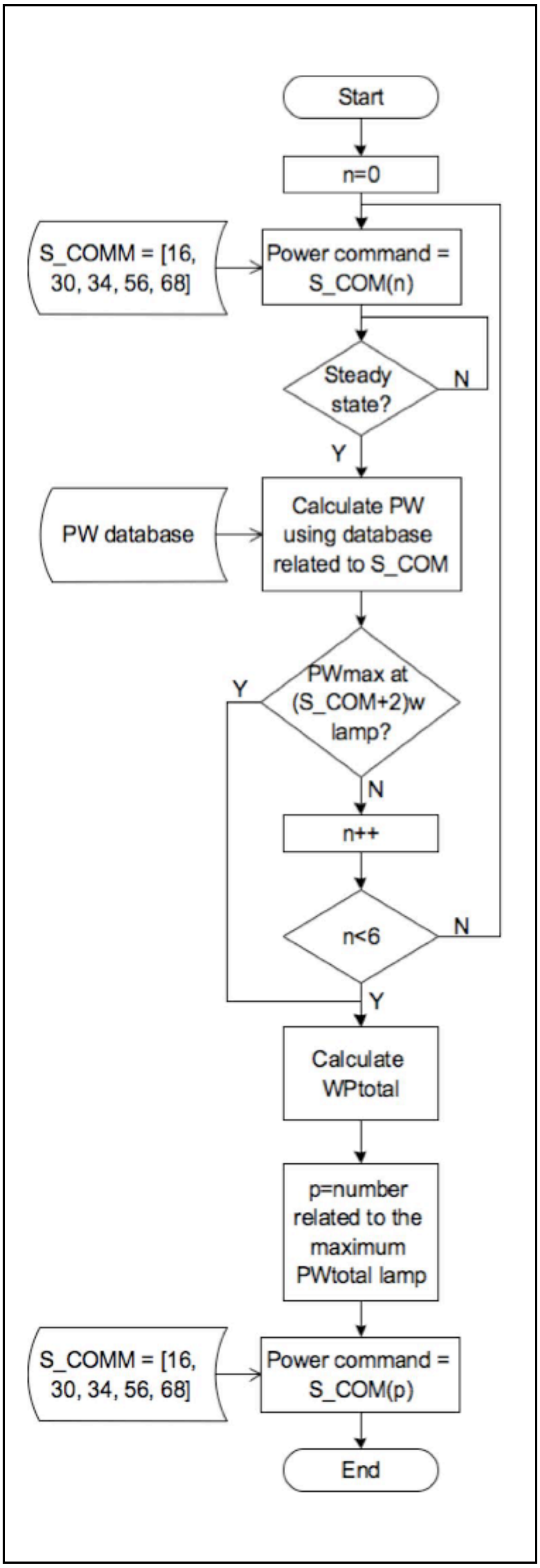

Figure 3.33 Flowchart of the lamp rating detection algorithm

The block diagram in figure 3.30 and the flowchart in figure 3.31 can be described as follows. The process starts with lamp power rating number (n) equal to 0. This number varies from 0 to 6 representing the lamp power regulation state from 18W to 70W. The S_COMM is the array of power_command that contains 16, 30, 34, 56 and 68 values. This power_command is used by the power control procedure. With n=0 the power_command is 16. The procedure waiting for the steady state flag from the power control procedure to be set. Then the operating frequency is used to calculate the possibility weight (PW: W_P) from the predefined formula in (3.31). After calculating all PW (PW of 18W lamp operating at 16W to PW of 70W lamp operating at 16W), the software then finds the maximum PW. If the maximum PW is PW of S_COMM(n)+2 lamp operating at S_COMM(n), the software will skip the next power_command and calculate the PWtotal. For example:

if n is 0, the software will check that is there the maximum PW is PW of S_COMM(0)+2=18W lamp operating at S_COMM(0))=16W.

If this condition return NO, the n variable will be increased and the software will jump back to the start. After n=6, the PWtotal are calculated. The maximum PWtotal indicates the lamp rating. Finally, the power_command is updated by the S_COMM that relates to the maximum PWtotal.

The Power control procedure uses the power_command as a set point. By comparing an ADC input with the power_command, if ADC input is higher than power_command, the software will increase the output frequency by 1 step. If ADC input is lower than power_command, the software will decrease the output frequency by 1 step. The steady state flag will set if the ADC and power_command is equal. This procedure is located in the 1 ms timer interrupt service routine.

An example of the possibility weight and decision result is shown in chapter 4. The operating frequency of the tested lamp is measured and used to calculate the possibility weight. After that, this possibility weight is used to determine the lamp rating. Starting at the 16 W power command, the running frequency is 76.26 kHz and all W_P at 16 W is calculated. It results in 0 possibility of this lamp to be 18WT8 ($WP_{18Wat16W}$), 36WT8 ($WP_{36Wat16W}$) and 70WT8 ($WP_{70Wat16W}$). It results 1 for both possibilities of this lamp being 32WT8 ($WP_{32Wat16W}$) or 58WT8 ($WP_{58Wat16W}$). The highest W_P is not at $WP_{18Wat16W}$. Thus, the software goes to the next 30 W power command. Then W_P at 30 W is calculated. The algorithm stops at 30 W power command according to the maximum on $WP_{32Wat30W}$ (0.2 out of 0). The summation of WP_{32W} is 1.2, which is the maximum, and the lamp is detected as a 32 W rated lamp at total possibility of 1.2. These results are shown in table 3.7.

Table 3.7 An experimental result of W_P for the 32 W T8 lamp using manual mode

Power Command / Lamp Rating	16 W	30 W	34 W	56 W	68 W	Total
18WT8	0	-	-	-	-	0
32WT8	1	0.2	-	-	-	1.2
36WT8	0	0	-	-	-	0
58WT8	1	0	-	-	-	1
70WT8	0	0	-	-	-	0

3.6 Preheating Condition

Although the multi-rating ballast has an advantage on that it can operate more than one lamp power rating, the preheat condition should be seriously considered. According to the literature [19], the filaments must be operated at temperatures between $700°C$ and $1000°C$, to avoid a premature wear of the emissive coating, reducing the average life of the lamp.

Since it is difficult to measure this temperature, there are recommendations and standards regarding correlate parameters, such as the voltage over the filaments or their equivalent electrical resistances [19], [20]. The ANSI C82.11-1993 [22] standard indicates that the proper filaments temperature should increase their resistance to 4.25 to 6.25 times of their resistance at room temperature ($R_{hc} = \frac{R_h}{R_c}$). These filaments temperature can be increased by applying the electrical current. The resistance ratio was derived by [19] as follows:

$$R_{hc}\left(i_{ph(rms)},t\right) = 1 + r_1\left(e^{\left(\frac{i_{ph(rms)}}{r_2}\right)} - 1\right)t \tag{3.34}$$

where $R_{hc}\left(i_{ph(rms)},t\right)$ is the resistance ratio between hot (R_h) and cold (R_c) filaments.

$i_{ph(rms)}$ is the filament current (A) during preheating.

t is the preheating time (s).

r_1 is the constant value depending on the lamp series and manufacturer. For T8, $r_1 = 0.112\, s^{-1}$.

r_2 is the constant value depending on the lamp series and manufacturer. For T8, $r_2 = 0.155\, A$.

According to [19], the suitable preheating time is between 0.5 and 1.5 second. Thus, the suitable preheating area can be illustrated as shown in figure 3.32. By substituting the R_{hc} and t with $(R_{hc},t)=(4.25,1.5s)$ and $(6.25,0.5s)$. This results in 467 mA minimum preheating current and 705.5mA maximum preheating current.

Considering 1 second preheating time, as used for the prototype in this paper, the preheating current are:

$$i_{ph(rms)} = 0.155\ln\left(\frac{R_{hc}\left(i_{ph(rms)},1s\right)-1}{0.112\times 1}+1\right) \tag{3.35}$$

The minimum and maximum preheat currents are 527.3 mA and 599.6 mA where $R_{hc}\left(i_{ph(rms)},1s\right)$ is 4.25 and 6.25

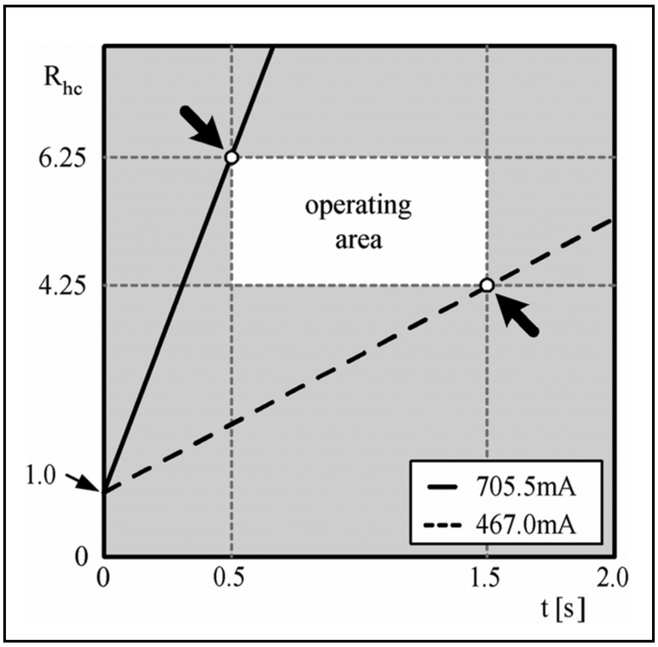

Figure 3.34 Acceptable variation of resistance ratio (R_{hc}), considering the operating area defined for the preheating process [19]

Using the constant current method may overheat the filament when the lamp is turned on immediately after turning off. This muti-rating ballast controls its power by adjusting the frequency (assume that the DC supply voltage is constant). This process using the same method as in the running state as shown in figure 3.33. Only one constant that the frequency cannot be decreased if the lamp peak voltage (V_{pk}) is higher or equal to the threshold to prevent the lamp from striking immaturely. The maximum allowable preheat voltages for the T8 series are as follows: (18W:250V, 32W:300V, 36W:300V, 58W:350V and 70W:400V)[15].

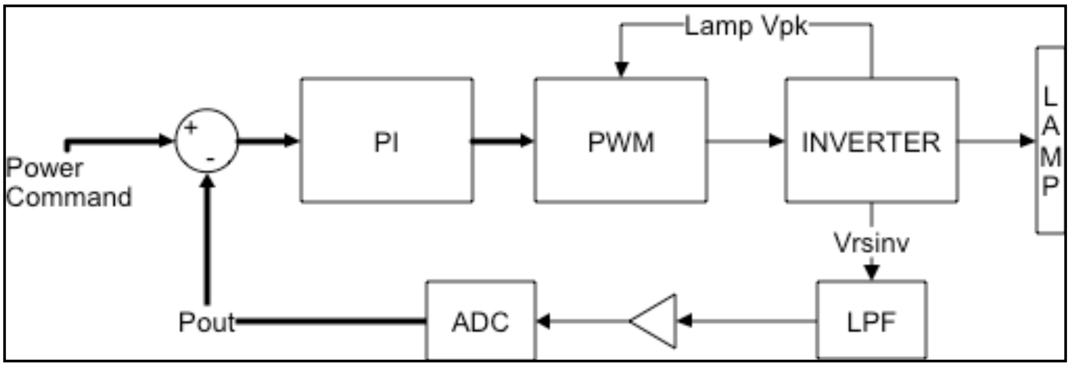

Figure 3.35 The block diagram of the preheat controller

According to the power control method, the proper power command is needed. From (3.33), the preheat energy (E) is calculated by:

$$E = \int I^2 R dt = \int_{t=0}^{T} i_{ph(rms)}^2 (1 + r_1 \left(e^{\left(\frac{i_{ph(rms)}}{r_2}\right)} - 1 \right) t) R_C dt$$

$$= \int_{t=0}^{T} i_{ph(rms)}^2 R_C + i_{ph(rms)}^2 r_1 \left(e^{\left(\frac{i_{ph(rms)}}{r_2}\right)} - 1 \right) t) R_C dt$$

$$= i_{ph(rms)}^2 R_C t + \frac{1}{2} i_{ph(rms)}^2 R_C r_1 \left(e^{\left(\frac{i_{ph(rms)}}{r_2}\right)} - 1 \right) t^2 \Bigg|_{t=0}^{T}$$

$$= i_{ph(rms)}^2 R_C T + \frac{1}{2} i_{ph(rms)}^2 R_C r_1 \left(e^{\left(\frac{i_{ph(rms)}}{r_2}\right)} - 1 \right) T^2 \qquad (3.36)$$

where R_c is the filament resistance at room temperature. From measurement, the resistance values are 2.5 ohm for 18, 32 and 36 W and 2.0 ohm for 58 W and 70 W. T is the preheat time which is 1 second. Substituting the 1 second preheat current results in the preheat energy varied from 1.311 J to 3.94 J for 2.5 ohm filaments and 1.049 J to 3.152 J for 2 ohm filaments. The possible preheat energy for both filament resistance values is varied from 1.311 J to 3.152 J. As a result, the power command of 2.3 W is chosen to supply the 2.3 W preheat energy for 1 second.

3.6.1 Numerical Calculation

According to the maximum allowable preheat voltage limitation, there are 2 steps in preheating the lamp. Initially because the filament resistance is low, the current is controlled at the maximum value. From (2.14), the maximum preheat current is 0.56 A at 250 V. As the filament resistance increases, the applied power at the filament will be increased. In the second step, the power at filament is controlled at allowable maximum for overheat protection. The power at the filament can be calculated as:

$$P_{ph} = I_{ph}^2 .R_h(t)$$

or $$I_{ph} = \sqrt{\frac{P_{ph}}{R_h(t)}} \tag{3.37}$$

Since the power control method is used, the reference power (P_{ph}) must be calculated. The preheat current can be divided into two conditions. Because the lamp voltage is limited, the filament current is also limited. Therefore, the power is lower than the command value. The second condition is that the filament resistance is high enough to make the preheat current below the limited current while power is controlled. By limiting peak lamp preheat voltage (V_{ph}) at 250 V, to ensure that the lamp will not strike in this state, the preheat current cannot be higher than 0.56 A. The preheat current can be calculated by using (2.14) by substance V_{ph} with 250 V. From this current limitation, the preheat condition is divided into 2 states that are constant current and constant power. Thus, the control conditions for both steps are as follows:

1. Constant Current Control

The preheat ($i_{ph(rms)}$) is kept at 0.56 A, when $0.56^2 R_h(t)$ is less than $P_{command}$ (2.3W). Solving this condition

$$R_{hc(R_c=2.5\Omega)}(t) < 2.93$$

and $$R_{hc(R_c=2.0\Omega)}(t) < 3.67 \tag{3.38}$$

From (3.37), the preheat current is 0.56 A when the filament resistance is below 2.93 ohm for 18, 32 and 36 W lamp and below 3.67 ohm for 58 and 70 W lamp.

2. Constant Power Control

The power command is 2.3W when $0.56^2 R_h(t)$ become larger than $P_{command}$. From (3.33), the variation of filament resistance over the time is:

$$\frac{\Delta R_h(t)}{\Delta t} = R_c r_1 \left(e^{\left(\frac{i_{ph(rms)}(t)}{r_2}\right)} - 1 \right) \tag{3.39}$$

Thus: $$\Delta R_h(t) = R_c r_1 \left(e^{\left(\frac{i_{ph(rms)}(t)}{r_2}\right)} - 1 \right) \Delta t \tag{3.40}$$

from (3.39): $$i_{ph(rms)}(t) = r_2 \ln\left(\frac{\Delta R_h(t)}{R_c r_1 \Delta t} + 1 \right) \tag{3.41}$$

$$P_{ph}(t) = i_{ph(rms)}^2(t) R_h(t) = \left(r_2 \ln\left(\frac{\Delta R_h(t)}{R_c r_1 \Delta t} + 1 \right) \right)^2 R_h(t)$$

$$= R_h(t) r_2^2 \ln^2\left(\frac{\Delta R_h(t)}{R_c r_1 \Delta t} + 1\right) \quad (3.42)$$

From (3.41), by using the numerical calculation based on iteration method yields the result of the preheat current and filament resistance as shown in figure 3.36. Initially, the lamp voltage is limited to 250 V through the frequency to avoid undesirable premature ignition. The lamp currents remain constant until the filament temperature increases. At the same time, the lamp power is continually increasing. Once the lamp filament is heated, the resistance is reduced. The power regulation is done through current reduction. Notice that it takes longer for the lower value of R_c, to reach the regulated power.

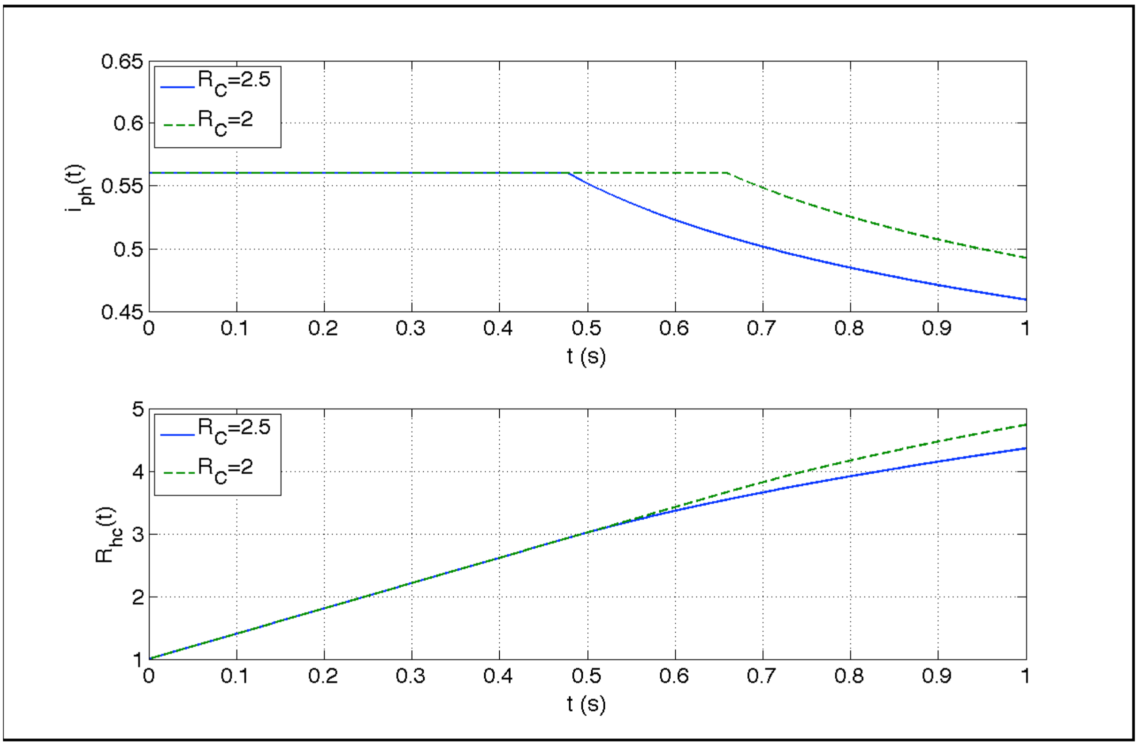

Figure 3.36 The numerical calculation results $(i_{ph}(t))$ and filament resistance ratio $(R_{hc}(t))$

Table 3.8 At 1 second preheating time, the calculated $R_{hc}(1s)$ and $i_{ph}(1s)$

	18W, 32W, 36W	58W, 70W
$R_{hc}(1s)$	4.36 ohm	4.74 ohm
$i_{ph}(1s)$	460 mA	490 mA

From table 3.8, the numerical calculation resistance ratio values are higher than 4.25 and lower than 6.25. This confirms that the $2.3W$ power command calculated by (3.35) and the $250V$ peak lamp voltage threshold can be used.

3.7 The Implementation

A hardware prototype of the electronic ballast was built. The values for the resonant inductance and capacitance match those used in the simulation. These resonant inductance and capacitance are 2.2mH and $4.7\mu F$, respectively.. The PFC boost inductance and the DC bus capacitance are 0.94 mH and $22\mu F$, respectively. The ballast circuit is divided into 3 parts, PFC boost converter, resonant inverter and control part. Figure A.1, A.3 and A.4 of appendix A show the schematic diagram of those 3 parts. The MOSFET driving circuit is implementated using ST L6382 because of the ability to drive a PFC MOSFET and 2 inverter MOSFETs. A +5V is supplied by a PI LNK302 chip as shown in figure A.2 of Appendix A.

The microcontroller controls the PFC boost converter in critical conduction mode. The lamp peak voltage (V_lamp_PK), lamp end of life (EOL), hard switching (CSI) and lamp present (Lamp_present) are used for the protection purpose. If any abnormal condition occurs, the microcontroller will shut down the ballast.

CHAPTER 4 EXPERIMENTAL RESULTS

A hardware prototype of the electronic ballast, shown in figure 4.1, was built. The ST7 microcontroller (MCU) from STMicroelectronic plays a role of main controller. It is based on a common 8-bit core with 8 MHz internal clock. Therefore, the complicate mathematic functions like multiplication or division should not be used. The values for the resonant inductance and capacitance match those used in the simulation. The Philips TLD, Super TLD and Toshiba fluorescent lamp series are used. However, the 32 W lamps are from Philip Super TLD since this type of lamp is only available by Philips Super TLD. The list of measurement device are shows in Appendix B.

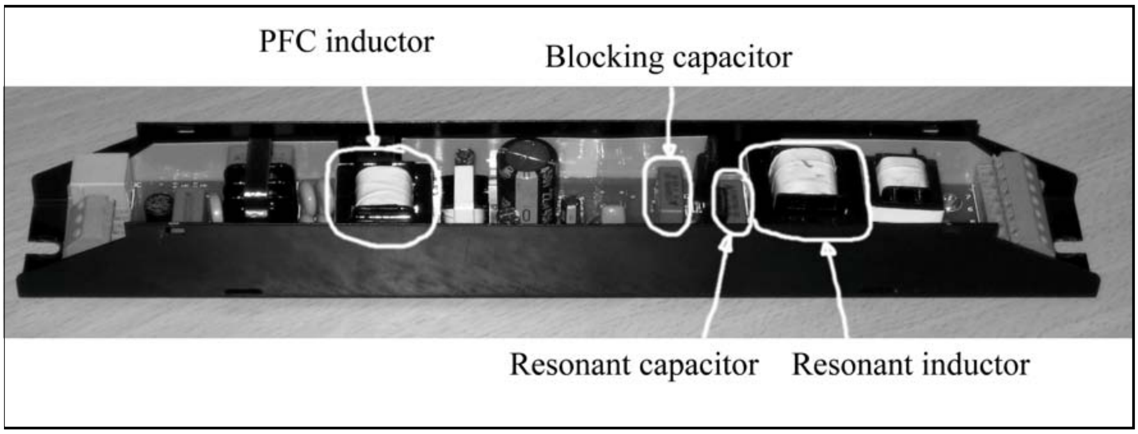

Figure 4.1 Prototype electronic ballast

4.1 The PFC Boost Converter

The input line voltage and current were captured and shown in figure 4.2. The current distortion was more than the ballast using the dedicate PFC controller IC or high performance MCU because it doesn’t have an error multiplying process due to the limitation of MCU. This is a limitation of using a low cost MCU. However, the PF is more than 0.9 and THD less than 25%.

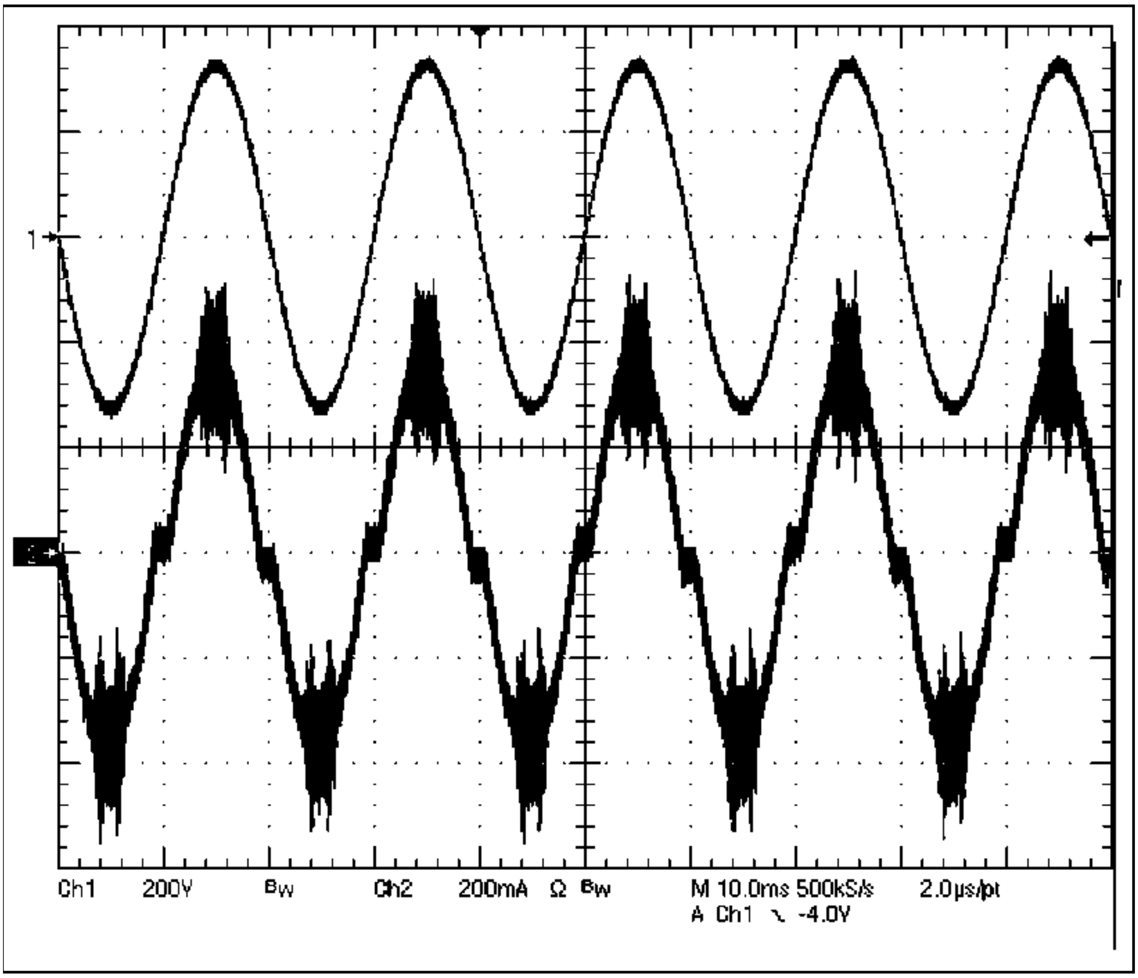

Figure 4.2 The line input voltage (1) and current (2)

Since this is multi-rating ballast, the PF and THD are measure for each lamp rating as illustrated in table 4.1. From this table, the highest lamp power yields the best value cause the configuration is calculated base on the highest one.

Table 4.1 PF and THD of ballast with 220 VAC 50 Hz line voltage

Power Rating	PF	THD
18W	0.95	20.1%
32W	0.97	17%
36W	0.97	15.8%
58W	0.98	13.7%
70W	0.99	10.5%

Figure 4.3 shows the voltage of the DC bus when the ballast is turning on. From the results, the ballast is turned on at 100 ms. At 120 ms, the boost converter is starting up.

Then the controller controls the DC bus output voltage at 400 V. With full load, the settling time is around 100 milliseconds. As the result, the 100 milliseconds delay should be added before stating up the preheat state. The Init state of the software that drives the inverter with constant 100 kHz for 100 milliseconds takes this role.

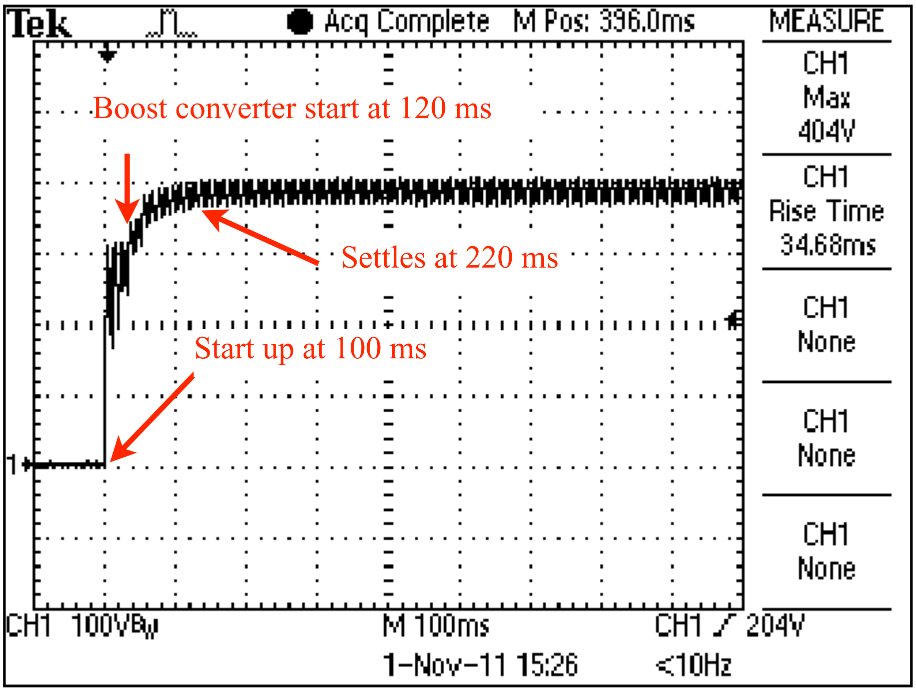

Figure 4.3 The DC bus voltage (Vdc) with 75W load

Figure 4.4 shows the response of the DC bus voltage when the load is changing from 45 W to 75 W. It shows how the boost controller handles the step load. The settling time is approximately 100 milliseconds.

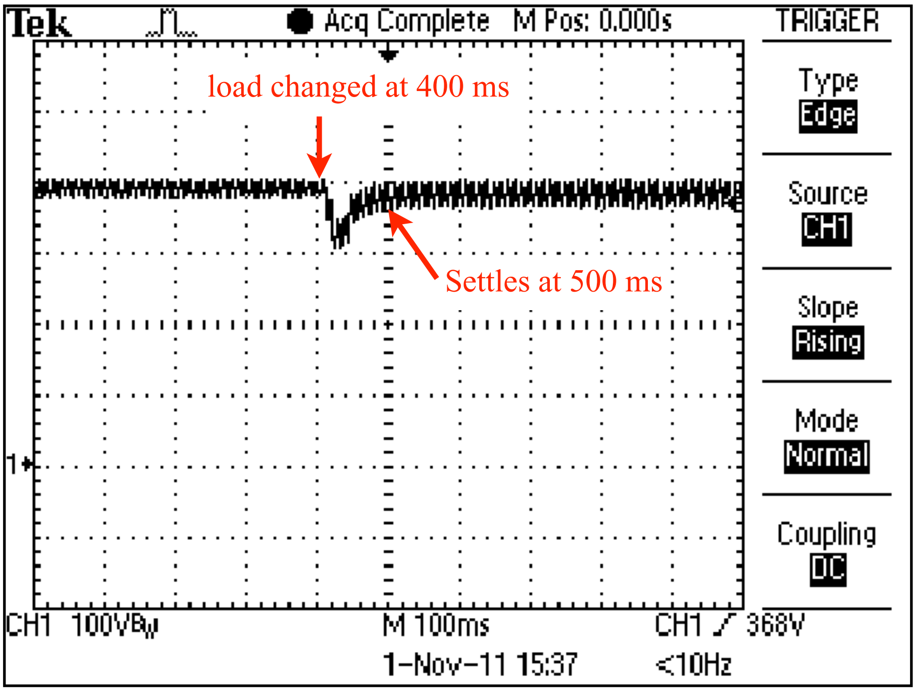

Figure 4.4 The DC bus voltage (Vdc) with step load from 45W to 75W load

Figure 4.5 shows the DC bus voltage when the 36 W lamp is starting up. The system is tuning on at 450 milliseconds. Then the ballast starting with Init state. After 100 milliseconds, the Preheat state is starting. The preheat state takes around 750 millisecond. After that, the software state moves to the Ignition state at around 1400 milliseconds. Finally, Running state start at 1450 ms. Therefore, the lamp startup process takes approximately 1 second.

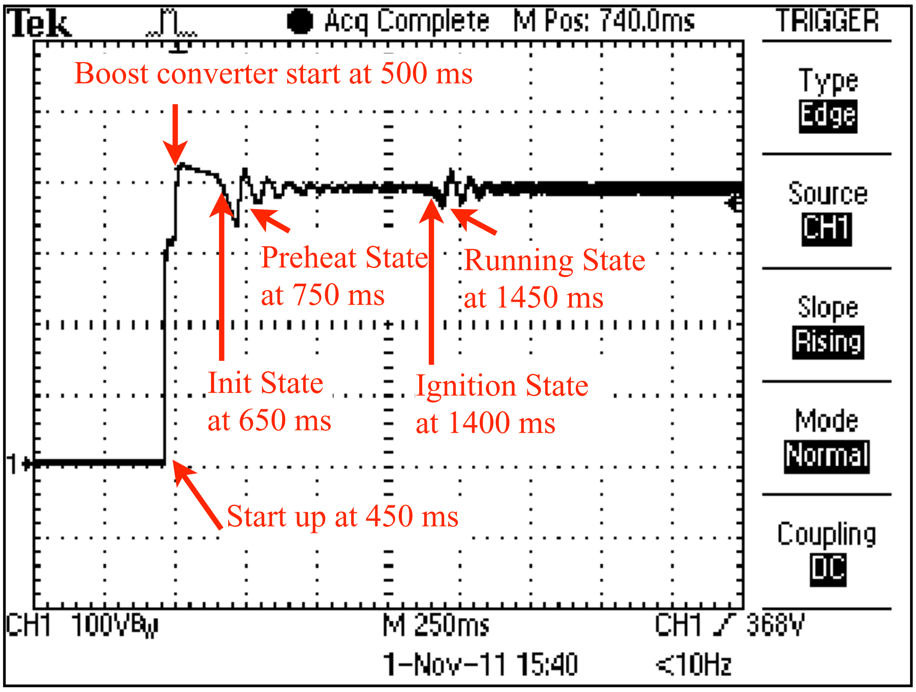

Figure 4.5 The DC bus voltage (Vdc) with 36w lamp starting

4.2 The Preheat Condition

By measuring, the preheat resistance values are divided into two conditions that are cold start and warm start. The cold start is that the ballast starts when the lamp filaments are cold. And the warm start is that the ballast starts when the lamp filaments are hot. This causes by suddenly turn on the lamp after turning off. The average filament resistance ratio values are shown in table 4.2. These values are within 4.25 and 6.25. Therefore, the filament temperature values before striking are safe for all lamp in T8 series.

Table 4.2 At 1 second preheat time, the actual filament resistance ratio values $R_{hc}(1s)$ and final preheat current values $i_{ph}(1s)$ are:

Cold start	**18W, 32W, 36W**	**58W, 70W**
$R_{hc}(1s)$	4.44	4.6
$i_{ph}(1s)$	450mA	500mA
$v_{ph}(1s)$	5.1V	4.6V
Warm start	**18W, 32W, 36W**	**58W, 70W**
$R_{hc}(1s)$	5.8	6.16
$i_{ph}(1s)$	400mA	430mA
$v_{ph}(1s)$	5.8V	5.3V

4.3 The Running Frequency

This experiment is processed by setting the power command to 16W, 30W, 34W, 56W and 68W for 18W, 32W, 36W, 58W and 70W T8 lamp in sequence. The running frequencies of those lamps are measured to compare with the calculation in 3.3.1. The results are shown in table 4.3. This frequency is directly measure at the G pin of a low side MOSFET of the inverter.

Table 4.3 The average running frequency of the electronic ballast using L = 2.2 mH and C = 4.7 nF

Power rating	Running frequency (Calculated)	Running frequency (Measured)
18 W	49.9 kHz	49.5 kHz
32 W	53 kHz	55.4 kHz
36 W	39 kHz	40.6 kHz
58 W	24.1 kHz	25.2 kHz
70 W	20.8 kHz	21.8 kHz

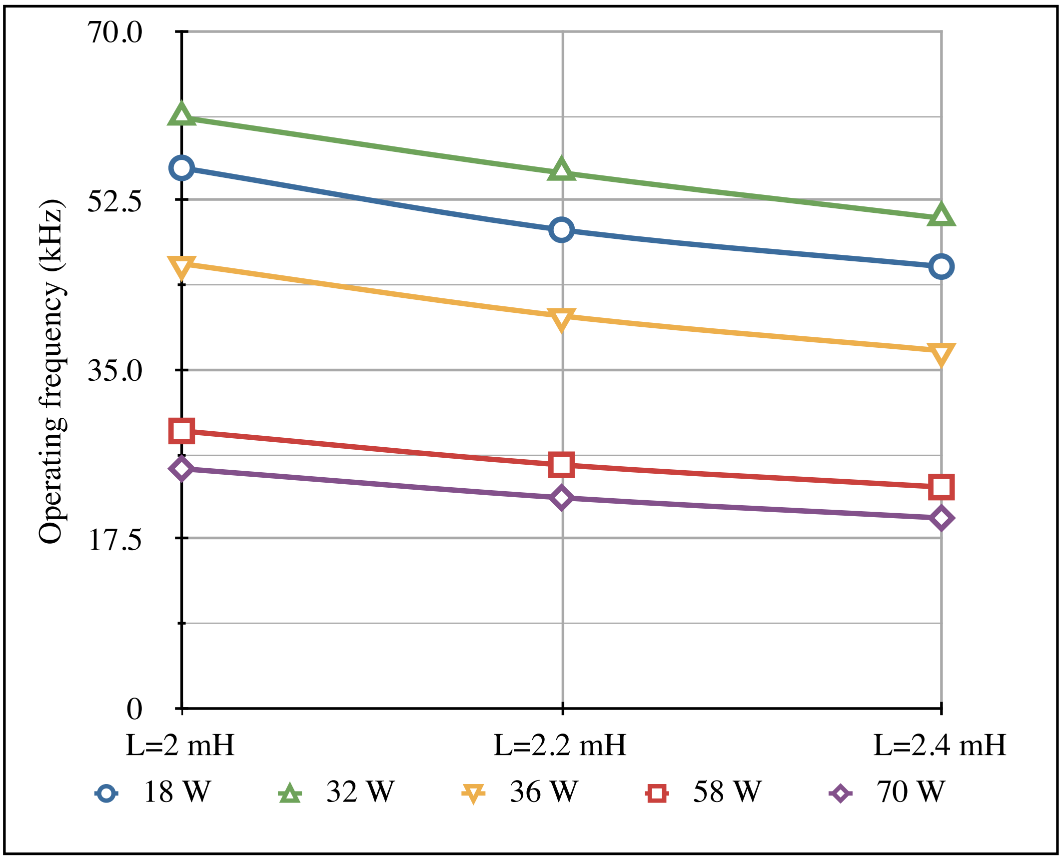

Figure 4.6 The average running frequency of the electronic ballast using L = 2 mH, 2.2mH and 2.4 mH

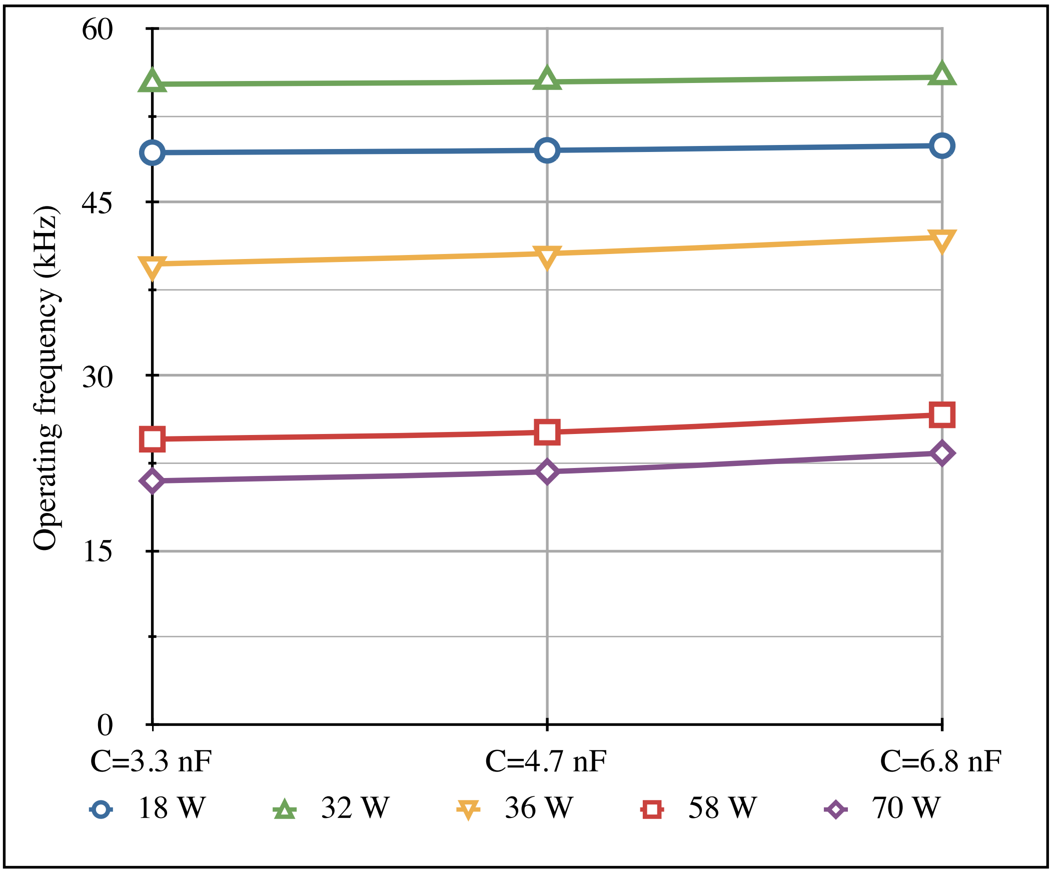

Figure 4.7 The average running frequency of the electronic ballast using C = 3.3 nF, 4.7 nF and 6.8 nF

From figure 4.6, the variation of the resonant inductance affects the operating frequency of ballast. By increasing this inductance by 10%, the operating frequencies decrease by 8-14%. Figure 4.7 shows the variation of the operating frequencies when the resonant capacitor value is changed. The operating frequencies increase 4-7% when the capacitance reduces by 30-45%. The experimental results show how the resonant inductor and capacitor affect the operating frequency. Therefore, it may confuse the lamp detection procedure. However, the possibility weight can be adapted in order to avoid the detection error.

4.4 Electrical Efficiency

This experiment is processed by setting the power command to 16W, 30W, 34W, 56W and 68W for 18W, 32W, 36W, 58W and 70W T8 lamp in sequence.

Table 4.4 The input power, output power and efficiency of the electronic ballast

Power rating	Output Power (W)	Input Power (W)	Efficiency of proposed ballast	Efficiency of single rating electronic ballast [6]
18 W	16.1	21.0	0.77	0.62 to 0.76
32 W	29.9	33.0	0.91	-
36 W	33.7	37.6	0.89	0.84 to 0.89
58 W	55.8	59.1	0.94	0.85 to 0.91
70 W	68.2	71.6	0.95	0.83 to 0.88

From this table, the efficiency depends on the lamp power. Since the power loss of this ballast is around 3 W for all lamp rating, the higher lamp power has higher efficiency. Comparing with the single rating ballast, this ballast has almost the same efficiency since this ballast has the same configuration as the ordinary ballast. However, the 58W and 70W lamp in [6] was operated at 50 W and 60 W instead of 56W and 68W in this ballast. This results a different of their efficiency. Remark that, there is no information of 32W lamp in [6] since this lamp type was manufactured by Philips for a short time and it had been obsolete.

4.5 Light Efficacy

Figure 4.8 shows the experiment configuration to compare the light efficacy of this proposed ballast to the single rating ballast. The fluorescent lamp is stabbed into the closed box. The illuminance is measured by using the lux-meter. This lux-meter is attached to one side of the box. Table 4.5 shows the relative light efficacy.

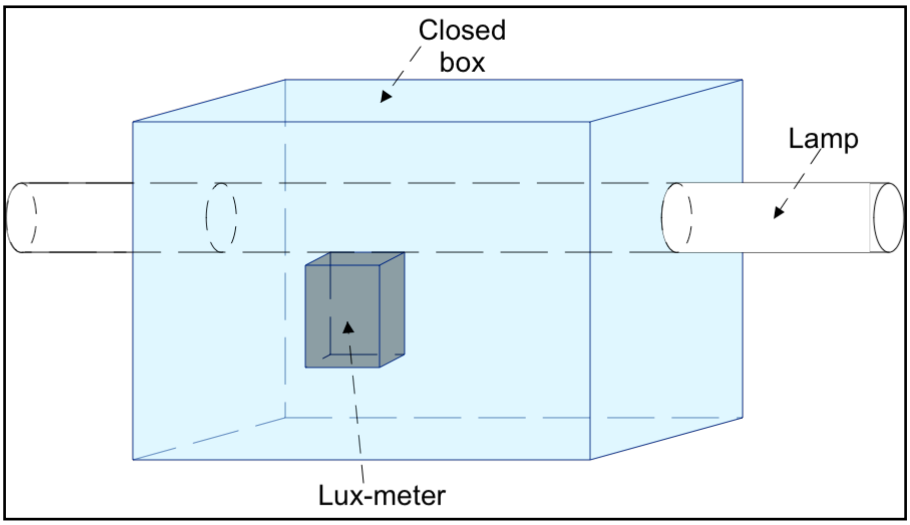

Figure 4.8 The configuration of the illuminance test set

Table 4.5 The comparison of the illuminance output and the efficacy of the electronic ballasts and the proposed ballast

Power rating	Measured illuminance of electronic ballast (Lux)	Measured illuminance of proposed ballast (Lux)	Relative efficacy of electronic ballast (Lux/W)	Relative efficacy of proposed ballast (Lux/W)
18 W	300.0	298.0	18.75	18.63
32 W	346.0	354.0	11.53	11.80
36 W	379.0	404.0	11.84	11.88

The results show that the multi-rating electronic ballast has almost the same light efficacy as the single rating electronic ballast since they share the same hardware configuration.

4.6 Running Frequency VS Time

This experiment is processed by setting the power command at rating. Starting from cold lamp (0 s), the running frequency is continuously decreased until the frequency becomes steady. Figure 4.9 shows that the cold lamps have lower running frequency than the warm lamp. As time proceeds, the running frequency will be continuously increased since the lamp is warming up. This is an important characteristic that has to be concerned. From figure 4.9, the running frequency seems to be stable after 20-30s. The software can't know whether the lamp is cold or warm. Therefore, a delay should be added to allow the running frequency to be stable before acquiring it. From this experiment, a 30s delay time should be the best. However, the more delay time causes more start up time to the ballast. In addition, the operating frequency of 18W lamp is significantly far from the other lamps. Thus, the possibility weight graph can be wider. The 10s delay for each power regulation step could be enough. Therefore, the delay time will be accumulated from 10s at the first step to 40s for the forth step. Since 40s of delay time is more than enough, there is needless to add any more delay time at the last 68w power regulation step.

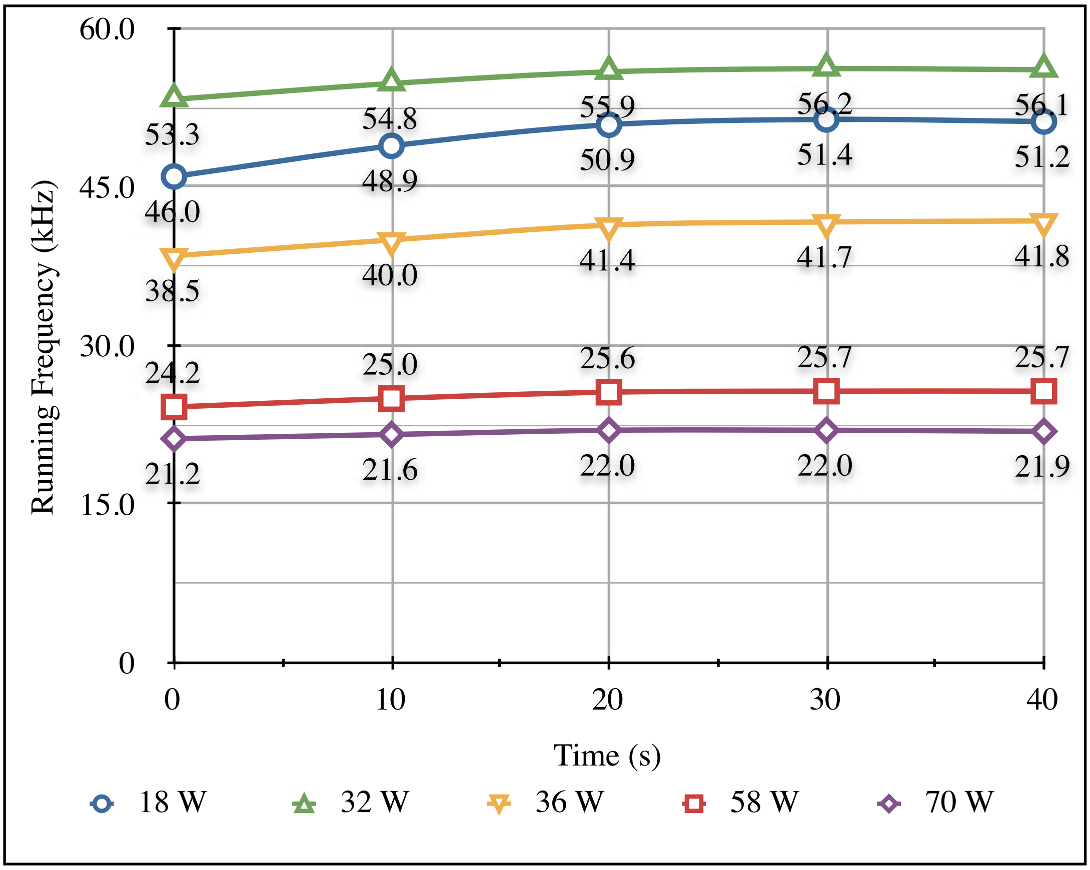

Figure 4.9 The running frequency of the electronic ballast VS time

4.7 The Lamp Detection by Using Voltage Detection Method (V.D.)

The voltage detection has been used method in detecting ballast's rating. With different power ratings, the lamp resistances may be different and the lamp peak voltages after strikes may be used to classify the power ratings. In figure 4.10, the lamp voltages are obtained from 50 samples of each of the T8 series lamp rating with the total number of 250 lamps. The voltages after strikes of the 32W and 58W lamps are located in the ranges of 162 V to 177 V and 166 V to 177 V, respectively. The detection result is very likely to be incorrect for both lamp ratings. This method yields the accuracy of detection rate as 86%.

The lamp peak voltage is measured by using the lamp peak voltage sensing circuit. This lamp peak voltage sensing circuit is also used to detect the success of striking. Testing with 250 bulbs which are divided into 5 power rating groups, the results are shown in figure 4.10. From this figure, the X axis is divided into 5 lamp ratings. The peak lamp voltages are plotted. The results show that the 18W, 36W, 58W and 70W lamp ratings can be classified since the voltages are not overlap. However, the 32W and 58W peak voltage are overlap and hard to be distinguished. Therefore, this V.D. method is appropriate for detecting T8 lamps if 32W or 58W lamp is not included. By using hard threshold, the results has been illustrated in table 4.8.

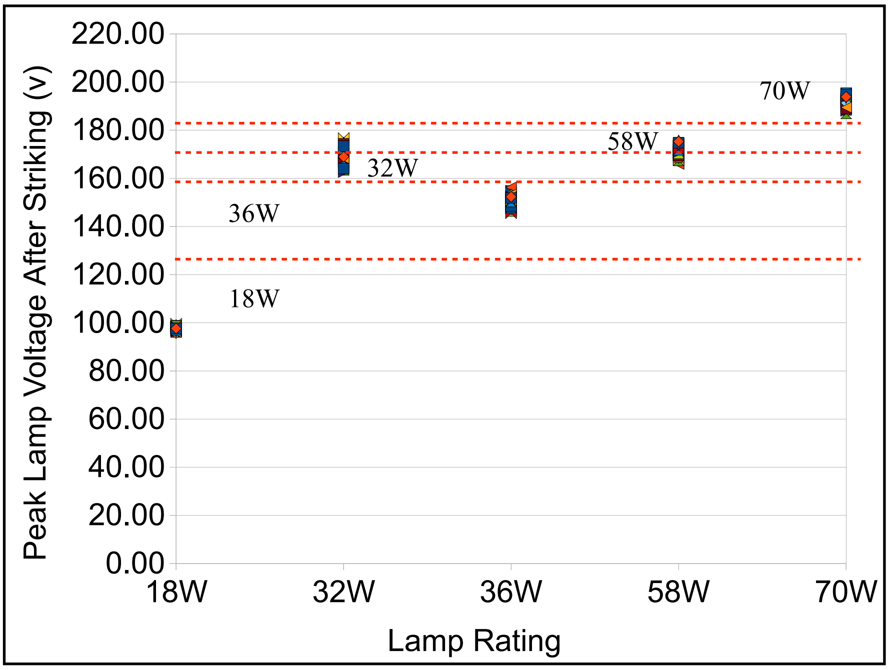

Figure 4.10 Lamp voltage after striking using 5 lamp ratings. Each rating have 50 bulbs

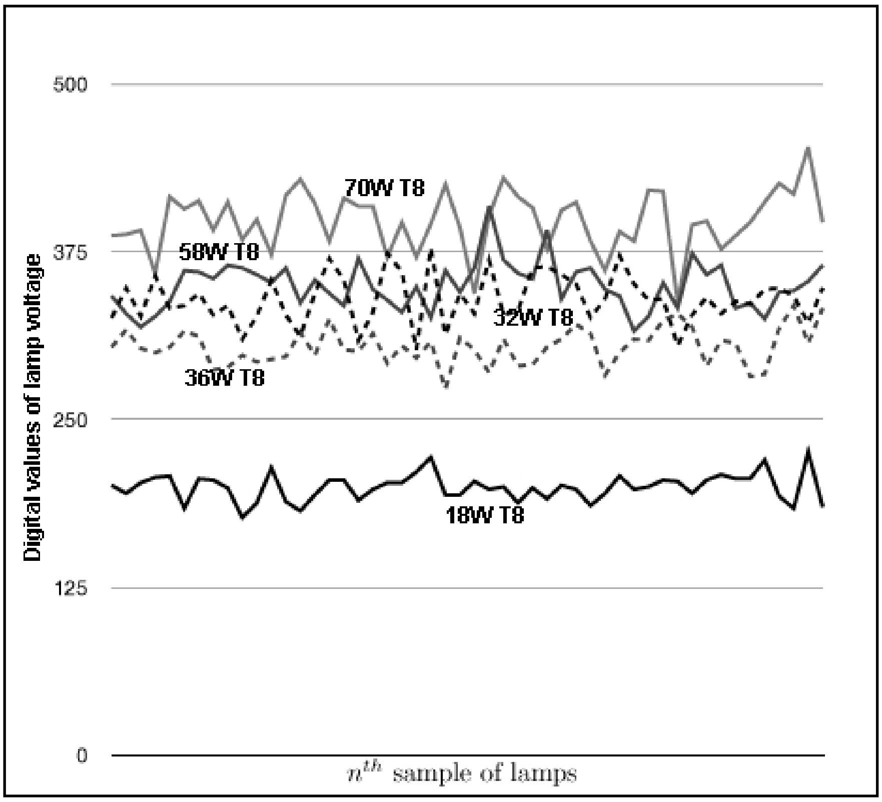

Figure 4.11 Lamp voltage after striking using 5 lamp ratings. This voltage was captured by ADC without input filter

The use of A/D converter in micro-controller will cause the noise amplification as shown in figure 4.11. The noisy switching environment will worsen the accuracy.

4.8 The Lamp Detection by Using Frequency Detection Method

The Frequency Detection with Multi-step Power Regulation method varies the regulated power from the lowest to the highest. The power steps are divided into 5 steps that are 16W, 30W, 34W, 56W and 68W. At each step, the operating frequency is acquired in order to detect the lamp rating by using the pre defined possibility weight functions. The experiments of this method are divided into 2 sets that are:

To evaluate this proposed method, hundreds of arbitrarily chosen fluorescent lamps with varied age are tested with proposed ballast. The operating frequencies of tested lamps are shown in figure 4.12-4.15, respectively. At 30W power regulation, the operating frequencies of all lamps are in the areas of their possibility weight. Thus, the proposed method can distinguish between 32W and 58W lamps. Note that some lamps with low possibility weight might have the chance of type I error (the false positive - the error of rejecting lamp when it is actually at rating) as well as the type II error (the false negative - the error of failing to reject a lamp when it is in fact not at rating). The lamp detection rate, type I error rate and type II error rate are calculated as:

$$D.R. = \frac{N_{Correct}}{N_{Lamp}} \times 100 \tag{4.1}$$

where D.R. is detection rate, $N_{Correct}$ is number of the accurately detected lamps and N_{Lamp} is number of tested lamp.

$$TypeI = \frac{N_{Reject}}{N_{Lamp}} \times 100 \tag{4.2}$$

where N_{Reject} is number of lamps that are rejected when it is actually at its rating.

$$TypeII = \frac{N_{WrongAccept}}{N_{Lamp}} \times 100 \tag{4.3}$$

where $N_{WrongAccept}$ is number of lamps that are accepted when it is not at its rating.

The experiments of this method are divided into 2 sets that are Fast Frequency Detection and Slow Frequency Detection.

4.8.1 Fast Frequency Detection (F.D.1)

In this detection method, the controller acquires the running frequency as soon as the power is equal to the power command. The Results at 16W power regulation show the type II error of 32-70W lamps are 100%. These come from the same possibility weight function of those lamps. For example, the 36W lamps will be detected as entire 32W, 36W, 58W and 70W. At the next step, from the results shown in figure 4.12a-4.15a, the 32W and 58W lamp have the small overlap region. This results the type I and type II error of those lamps. However, at 34W power regulation, the 32W lamps that were detected as 58W in the previous state give the highest possibility at 32W. This stop the detection process and driving signal simultaneously. The detection results are shown in table 4.6 and 4.8. At the final decision state, it results 6% undetected 32W lamps (shut down) and 8% dimmed 58W lamps.

Table 4.6 Detecting results of T8 lamp at 16W, 30W, 34W, 56W and 68W power regulation state using fast frequency detection

Lamp rating	18W	32W	36W	58W	70W
16W Power regulation					
%Detection rates	100	100	100	100	100
%Type I error	0	0	0	0	0
%Type II error	0	100	100	100	100
30W Power regulation					
%Detection rates	-	94	100	92	100
%Type I error	-	6	0	8	0
%Type II error	-	8	0	6	0
34W Power regulation					
%Detection rates	-	-	100	92	100
%Type I error	-	-	0	8	0
%Type II error	-	-	0	0	0
56W Power regulation					
%Detection rates	-	-	-	92	100
%Type I error	-	-	-	8	0
%Type II error	-	-	-	0	0
68W Power regulation					
%Detection rates	-	-	-	-	100
%Type I error	-	-	-	-	0
%Type II error	-	-	-	-	0

4.8.2 Slow Frequency Detection (F.D.2)

Increase the delay time to 10s after the power set point and process variable are about the same before acquiring the frequency. Therefore, the minimum detection time of 18W lamp, 32W lamp, 36W lamp and 58W lamp are 10 s, 20 s, 30 s and 40 s. Since 70W lamp that pass the 56 W power regulation state has run for 40 s, the operating frequency is stable enough to be used without an additional delay. Thus, the minimum delay time of 70W lamp is equal to 56W that is 40 s.This increases the maximum lamp detection time to about 40s for 58W and 70W lamp. The operating frequency of hot lamp (turn on for some period) is more stable than the cold lamp.

Table 4.7 Detecting results of T8 lamp at 16W, 30W, 34W, 56W and 68W power regulation state using slow frequency detection

Lamp rating	**18W**	**32W**	**36W**	**58W**	**70W**
16W Power regulation					
%Detection rates	100	100	100	100	100
%Type I error	0	0	0	0	0
%Type II error	0	100	100	100	100
30W Power regulation					
%Detection rates	-	94	100	92	100
%Type I error	-	6	0	8	0
%Type II error	-	8	0	6	0
34W Power regulation					
%Detection rates	-	-	100	92	100
%Type I error	-	-	0	8	0
%Type II error	-	-	0	0	0
56W Power regulation					
%Detection rates	-	-	-	92	100
%Type I error	-	-	-	8	0
%Type II error	-	-	-	0	0
68W Power regulation					
%Detection rates	-	-	-	-	100
%Type I error	-	-	-	-	0
%Type II error	-	-	-	-	0

Table 4.8 The comparison results of the Voltage Detection, Frequency the Detection with Multi-step Power Regulation and the Adapted Frequency Detection with Multi-step Power Regulation method.

Lamp rating	18W	32W	36W	58W	70W
V.D.					
%Detection rates	100	60	100	100	100
%Type I error	0	40	0	30	0
%Type II error	0	30	0	40	0
F.D.1					
%Detection rates	100	94	100	92	100
%Type I error	0	6	0	8	0
%Type II error	0	8	0	6	0
F.D.2					
%Detection rates	100	100	100	100	100
%Type I error	0	0	0	0	0
%Type II error	0	0	0	0	0

The frequency data are shown in figure 4.12b-4..15b. The detection results have been shown in Table 4.7 and 4.8.

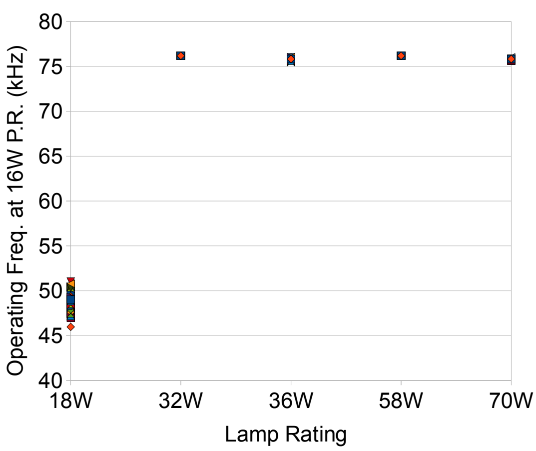

a.

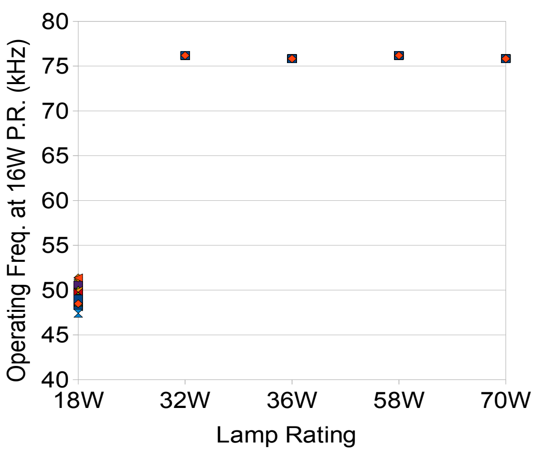

b.

Figure 4.12 The operating frequency of each lamp rating when regulated at 16W. These data are acquiring from 250 bulbs which are divided into 5 power rating groups.

a. Immediately acquiring the frequency right after steady state.

b. Acquiring the frequency after 10s.

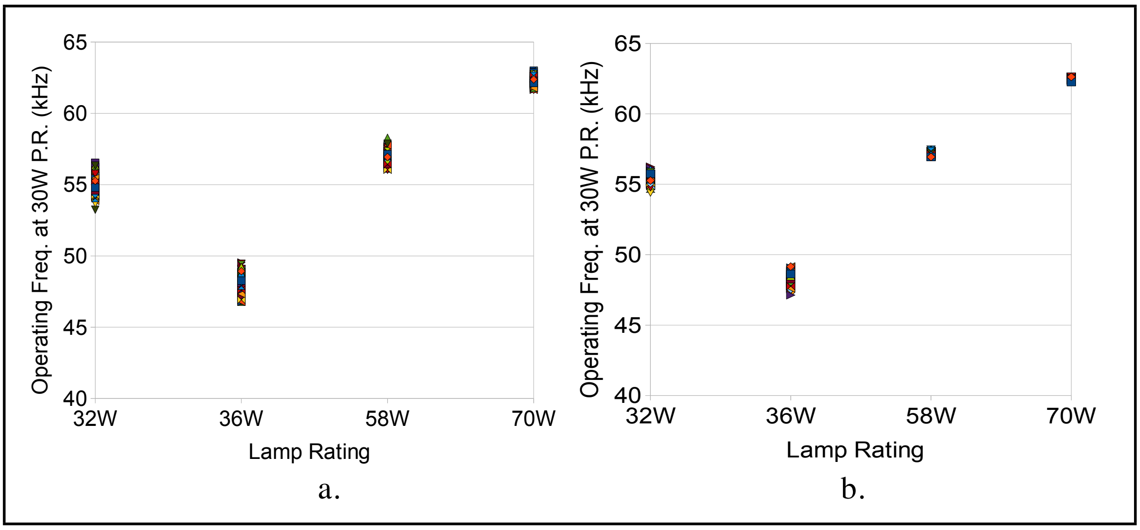

Figure 4.13 The operating frequency of each lamp rating when regulated at 30W

a. Immediately acquiring the frequency right after steady state.

b. Acquiring the frequency after 10s.

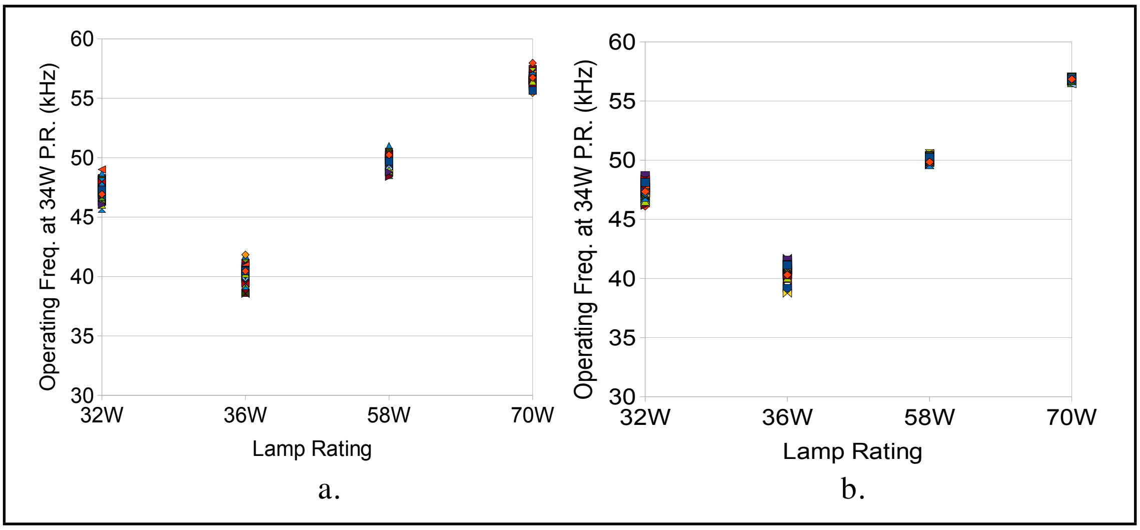

Figure 4.14 The operating frequency of each lamp rating when regulated at 34W

a. Immediately acquiring the frequency right after steady state.

b. Acquiring the frequency after 10s.

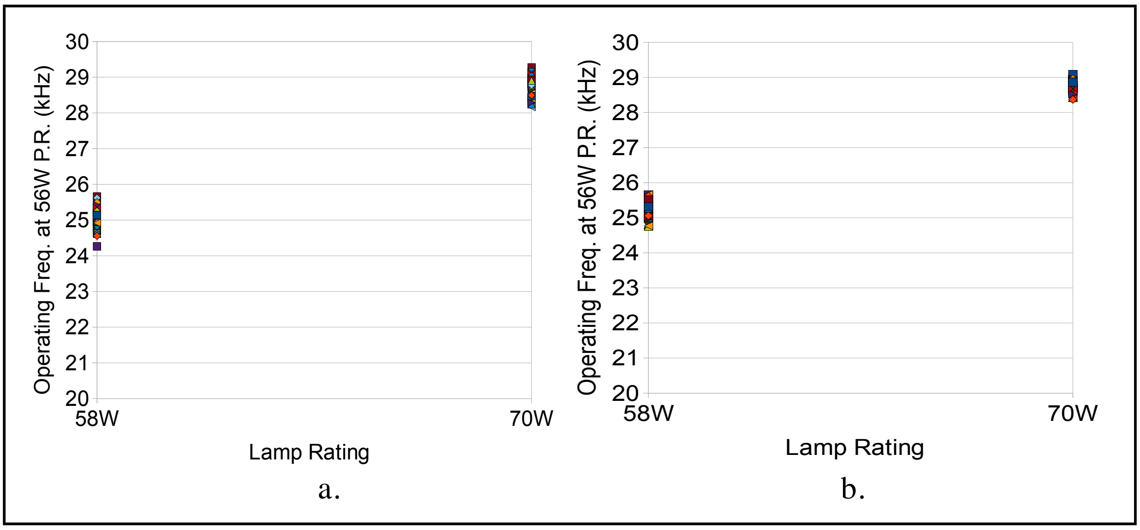

Figure 4.15 The operating frequency of each lamp rating when regulated at 56W

a. Immediately acquiring the frequency right after steady state. b. Acquiring the frequency after 10s.

From table 4..8, the F.D. method with 10s delay time results 100% detection rate, F.D. method without delay time results 97.2% detection rate and V.D. method results 86% detection rate. Because of the overlapped possibility weight of the 32 W and 58 W lamp, the high type I and type II error of 58W lamps are occurred during 16W power regulation. Even the low accuracy occurs in 16W power regulation state, the next power regulation state results in the high detection accuracy implying the right rating will be detected at the final decision. Therefore, this algorithm results in a 100% detection rate of all tested lamps. An example of the lamp voltage and lamp current of this ballast running with 36W lamp is illustrated in figure 4.16. For the testing with very old lamps, the inaccurate detection is occurred but the protection algorithm stops the ballast operation due to the rectifying effect.

Comparing the proposed detection with the voltage detection method, the experiment for measuring lamp voltages after ignition are carried out as shown in figure 4.10. Using this method, the 70W and 18W lamps are easily detected but the detection between 32W and 58W lamps is not possible. The main reason is that the lamp voltage after ignition varies with the lamp temperature, age, and manufacturer. Moreover, the use of A/D converter in micro-controller will cause the noise amplification as shown in figure 4.11. The noisy switching environment will worsen the detection accuracy. With the proposed method, the frequency is generating by the micro-controller itself which is not interfered by noise. And the multi-step power regulation constrains the lamp operating condition during the detection as well.

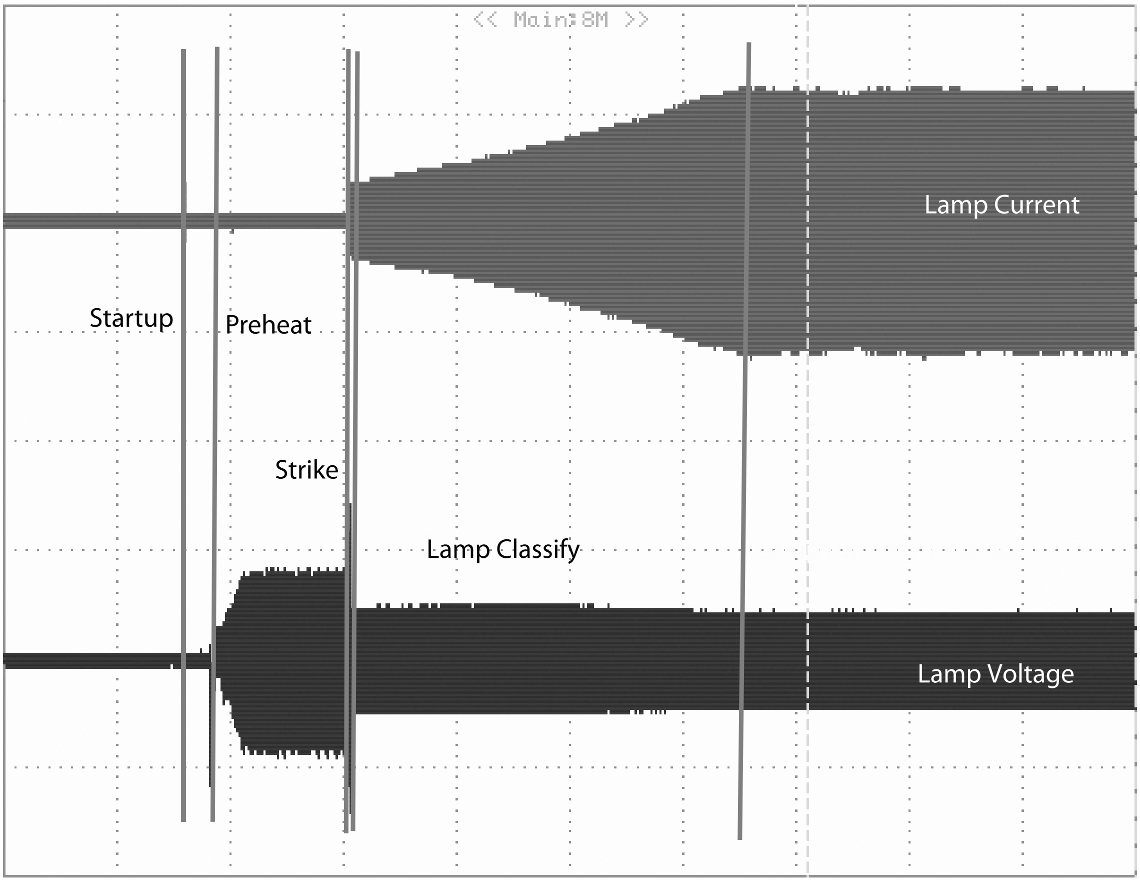

Figure 4.16 An example of voltage (Bottom) and current (Top) of 36W lamp running with multi-rating electronic ballast.

4.9 Conclusion and Limitation

Clearly, the frequency detection method does not suffer from overlapping range of the detection parameter. The detection results of the proposed method are evidently more accurate. It is even better if we set a delay of 40s before obtaining the operating frequency, 100% detection accuracy may be achieved since the lamp resistance is allowed to reach its stable state.

From table 4.8, the detection rates of the 32W and 58W lamps are lower than another rating. The type I error of 58W lamp shows that 8% of 58W lamps are rejected due to the operating frequencies of those lamps have crossed the line to the 32W lamp rating region. These 58W lamps are classified as 32W lamps and also cause the Type II error as 8 %. When these lamps are rejected from being 32W rating and are classified as 58W lamps, the lamps filaments are damaged by the huge over wattage caused by the abnormal condition of ballast. This condition leads to the fault state and stops the inverter. This causes 0 % Type II error of 58W due to the fault state and the controller resets the detection results to 0, causing these lamps to become unknown. However, if the fault state had not been included, this Type II error of 58W lamp rating would have been 6 % instead of 0 %.

To reduce the over wattage problem that damage the lamp, we should expand the region of 32W lamp frequency and shrink the 58W region. This could decrease the Type I error so that none of 32W lamp would be rejected. However, this method will cause a lot of

58W lamps to be classified as 32W lamps that increases the Type I error of 58W. Compromising with the detection speed, the more delay time reduces the deviation of operating frequency. This method increases the detection rate to 100% as shown in table 4.8.

Another limitation is that the frequency determination method depends on the resonant devices (L and C). The error these devices values lead to the deviation of operating frequency. Thus, these resonant devices should be precisely selected.

CHAPTER 5 CONCLUSIONS

A multi-rating electronic ballast for fluorescent lamps based on operating frequency determination has been presented. The detection algorithm is based on the probability weight distribution of the lamp operating frequency, and multi-step lamp power regulation. The proposed algorithm has shown great accuracy in detecting the targeted lamp power rating compared with the commonly used voltage detection method. In some cases, aging lamps may result in misclassification of the lamps therefore, a protection circuit must be implemented with the ballast. With the proposed detection algorithm, the multi-rating ballast will help eliminate concerns about matching the ballast circuit with the designated lamp power rating. However, the frequency determination method depends on the resonant devices (L and C) and the operating frequency is highly sensitive to the L and C values. Therefore, care must be taken in selection of these devices in terms of types and values to eliminate the difference between the chosen and the actual values.

5.1 Summary of Contributions

The proposed multi-rating electronic ballast has four main contributions that are listed as follows.

- The Multi-rating Electronic Ballast reduce the complicated task of choosing the ballast to match with the appropriate lamp. This benefit allows inexperience users, such as householders, to buy the ballasts with a variety of selections of lamp wattages. In addition, for large organizations that have a lot of lamps with more than one rating can stock only one model of ballast.

  However, the aging effect from an increased filament resistance and lamp discharge characteristics may cause inaccuracy in the detection results. For example; the overlapped operating frequency of 32WT8 and 58WT8 might occur during the 30 W power regulation. In our designed ballast, the 18W, 32W and 36W T8 lamps, which are commonly used in Thailand, are selected. The operating frequencies of these lamps are different from one another resulting in high accuracy in detection results. Moreover, the cost of the proposed ballast is reduced because the software has been designed and implemented with less number of components.

  The PFC boost controller is simplified by removing the multiplying process that is a very complicated task for a low cost microcontroller. This algorithm was done by setting the update time of the pulse width of the driving command to the time that the zero crossing of an AC line voltage occurs. This algorithm enables the low cost microprocessor to do a PFC boost controller task together with another important process. Note that, without the multiplying function, the total current harmonic distortion (THD) is higher. If the %THD lower than 10 was required, a dedicated PFC controller IC would be needed.

- The simplified normal distribution that is used in the lamp detection process enables the use of a low cost micro processor to do a complicated task like a pattern recognition without using high processing task.

- By using the frequency information to identify the lamp power rating rather than using the voltage information, the lamp detecting process has more immunity to noise.

5.2 Future Work

This thesis has presented several aspects regarding lamp detection algorithms. Issues in hardware implementation of the proposed idea are addressed in a way that it is realizable on a low-cost microcontroller. The future work in perfecting the multi-rating electronic ballast includes the followings.

Determination of the possibility weight function is a time-consuming process for a series of lamps of interest due to the total number of sampled frequency must be collected to ensure accuracy in detection results. The more number of samples, the better detection results. Each lamp sample must be operated at a variety of frequencies to construct a database of the lamp frequency. This means that data collection is an elaborated task where the recorded data is sensitive to the detection results. To facilitate the data collection process, methods such as artificial neural network may be considered to reduce the complexity of the data collection to only turning the lamps on and off where accuracy is not sacrificed.

The multi-rating ballast is designed to be able to use with a series of lamps. This means that the ballast must be able to handle the highest power rating lamp in the series. For example, the T8 series lamps is ranging from 18 W to 70 W. On the one hand, the ballast is capable of operating at 70 W. On the other hand, the 18 W lamp may be used with the same ballast. The redundancy in the ballast rating results in unnecessary cost and may be reduced by targeting many lamp series with narrower range of power ratings instead of aiming the design to accommodate only a single lamp series. For example, the desired power could be set to 40 W or less for both T5 and T8 series.

REFERENCES

1. L. Davies, H. Ruff, and W. Scott, 1942, "Fluorescent Lamps", **Journal of the Institution of Electrical Engineers - Part II: Power Engineering**, Vol. 89, pp. 447–465.

2. l. John, E. Kaufman, and J. F. Christensen, 1984, **IES Lighting Handbook**, Illuminating Engineering Society.

3. M. Kazimierczuk and W. Szaraniec, 1993, "Electronic Ballast for Fluorescent Lamps", **IEEE Transactions on Power Electronics**, Vol. 8, pp. 386–395.

4. M. Matsuo, T. Suetsugu, S. Mori, and I. Sasase, 1999, "Class DE Current-source Parallel Resonant Inverter", **IEEE Transactions on Industrial Electronics**, Vol. 46, pp. 242–248.

5. J. Cosby, M.C. and R. Nelms, 1994, "A Resonant Inverter for Electronic Ballast Applications", **IEEE Transactions on Industrial Electronics**, Vol. 41, pp. 418–425.

6. C. Liu, F. Teng, C. Hu, and Z. Zhang, 2003, "LCLC Resonant Converter for Multiple Lamp Operation Ballast", **Applied Power Electronics Conference and Exposition,** Eighteenth Annual IEEE APEC '03, Feb, Vol. 2, pp. 1209–1213.

7. J. Alonso, J. Cardesin, Calleja, Rico-Secades, and J. Gar- cia, 2005, "A Fluorescent Lamp Electronic Ballast for Railway Applications Based on Low-cost Microcontroller", **IEEE Transactions on Industry Applications**, Vol. 41, pp. 1391–1400.

8. R.-L. Lin and Y.-T. Chen, 2006, "Electronic Ballast for Fluorescent Lamps with Phase-Locked Loop Control Scheme", **IEEE Transactions on Power Electronics**, Vol. 21, pp. 254–262.

9. Y. Ji, R. Davis, C. O'Rourke, and E. Chui, 1999, "Compatibility Testing of Fluorescent Lamp and Ballast Systems", **IEEE Transactions on Industry Applications**, Vol. 35, pp. 1271–1276.

10. L. Lee, S. Hui, and H. Chung, 2005, "An Automatic Lamp Detection Technique for Electronic Ballasts", **Twentieth Annual IEEE Applied Power Electronics Conference and Exposition**, March, Vol. 1, pp. 575–581.

11. L.-M. Lee and S. Hui, 2009, "Automatic Lamp Detection and Operation for Warmstart Tubular Fluorescent Lamps", **IEEE Transactions on Power Electronics**, Vol. 24, pp. 2933 –2941.

12. S.-M. Chen, Y.-K. Ko, Y.-C. Chang, and J.-S. Pan, 2009, "Weighted Fuzzy Interpolative Reasoning Based on Weighted Increment Transformation and

Weighted Ratio Transformation Techniques", **IEEE Transactions on Fuzzy Systems**, Vol. 17, pp. 1412–1427.

13. T.-F. Wu, Y.-C. Liu, and Y.-J. Wu, 1999, "High-efficiency Low-stress Electronic Eimming Eallast for Multiple Fluorescent Lamps", **IEEE Transactions on Power Electronics**, Vol. 14, pp. 160– 167.

14. T.-F. Wu and T.-H. Yu, 2000, "An Electronic Dimming Ballast with Bifrequency and Fuzzy Logic Control", **IEEE Transactions on Industry Applications**, Vol. 36, pp. 1308–1317.

15. Thomas J Ribarich, Perter B Green, John J Ribarich, John E Parry and Cecilia Contenti, 2006, "I.R. Ballast Designer Version 4.1.7", **I. R. Corporation** [Software].

16. T. Ribarich and J. Ribarich, 2001, "A New Procedure for High-Frequency Electronic Ballast Design", **IEEE Transactions on Industry Applications**, Vol. 37, pp. 262–267.

17. S. S. M. Chan, H. S.-H. Chung, and Y.-S. Lee, 2007, "Design and Implementation of Dimmable Electronic Ballast Based on Integrated Inductor", **IEEE Transactions on Power Electronics**, Vol. 22, pp. 291–300.

18. H. Sartori, H. Hey, and J. Pinheiro, 2009, "An Optimum Design of PFC Boost Converters", **EPE '09. 13th European Conference on Power Electronics and Applications**, Sept., pp. 1– 10.

19. F. Wakabayashi, M. de Brito, C. Ferreira, and C. Canesin, 2007, "Setting the Preheating and Steady-state Operation of Electronic Ballasts, Considering Electrodes of Hot-cathode Fluorescent Lamps", **IEEE Transactions on Power Electronics**, Vol. 22, pp. 899–911.

20. D. Klien, 2003, "A Sensing and Regulation Concept for High end Dimming Ballasts", **38th IAS Annual Meeting. Conference Record of the Industry Applications Conference**, Oct, Vol. 2, pp. 785–790.

21. Y. Ji, R. Davis, C. O'Rourke, and E. Chui, 1999, "Compatibility Testing of Fluorescent Lamp and Ballast Systems", **IEEE Transactions on Industry Applications**, Vol. 35, pp. 1271– 1276.

22. American National Standard for Ballasts for Fluorescent Lamps: Specifications, 1985, **ANSI C82.1-1985**.

23. P. Tam, S. Lee, S. Hui, and H.-H. Chung, 2006, "Practical Evaluation of Dimming Control Methods for Electronic Ballasts", **IEEE Transactions on Power Electronics**, Vol. 21, pp. 1769–1775.

24. Z. Li, P. Mok, W.-H. Ki, and J. Sin, 1997, "A Simple Method to Design Resonant Circuits of Electronic Ballast for Fluorescent Lamps", ISCAS '97, **Proceedings of**

1997 IEEE International Symposium on Circuits and Systems, June, Vol. 3, pp. 1744–1747.

25. A. Ng, W.-H. Ki, P. Mok, and J. Sin, 2000, "Lamp Modeling for Design of Dimmable Electronic Ballasts", **IEEE 31st Annual Power Electronics Specialists Conference**, Vol. 3, pp. 1358–1362.

26. S. Glozman and S. Ben-Yaakov, 2001, "Dynamic Interaction Analysis of HF Ballasts and Fluorescent Lamps Based on Envelope Simulation", **IEEE Transactions on Industry Applications**, Vol. 37, pp. 1531–1536.

27. T.-F. Wu, J.-C. Hung, and T.-H. Yu, 1995, "A Pspice Model for Fluorescent Lamps Operated at High Frequencies", **Proceedings of the 21st IEEE International Conference on Industrial Electronics, Control, and Instrumentation**, Nov., Vol. 1, pp. 359–364.

28. M. Sun and B. Hesterman, 1998, "Pspice High-frequency Dynamic Fluorescent Lamp Model", **IEEE Transactions onPower Electronics**, Vol. 13, pp. 261–272.

29. J.P.Hua, 1998, **Detection and protection circuit for fluorescent lamps operating at failure mode**, USA, U.S. Patent 5777439.

30. A. Chee and J. Sampson, 1999, "A Novel Triple-frequency Controlled Lamp Network with End-of-life Detection for Architectural Dimming of Compact Fluorescent Lamps", **Proc. 14th Annu. IEEE Appl. Power Electron. Conf. Expo. (APEC '99)**, 14–18 Mar., Vol. 2, pp. 734–738.

31. Z. Huang and T. Ribarich, 2006, "Designing a Wide Range High Performance T5HO Electronic Ballast Platform", **Proc. 21st Annu. IEEE Appl. Power Electron. Conf. Expo. (APEC '06)**, 19–23 Mar., pp. 1051–1057.

32. Q. Yu and J. Parisella, 2007, "Frequency Diagnostic Universal Fault Protection for Current Fed Parallel Resonant Electronic Ballast", **IEEE Trans. Power Electron.**, Vol. 22, no. 3, pp. 881–888.

33. J. J. LoCascio and U. H. Mader, 1997, **Lamp Out Detection for Miniature Cold Cathode Fluorescent Lamp System**, USA, U.S. Patent 5652479.

34. D. Liu, 2008, **Open Lamp Detection in an EEFL Backlight System**, USA, U.S. Patent 7253569.

35. U. Mader, 1996, "Steady-state Analysis of a Voltage-fed Inverter with Second-order Network and Fluorescent Lamp Load", **IEEE Applied Power Electronics Conference and Exposition**, Vol. 2, Mar 1996, pp. 609–615.

36. Lighting Research Center, 2000, **Electronic Ballast Non-Dimming Electronic Ballasts for 4-foot and 8-foot Fluorescent Lamps**, National Lighting Product Information Program (NLPIP), Vol. 8, No. 1, pp. 4-29.

37. Australian Communications and Media Authority, 1968, **Better television and radio reception. Identifying your analog TV and radio interference problem**, Australian Communications and Media Authority (ACMA), Australia, pp.17.

38. R.M. Gray and L.D. Davisson, 2004, **Introduction to Statistical Signal Processing**, 1st ed., Cambridge University Press, England, pp. 447.

APPENDIX A

The Schematic Diagram of Multi-rating Electronic Ballast

This schematic is divided into 4 parts that are microcontroller, 5V power supply, boost converter and inverter as illustrated in figure A.1-A.4.

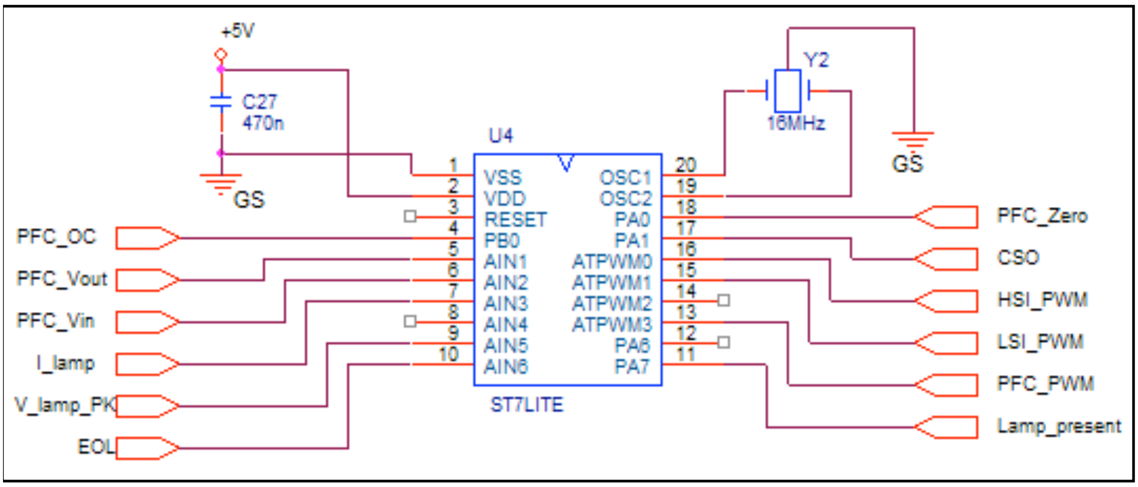

Figure A.1 The schematic diagram of the microcontroller

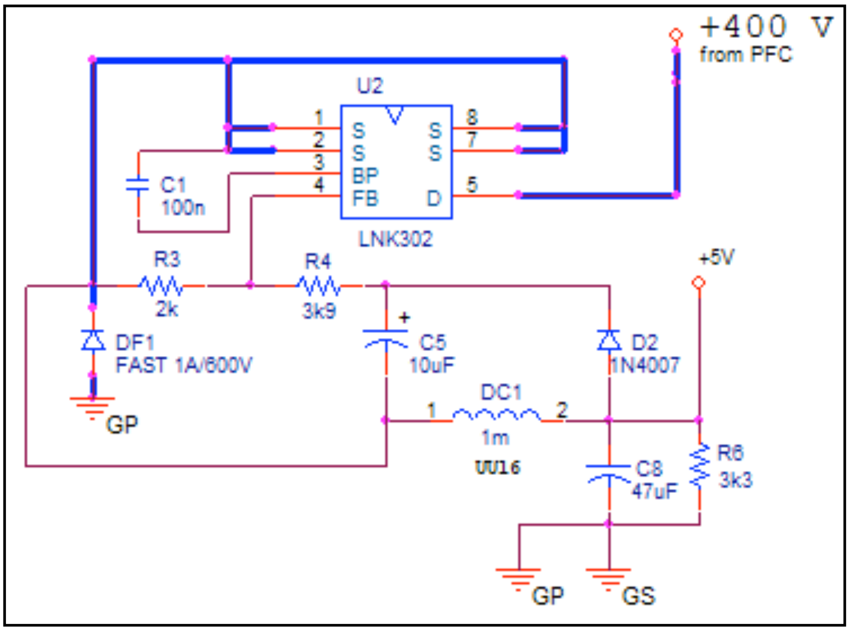

Figure A.2 The schematic diagram of the 5V power supply

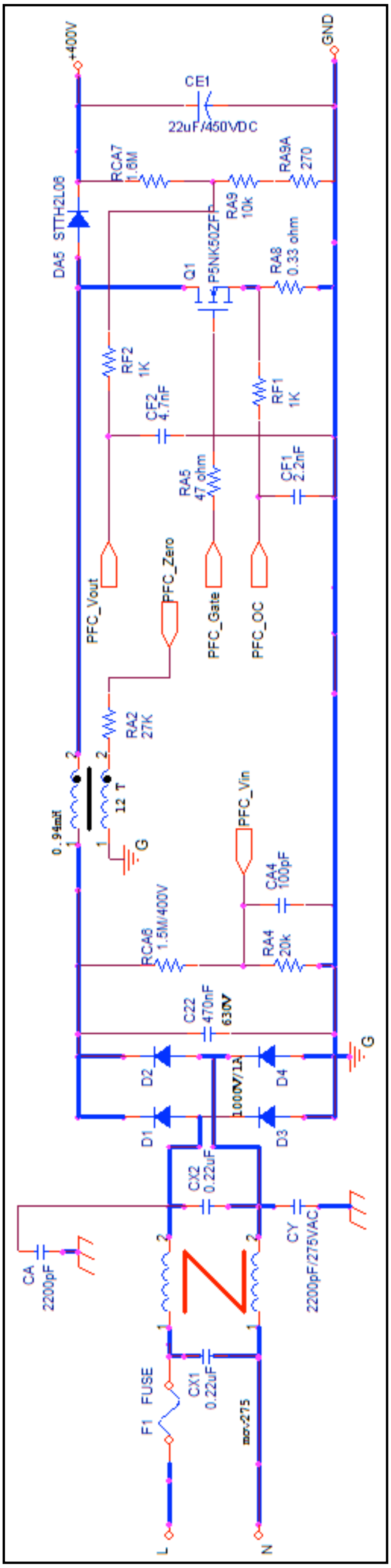

Figure A.3 The schematic diagram of the PFC boost converter

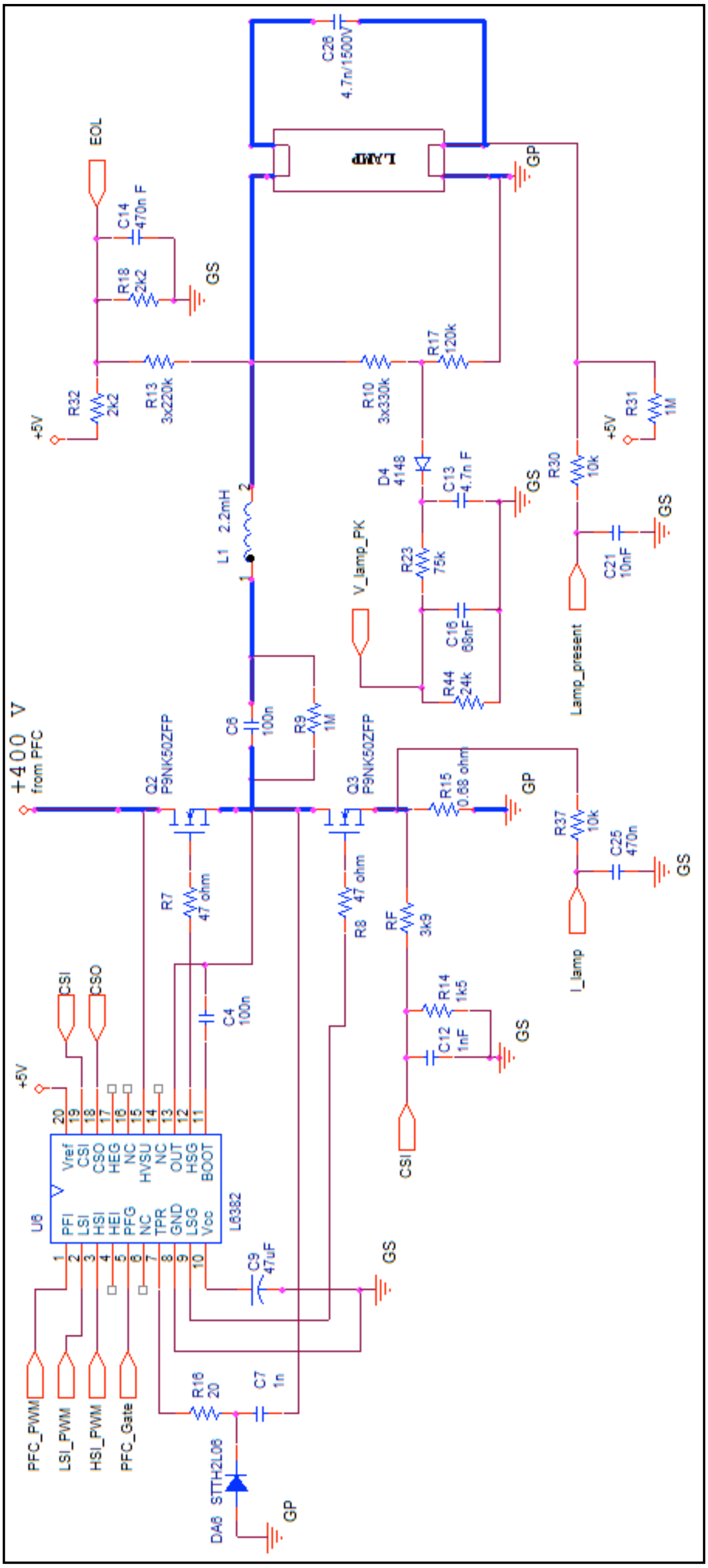

Figure A.4 The schematic diagram of the resonant inverter and the MOSFET driver

APPENDIX B
The Measurement Devices

APPENDIX B

B.1 Power Quality Measurement

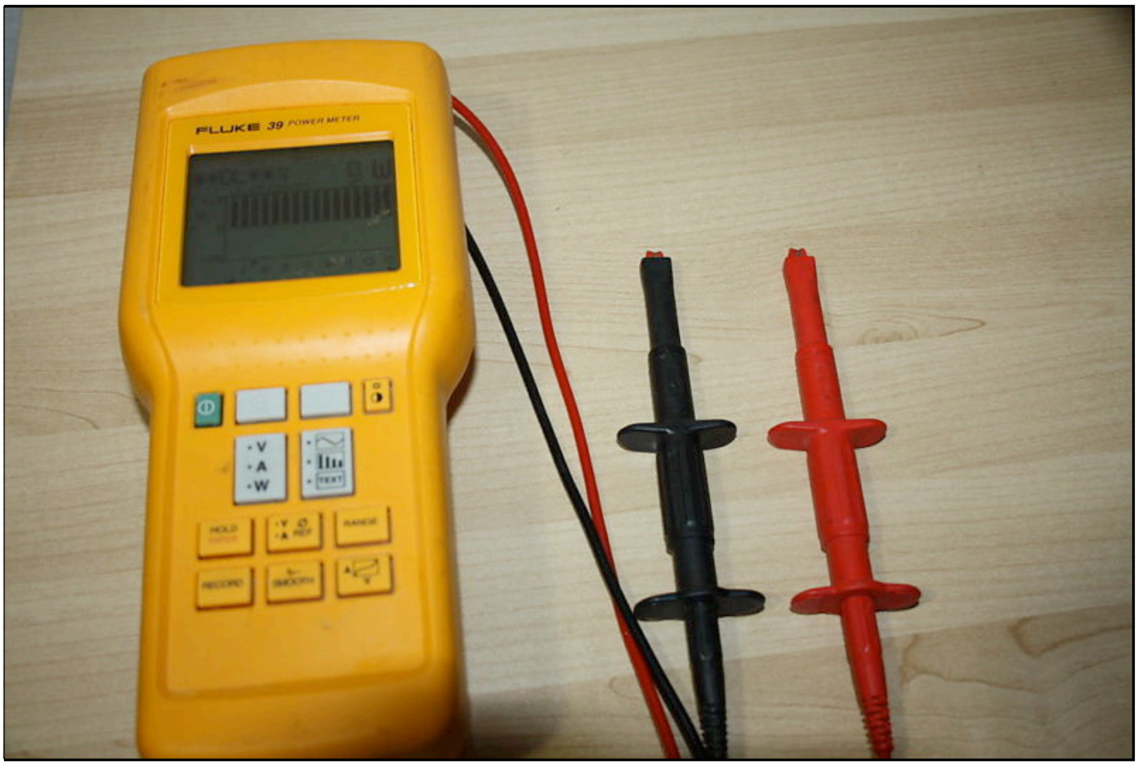

Figure B.1 The Fluke 39 is used to measure the PF and THD of the electronic ballast in chapter 4.1

Figure B.1 shows the picture of Fluke 39 power meter. This meter is used to measure the power quality of the electronic ballast include power factor (PF) and total harmonic distortion (THD). The specification of fluke 39 is:

Table B.1 Fluke 39 specification

Voltage	Range and Resolution: 5.0V to 600V rms (AC+DC); ±5.0V to ±933V peak Accuracy: rms: ±(0.5% + 2 digits); Peak or DC: ±(2% + 3 digits) (Add 2 digits if < 15V rms)
Current (1mV/A) Isolated input	Range and Resolution: 1.00A to 1000A rms (AC+DC); ±1.0A to ±2000A peak Accuracy: rms: ±(0.5% + 3 digits)+probe specs; Peak or DC: ±(2% + 4 digits) + probe specs
Watts/Volt-Amps (1mV/A) isolated input	Range and Resolution: 0.0W(VA) to 600kW(kVA) average; 0.0W(VA) to ±2000kW(kVA) peak Accuracy: AC+DC: ±(1% + 4 digits) + probe specs
Harmonics (harmonic level >5% using Smooth 20)	Volts: Fundamental to 13th ±(2%+2 digits); At 31st ±(8%+2 digits); Amps or Watts: Fundamental to 13th ±(3% + 3 digits) + probe specs; At 31st ±(8% + 3 digits) + probe specs
Frequency	Range & Resolution: 6.0 Hz to 99.9 Hz Accuracy: ±0.3 Hz
Input Bandwidth	DC, 6 Hz to 2.1 kHz
Crest Factor (CF)	Range & Resolution: 1.00 to 5.00 Accuracy :±4%
Power Factor (PF)	Range & Resolution: 0.00 to 1.00 Accuracy: ±0.02
Displacement Power Factor (DPF)	Range & Resolution: 0.00 to 1.00 Accuracy: ±0.04 to ±0.03 (0.30 to 0.89) ±0.02 (0.90 to 1.00)
Phase	Range & Resolution: -179 to 180 degree Accuracy (Fundamental): ±2o + probe specs
K-Factor (KF)	Range & Resolution: 1.0 to 30.00 Accuracy: ±10%
% THD-F	Range & Resolution: 0.00% to 799.9% Accuracy: ±(0.03 Reading + 2.0%)
% THD-R	Range & Resolution: 0.0% to 99.9% Accuracy: ±(0.03 Reading + 2.0%)

Figure B.2 The Fluke 80i current probe

For the current measurement, this meter is connected with Fluke 80i current probe. This probe is illustrated in figure B.2. The specification is:

Table B.2 Fluke 80i specification

Input Current Range	1A to 600A
Output	1 milliamp per ampere of input current (1mA/A)
Accuracy	±2% of reading, 50 Hz to 1 kHz ±3% of reading (typical), 30 Hz to 50 Hz or 1 kHz to 10 kHz.
Working Voltage	750V ac rms maximum
Typical Bandwidth	-10% at 10 Hz and 50 kHz (1A, 400 Hz reference, excludes multimeter response)
Usable Current Range	0.1A to 2000A, 5 seconds maximum above 600A
Safety: Protection Class	Class II as defined in IEC 348 and ANSI C39.5

B.2 Waveform Measurement

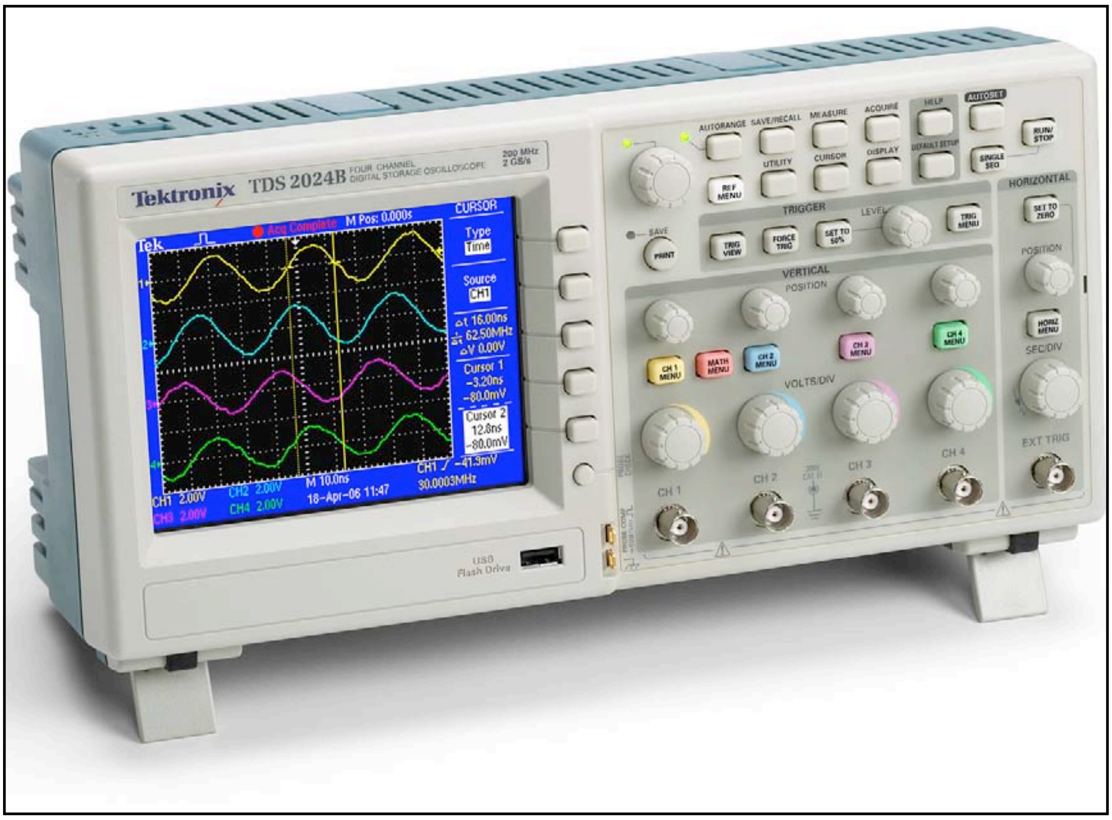

Figure B.3 Tektronix TDS2024 digital oscilloscope

Figure B.3 shows the picture of Tektronix TDS2024 digital oscilloscope. This oscilloscope is used to measure the waveform of the AC input voltage, input current and DC output voltage of the PFC boost converter in chapter 4.1. The specification of TDS2024 is:

- 100 MHz, 60 MHz, 40 MHz bandwidth models
- 2 channels
- Up to 1 GS/s sample rate on all channels
- 2.5k point record length on all channels
- Advanced triggers including pulse width trigger and line-selectable video trigger
- USB 2.0 host port on the front panel for quick and easy data storage

The preheat current and filaments voltage in chapter 4.2, the running frequency in chapter 4.3 and 4.6, the input power and output power in chapter 4.4 are measured by using mathematic function of Yokogawa DL1620 digital oscilloscope. This oscilloscope is used to measure the lamp current and lamp voltage waveform in figure 4.16 too. This oscilloscope is appropriate for recording the waveform for a longer period of time. The specification of DL1620 is:

- 2 channels 200 MS/s
- 200 MHz analog bandwidth
- Maximum memory length: 8M point record length
- 6.4-inch wide-angle-view TFT color liquid crystal display

- USB compliant
- Ethernet connectivity
- Real-time digital filtering

Figure B.4 Yokogawa DL1620 digital oscilloscope

The AC line voltage and lamp voltage are higher than the allowable input range of these oscilloscope. Therefore, the Yokogawa 700924 voltage probe is used. Figure B.5 shows the picture of this voltage probe. The specification of this probe is:

Table B.3 Yokogawa 700924 specification

Input type	Balanced differential input
Frequency band	DC up to 100 MHz (-3 dB)
Input attenuation ratio	Switched between 1/100 and 1/1000
Input impedance	4 MΩ, approximately 10 pF parallel
Gain accuracy	±2% (common mode voltage ≤ 400 V) ±3% (common mode voltage ≤ 1000 V)
Maximum allowed differential voltage	±350 V (DC + ACpeak) or 250 Vrms (1/100 range) ±1400 V (DC + ACpeak) or 1000 Vrms (1/1000 range)
Maximum common mode input voltage	±1400 V (DC + ACpeak) or 1000 Vrms (both 1/100 and 1/1000 ranges)
Common Mode Rejection Ratio (CMRR)	-80 dB (60 Hz), -50 dB (1 MHz)
Output voltage	±3.5 V
Output impedance	Used with 1 MΩ input impedance
Power supplies	Dry cells, four R6P (SUM-3); when using the AC/DC adapter, use an output voltage of 6 V/200 mA or greater/center plus
Safety	EN61010-1: 1993 + A2: 1995 EN61010-2-031: 1994

Figure B.5 Yokogawa 700924 voltage probe

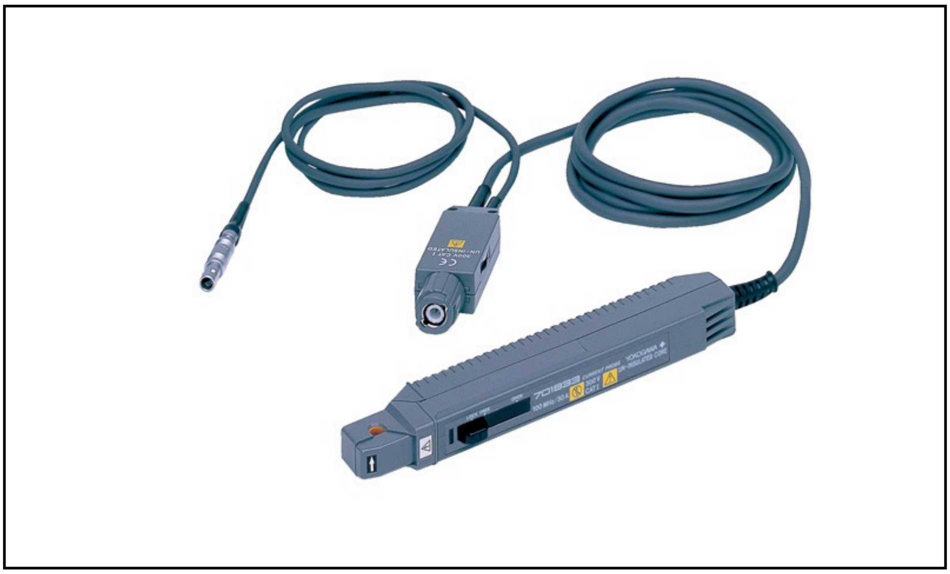

Figure B.6 Yokogawa 700937 current probe

The current waveform is acquired by using Yokogawa 700937 current probe. Figure B.6 shows the picture of Yokogawa 70093 current probe. This probe specification is:

Table B.4 Yokogawa 700937 specification

Frequency range	DC to 50 MHz (-3dB)
Maximum continuous input range	15 Apeak (AC + DC components)
Maximum peak current value	Non-continuous 30 Apeak ; at pulse width ≤ 10 μs, 50 Apeak
Output voltage rate	0.1 V/A
Amplitude accuracy	±0.5% rdg. ±1 mV
Noise	Equivalent to 2.5 mA rms or less
Temperature coefficient for sensitivity	±2% or less (within a range of 0 to 40°C)

B.3 Illuminance Measurement

Figure B.7 Kyoritsu 5202 digital light meter (Lux-meter)

Figure B.7 shows the picture of Kyoritsu 5202 digital light meter (Lux-meter). This light meter is used in chapter 4.5. The specification of this meter is:

Table B.5 Kyoritsu 5202 specification

Ranges	0.1~19990Lux	
Accuracy (23ºC±5ºC)	Lux	Accuracy
	200	±(4% rdg+5 dgt)
	2000	±(4% rdg+5 dgt)
	20000	±(5% rdg+4 dgt)
Angular Incident Light Characteristics	30º Less than ±3% 60º Less than ±10% 80º Less than ±30%	
Spectral Response Characteristics	JIS C1609 CLASS A	

APPENDIX C
Publication

1. P. Navaratana, S. Naetiladdanon, and A. Sangsawang, 2008, “Automatic Fluorescent Lamp Detection Technique for Electronic Ballasts”, **IEEE International Conference on Robotics and Biomimetics**, Feb., pp. 1047–1052.

Proceedings of the 2008 IEEE
International Conference on Robotics and Biomimetics
Bangkok, Thailand, February 21 - 26, 2009

Automatic Fluorescent Lamp Detection Technique for Electronic Ballasts

Piyasawat Navaratana, Sumate Naetiladdanon and Anawach Sangsawang
Department of Electrical Engineering
King Mongkut's University of Technology Thonburi
Toongkru, Bangkok 10140, THAILAND
{piyasawat.nav, sumate.nae & anawach.san}@kmutt.ac.th

***Abstract* - Due to the variation of fluorescent lamp power rating and types, the specified ballast could be used to meet the appropriate operating power. Generally, electronic ballast drives fluorescent lamp with fixed operating frequency. Such method can be used for only the designed lamp type and power rating. An operation of this type of ballast with mismatch lamp will cause damage on the lamp and/or ballast. This paper presents an Automatic Fluorescent Lamp Detection for Electronic Ballasts. This proposed method enables the ballast to determine the connected lamp's power rating and drive the lamp with proper operating frequency. The experimental results show 100% accuracy on the 3 power rated T8 lamps which are 18 watt, 32 watt and 36 watt.**

Index Terms - Fluorescent lamp, Power Rated, Electronic ballast, Current control.

I. Introduction

Plenty of organizations have many types of lamps installed, the fluorescent lamps usually be the highest in quantities due to its power efficiency. With fluorescent lamps, there are many types and power rated. With the large number of fluorescent types used, the more stocked lamps and ballasts are required. For example ballast for 18W, 32W and 36W T8 lamp should be stocked separately. And with the same physical size of 32W and 36W lamps, they can't be replaced by each other. Therefore, both lamps should be also stock separately. Using the mismatch ballast and lamp can cause damage on lamp and/or ballast. To solve this problem, automatic lamp detecting method is presented. After lamp power rated is detected, ballast will run at the proper frequency.

Unfortunately, there are not many literature techniques mention about lamp detecting methods. One of them, claimed to be the best method, using voltage across the lamp[1]. This method can differentiate lamp power using the lamp voltage. At ignition state, the lamp voltage is collected and used to classify the lamp. However, by the classical method that quickly decrease the driving frequency until the lamp voltage suddenly drop (current can be starting to flow through the lamp), the frequency at this after ignite stage can be varied. It's up to the lamp temperature, age and manufacturer. Therefore, the voltage across the lamp is varied too. Most of all, from Table 1 some type of lamp has the same voltage range (mark with dark gray). And by varying the frequency to supply the lamp power from 100% to 2%, the lamp voltage of some different rate is also overlapped. For example, 32WT8 and 58WT8 voltage is overlapped between 117V to 127V. This can outcome the incorrect lamp recognition.

TABLE I
TYPE OF LAMP AND ITS CHARACTERISTICS AT FULL AND MINIMUM POWER[6]

Lamp type	Ratting //Run (W)	100% V	100% I	2% V	2% I	Rs (cal.)	Vh (cal.)
	96//94	198	0.475	166	0.011314	68.66	165.39
	40//38	99	0.384	95	0.007961	9.41	95.38
	34//32	71	0.453	100	0.006374	-66.56	100.83
T12	20//19	78	0.244	71	0.005374	29.60	70.55
	70//68	129	0.528	141	0.009617	-24.53	141.66
	58//56	113	0.495	127	0.008800	-29.09	127.54
	40//38	100	0.381	117	0.006514	-45.30	116.97
	36//34	100	0.341	117	0.005828	-50.63	116.97
	32//30	117	0.257	131	0.004587	-56.00	131.07
	18//16	69	0.231	67	0.004764	9.38	67.13
T8	17//16	81	0.197	78	0.004371	18.38	77.70
	54	152	0.355	205	0.005267	-151.55	205.86
	39	134	0.290	145	0.005381	-37.23	145.16
	35	219	0.160	301	0.002329	-516.83	301.72
	28	191	0.147	212	0.002640	-147.29	212.52
	24	88	0.272	99	0.004849	-39.77	99.19
	21	141	0.148	177	0.002376	-241.97	177.35
T5	14	98	0.143	106	0.002640	-60.25	106.23
	55	134	0.417	205	0.008193	-173.04	206.48
	40//38	170	0.224	198	0.005758	-129.65	198.74
	36//34	113	0.301	134	0.007592	-72.42	134.90
	24//23	75	0.307	99	0.006970	-80.17	99.55
PL-L	18//17	62	0.273	88	0.005770	-97.83	88.95
	42	177	0.238	212	0.005940	-152.63	213.04
	32	120	0.266	173	0.005541	-203.45	174.37
	26//24	99	0.242	166	0.004333	-282.13	167.39
TC-T	18//17	71	0.240	141	0.003606	-298.60	142.50
	26//24	106	0.226	134	0.005359	-128.03	135.04
	18//17	99	0.172	127	0.004007	-168.64	127.95
	13	99	0.131	127	0.003064	-220.53	127.95
TC-DEL	10	57	0.177	85	0.003536	-163.27	85.43
	11	75	0.147	99	0.003334	-167.63	99.55
	9//8	48	0.166	85	0.002828	-224.82	85.49
	7//6	37	0.163	71	0.002546	-211.30	71.25
TC-EL	5	27	0.186	42	0.003536	-85.22	42.73

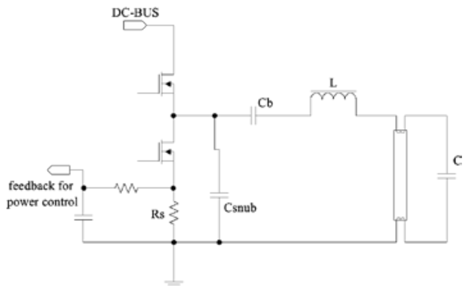

Fig. 1 a) Half bridge driver with resonance circuits

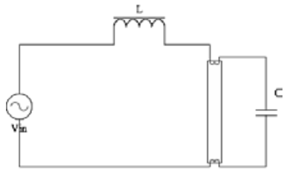

b) Simplified inverter and resonant circuits

To make it possible to implement, the constrain must be set. By regulating the lamp power after the ignition stage, the frequency is fixed. So the frequency variation is eliminated. The second problem is the lamp voltage overlapped between some different power rate lamp. Looking at the calculated Vh and Rs in Table 1, this represent the V-I characteristic of fluorescent lamp. This value is coming from the lamp dynamic model described in [2]. Its can also used to calculates the running frequency of lamp running with the ballast resonant circuit. Focus on the pair of overlapped voltage lamp, the Rd and/or Vh is differed. Therefore, detecting lamp characteristic is the better way. The frequency used to run the lamp at steady power is the easy way to determine the lamp characteristic. This idea is simulated using 2 stages general used circuit as shown in Figure 1a. The simplified inverter and resonant circuits[3] (Figure 1b.) is used to plot out the running frequency related to the running lamp power as shown in Figure 2.

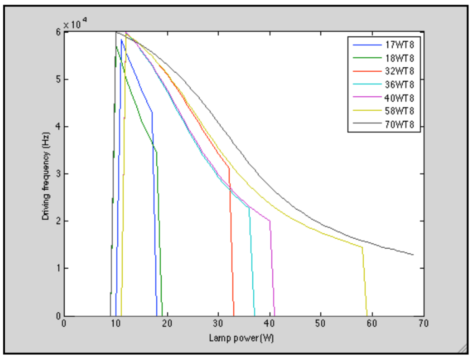

Fig.2 Frequency VS Lamp Power of T8

From Figure 2, the frequency is slightly difference between 36WT8 and 40WT8 and between 32WT8 and 58WT8. This graph show that the lamp detecting method can be implement using frequency at the steady lamp power.

This paper presents an automatic lamp detection using lamp power regulation and frequency detection. The lamp detecting algorithm divides into 3 steps which are the after ignition power regulation, possible step up power command and final decision. Using a microcontroller with PWM output, this algorithm is applied together with 2 stages general used circuit. The lamp power is regulated by using voltage across the resister(Rs) of low side driver MOSFET, assumed that power loss is constant related to the input power.

II. Lamp Detection Algorithm

A. Lamp power regulation

The average voltage across the Rs of low side driver MOSFET represent the current through the half-bridge driver (Figure 1a). This current is provide by DC-BUS which voltage is regulated by the high power factor boost converter.

$$P_{inv} = V_{DC} . I_{inv} \quad (1)$$

with constant V: $P_{inv} \alpha I_{inv}$ (2)

$$P_{inv} = P_{lamp} + P_{loss} \quad (3)$$

assume that P_{loss} is constant related to P_{inv} :

$$P_{inv} \alpha P_{lamp} \quad (4)$$

from (1): $P_{lamp} \alpha I_{inv}$ (5)

V_{DC} =DC voltage supplied by the boost converter

I_{inv} =Current through the inverter

P_{inv} = Power supplied by VDC through the inverter

P_{lamp} =Power using by the lamp

P_{loss} =Power loss by lamp filament and electrical componant

From equation (5), controls V_{RS} relatively controls P_{lamp}.

After preheat the filament, driving at high frequency, microcontroller quickly decrease the driving frequency until the voltage across the lamp suddenly dropped down. This is occur by the lamp suddenly change its impedance due to the complete ignition. The power command is then applied. This applied command is the lowest power rate of lamps to be detected. For example, use 16W power command for the group of T8. At the steady state (Pout=Pcommand), running frequency is collected. Because the frequency is commanded by microcontroller during power regulating loop, it already knows the running frequency itself. None of external frequency measurement is need. This frequency is used to classify the 18W(lowest) from the group. If frequency is in the range then it is the final decision and will step to the running procedure. To ensure that the lamp is recognized correctly, the possibility weight is introduced.

By the variation of lamps manufaturer, age and temperature, running frequency is not constant. From the experiment by regulating the lamp power, the results show the variation of running frequency. Table 2 and 3 present the average and standard deviation of running frequency at 16 to 68W of power regulation. The standard deviation is around 1-3% of average frequency. By simplifying the gaussian distribution, the trapezoid one is used. It is easier to implemented with the low-end 8 bits microcontroller. This trapezoid is what we call "possibility weight (*WP*)". Possibility weight of 18WT8 running at 16W (*WP18at16*)=1 means it is 100% possible that the lamp is 18W rate when considering at 16W power regulation.

TABLE II
AVERAGE RUNNING FREQUENCY OF BALLAST(KHZ)

Run(W) Lamp	16	30	34	38	56	68
T870W	56.97	41.46	35.83	30.60	<25kHz	<25kHz
T858W	56.47	36.31	30.77	26.35	<25kHz	
T840W	55.12	30.77	25.91	<25kHz		
T836W	54.99	30.19	25.36			
T832W	56.48	35.08				
T818W	39.81					
T817W	46.26					

TABLE III
STANDARD DEVIATION OF RUNNING FREQUENCY OF BALLAST(KHZ)

Run(W) Lamp	16	30	34	38	56	68
T870W	2.85	1.66	0.72	1.01		
T858W	2.43	1.27	0.62	0.79		
T840W	1.20	0.92	0.57			
T836W	2.42	1.72	0.61			
T832W	1.24	0.70				
T818W	2.07					
T817W	1.41					

Fig. 4 show the trapezoidal distribution using in this algorithm. From the Figure, the possibility weight is calculated by:

$$W_P = \begin{cases} 1; \bar{X} - 0.5SD, f, \bar{X} + 0.5SD \\ \dfrac{1}{SD} f - \dfrac{\bar{X} - 1.5SD}{SD}; \bar{X} - 1.5SD, f, \bar{X} - 0.5SD \\ \dfrac{-1}{SD} f + \dfrac{\bar{X} + 1.5SD}{SD}; \bar{X} + 0.5SD, f, \bar{X} + 1.5SD \end{cases} \quad (6)$$

Where $\bar{X} = \frac{1}{n}\sum_{i=1}^{n} f_i$, $SD = \sqrt{\frac{1}{n}\sum_{i=1}^{n}(f_i - \bar{X})^2}$ (7)

n=number of samples, f_i = frequency of sample i

The value of $\bar{X}$ and SD can be calculated by 2 methods. 1. from the real samples and 2. using frequency calculated by simplified inverter circuit and dynamic lamp model as mean and use 2-3% of calculated frequency as SD. Note that using the real samples will be better in performance depended on the number of samples used. If collecting the large number of sample is a difficult task, using the calculated one is fine (see the experimental results).

B. Possible step up power command

At this step, the power command is stepped up to the next power rated in the group if maximum W_P is not on the lamp that rated this power. For example, if maximum possibility weight is on 32WT8 running at 16W ($W_{P32at16}$)=1, it is the most possible that the lamp is 32W rate when considering at 16W power regulation. Nevertheless, the 32W lamp should run at 30W not 18W, the power command stepped up to the next level. After power command is stepped up, ballast will then regulates the output power to this new setting command. After controller reaches the steady state. The running frequency is collected. As the previous stage, the next power rated lamp is classified. The possibility weight is calculated using equation 6 also.

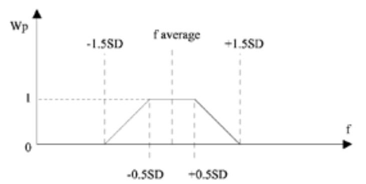

Fig. 4 possibility weight (W_P) VS running frequency

If lamp can not be classified in this stage, step up the power command and reclassify for the next power rated. Until the lamp is classified or reach the highest power command.

C. Final decision

In this stage, the possibility of all lamp rated is sum med. The highest summing weight determines the most possible lamp rated. If W_{P_TOTAL} is equal, the lower one is used. And if none of W_{P_TOTAL} is equal or above 1, lamp is not classified and will be shut down.

III. HARDWARE CONFIGURATION

First of all, the resonance circuit is designed using the simple resonant circuit design method[2]. Given DC supply is V_{DD} then:

$$V_{Lamp} = \frac{\sqrt{2}}{\pi} V_{DD} = 0.4502 V_{DD} \quad (8)$$

To calculate resonance inductor (L), the type of lamp and range of power rated should be defined.

In this paper we mention about T8 that is widely used. The power rated are 17W, 18W, 32W, 36W, 40W, 58 W and 70W. Using equation (9) [3], resonant L is calculated.

$$L = \frac{V_{DC}^{2}\eta}{4 f_{run}\sqrt{2}\pi^{2} P_{run}} \tag{9}$$

assume that efficiency (η) is 0.95 and V_{DC} is 400V, L is calculated using f_{run} = 25kHz and 55kHz (microcontroller we use can generated PWM output with frequency not more than 100kHz. And Frequency below 20kHz the lighting efficiency is significantly drop[4].)

TABLE IV
RESONANCE INDUCTOR CALCULATED RESULTS FOR T8

Power rated(W)	L for f=25kHz(H)	L for f=55kHz(H)
17	6.80E-03	3.09E-03
18	6.80E-03	3.09E-03
32	3.63E-03	1.65E-03
36	3.20E-03	1.45E-03
40	2.86E-03	1.30E-03
58	1.94E-03	8.83E-04
70	1.60E-03	7.27E-04

From Table 4, if we choose L=1.6mH this ballast will run with the lamp rated from 36W to 70W. If we choose 3.2mH, it will run with the lamp rated from 17W to 36W. If we choose 1.6mH, it will run with the lamp rated from 32W to 70W. The 32mH is selected because those rates are widely used in the market.

After that, with appropriate preheat current and preheat voltage, resonance C is calculated [3]:

$$C = \frac{I_{ph}^{2} L}{\left(V_{ph} + {V_{DC}}/{\pi}\right)^{2} - \left({V_{DC}}/{\pi}\right)^{2}} \tag{10}$$

that given C=4.26nF. Thus, 4.7nF is used.

IV. Simulation results

For working with T8 fluorescent lamp, the first control loop will start with 17W. Then the next power rates are applied until maximum W_P is on the lamp at its rate. Then W_P in every step will be summed by its relative power rated and classified by the maximum summing weight. Finally, if summation of W_P is not equal or above 1, lamp will not be classified.

To simulate the result, the fluorescent lamp dynamic model [2] is used

$$R_{lamp} = \frac{V_o R_s}{V_o - V_H} \tag{11}$$

The V_S and R_S can be found by measuring the lamp Voltage and Current. The results are in Table 1.

$$R_S = \frac{V_{fullpower} - V_{\min power}}{I_{fullpower} - I_{\min power}}$$

$$V_H = V_{\min power} - I_{\min power} R_S \tag{12}$$

Using these model, running frequency of designed ballast is calculated:

TABLE V
CALCULATED RUNNING FREQUENCY OF BALLAST WITH DESIGNED CIRCUIT

Run(W) Lamp	16	30	34	38	56	68
T870W	57.3kHz	39.6kHz	34kHz	29.1kHz	<20kHz	<20kHz
T858W	56.2kHz	34.1kHz	29.1kHz	25.3kHz	<20kHz	<20kHz
T840W	53.7kHz	29.5kHz	25.4kHz	22.3kHz	<20kHz	<20kHz
T836W	54.2kHz	30.2kHz	26kHz	22.7kHz	<20kHz	<20kHz
T832W	57.5kHz	35.4kHz	29.5kHz	25kHz	<20kHz	<20kHz
T818W	40kHz	20.4kHz	<20kHz	<20kHz	<20kHz	<20kHz
T817W	46.7kHz	23.9kHz	20.8kHz	<20kHz	<20kHz	<20kHz

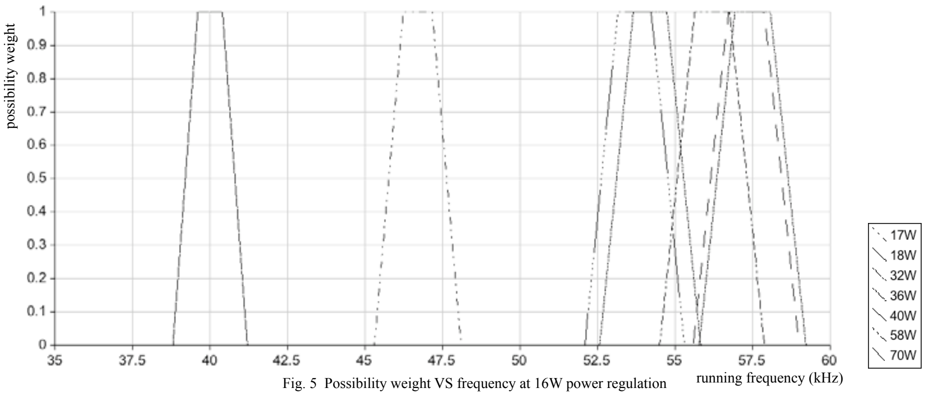

Fig. 5 Possibility weight VS frequency at 16W power regulation

Table 4 show that the designed ballast can run with T8-17W, 18W, 32W and 36W with full power. This ballast can also run with T8-40W, 58W and 70W but not the full power. The dark-gray highlight means “over rated running and can damage the lamp”. The gray means “frequency is lower than 25kHz”. By selecting SD 2%, from equation (6) with power command =16W:

$$W_{P17at16} = \begin{cases} 1; 46.23kHz, f, 47.17kHz \\ 1.07f - 48.5; 45.3kHz, f, 46.23kHz \\ -1.07f + 51.5; 47.71kHz, f, 48.1kHz \end{cases} \quad (13)$$

$\bar{X}$ =46.7kHz, SD=0.934kHz

$W_{P17at16}$ is possibility that the lamp is 17WT8 by determining at 16W power regulation.

$$W_{P36at16} = \begin{cases} 1; 53.66kHz, f, 54.74kHz \\ 0.92f - 48.5k; 48.5kHz, f, 53.66kHz \\ -0.92f + 51.5k; 54.74kHz, f, 55.83kHz \end{cases}$$

(14)

$\bar{X}$ =54.2kHz, SD=1.084kHz

$W_{P36at16}$ is possibility that the lamp is 36WT8 by determining at 16W power regulation.

Use the same equation by varying the power command and lamp type, the W_P related to them are calculated and used in this software. This calculation is plotted in Figure 5.

V. Experimental results

The experiments are divide into 2 part that are A. closed loop power control at 16W, 30W, 34W and 38W to find W_P of tested lamp and B. implement the automatic lamp detection to find out the classification rate. this experiment is set up by using designed ballast with 15 fluorescent lamps of each type. In each type, the lamp has 3 group of age include 5 out of the box lamps (new), 5 of 100 hours lamps and 5 of over 1000 hours lamps.
Note: Some of lamp is hardly to find (17W, 40W), less than 15 lamps is used and none of them are new.

A. Closed loop power control to find W_P

By picking up a 36W lamp, running at 16W regulated, the frequency is 55.8kHz. Using equation (6) given $W_{P17at16}$ = 0, $W_{P18at16}$ =0, $W_{P32at16}$ =0.32, $W_{P36at16}$ =0.32 and $W_{P40at16}$ =0. The $W_{P17at16}$ and $W_{P18at16}$ are not the highest one, power command is stepped up to 30W.

By running at 30W regulated, the frequency is 29.9kHz given $W_{P32at30}$ =0, $W_{P36at30}$ =1 and $W_{P40at30}$ =0.96. Also, the $W_{P32at30}$ is not the highest one, power command is stepped up to 34W.

By running at 34W the frequency is 25.8kHz given $W_{P36at34}$ =1 and $W_{P40at34}$ =0.87. the $W_{P36at34}$ is the highes, go to the final dicision.

In the final decision step, lamp will be classified into 36WT8 because the summation of W_{P36}=2.32 which is the highest as seen in Table 6.

TABLE VI
POSSIBILITY WEIGHTS OF TESTED 36W T8

Run Rate(W)	16	30	34	38	56	68	Sum
70	0.45	0.00	0.00				0.45
58	1.00	0.00	0.00				1.00
40	0.00	0.96	0.87				1.83
36	0.32	1.00	**1.00**				**2.32**
32	0.32	0.00					0.32
18	0.00						0.00
17	0.00						0.00

Again pick up a 32W lamp, the result is in Table 7. In step 2 of algorithm, ballast will step to final decision due to $W_{P32at30}$ is maximum ($W_{P32at30}$ =1). In the final decision, lamp will be classified as 32WT8 because the summation of W_{P32}=2 which is the highest as shown in Table 7.

TABLE VII
POSSIBILITY WEIGHTS OF TESTED 32W T8

Run Rate(W)	16	30	34	38	56	68	Sum
70	0.94	0.00					0.94
58	1.00	0.44					1.44
40	0.00	0.00					0.00
36	0.00	0.00					0.00
32	1.00	**1.00**					**2.00**
18	0.00						0.00
17	0.00						0.00

B. Implementation of automatic lamp detection

By testing with 3 type of lamps include 18W, 32W and 36W T8. The result show the 100% classification rate. This experiment is done by measuring the lamp output power after 30 seconds after switched on.

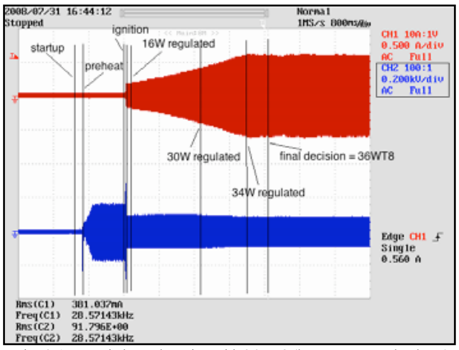

Fig. 6 Automatic lamp detection with 36WT8 (lamp current and voltage)

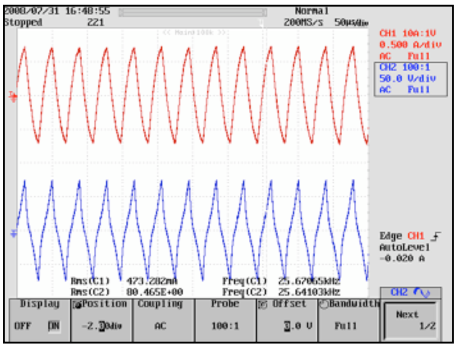

Fig. 7 Lamp current and voltage (zoom) of running 36WT8

3 seconds after ignited, 36W lamp is detected. This make the lamp not flash to the maximum power but slowly increase its power to the maximum. Figure 7 show running frequency is 25.6 kHz.

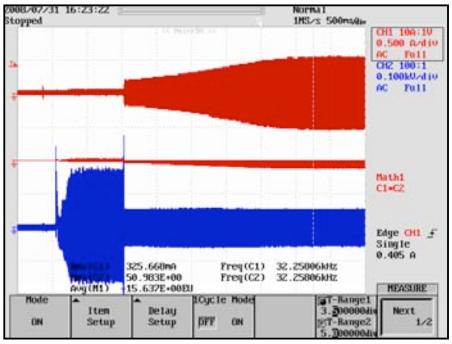

Fig. 8 Automatic lamp detection with 18WT8 (lamp current and voltage)

Figure 8 show that about 2 seconds after ignite, the lamp is classified as 18W. Therefore, the “Avg(M1)” show the regulated lamp power at running stage = 15.637W. The running lamp current, lamp voltage and frequency is shown in Figure 9.

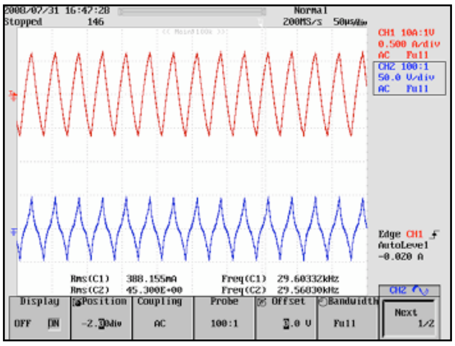

Fig. 9 Automatic lamp detection with 18WT8 (lamp current and voltage)

VI. CONCLUSIONS

By the method presented, it shows the trustability of detected results. This method combines with lamp power regulation and lamp power rate classification using its running frequency. It results in correct determination of lamp power rating on all of samples. To complete this algorithm, ballast take less than 5 seconds after ignition stage. The only thing to be concerned is the variation of resonance inductor value. It highly affects the operating frequency that is the most important role in this method.

REFERENCES

[1] L.M. Lee, S.Y.R. Hui and H.S.H. Chung, “An Automatic Lamp Detection Technique for Electronic Ballasts”, *IEEE*, 2005, pp 575-581

[2] T.-F. Wu, J.-C. Hung and T.-H. Yu, “A PSpice Model for Fluorescent Lamps Operated at High Frequencies”, *IEEE*, 1995, pp. 359-364

[3] Zhi Lie, Philip K. T. Mok, Wing-Hung Ki and Johnny K. 0. Sin, “A Simple Method to Design Resonance Circuits of Electronic Ballast for Fluorescent Lamps”, *IEEE International Symposium on Circuits and Systems*, pp 1744-1747, 1997

[4] 1. John, E. Kaufman, Jack F. Christensen and Illuminating Engineering Society of North America, 1984, “IES Lighting Handbook”, Illuminating Engineering Society

[5] Thomas J. Ribarich and John J. Ribarich (conslt.), “A New Procedure for High-Frequency Electrßonic Ballast Design”, *IEEE Industry Applications Society Annual Meeting, New Orleans, Louisiana, October 5-9, 1997*

[6] International Rectifier Corporation, IR Ballast Designer version 4.1.7, lamp characteristics, 2006

2. P. Navaratana, S. Naetiladdanon, and A. Sangswang, 2009, "Automatic Fluorescent Lamp Detection for Electronic Ballasts Based on Operating Frequency and Phase Shift Compensation", **IEEE International Symposium on Industrial Electronics**, July, pp. 53–58.

IEEE International Symposium on Industrial Electronics (ISIE 2009)
Seoul Olympic Parktel, Seoul, Korea July 5-8, 2009

Automatic Fluorescent Lamp Detection for Electronic Ballasts Based on Operating Frequency and Phase Shift Compensation

Piyasawat Navaratana Na Ayudhya, Sumate Naetiladdanon and Anawach Sangswang
Electrical Engineering, King Mongkut's University of Technology Thonburi
Toongkru, Bangkok 10140, THAILAND
Email: piyasawat.nav@kmutt.ac.th, sumate.nae@kmutt.ac.th and anawach.san@kmutt.ac.th

***Abstract*—Generally, an electronic ballast drives a fluorescent lamp at fixed operating frequency or by regulating the lamp current. Such methods can be used for the designed lamp type and power rating. This paper presents an automatic fluorescent lamp detection for electronic ballasts based on operating frequency and phase shift compensation. The classification of lamp power rating is based on the possibility weight distribution of the lamp operating frequency. Moreover, the phase shift compensation is also included in the detection algorithm in order to address the variations of the resonant circuit parameters. The results from simulation and experiment verify that an electronic ballast with the proposed detection algorithm can automatically detect and drive the fluorescent lamp at the correct lamp power rating.**

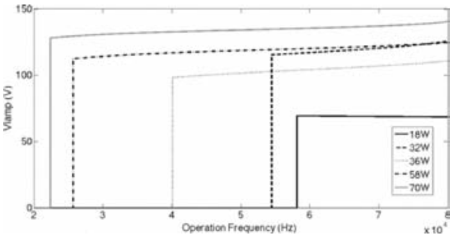

Fig. 1. Operating frequency VS Lamp voltage

I. INTRODUCTION

The fluorescent lamps are accepted as one of the highest power efficiency lamp. These lamps are widely used in many organizations. The problem is that there are many types and power ratings. With a large number of fluorescent types used, the more stocked lamps and ballasts are required, since ballasts for 18W, 32W and 36W T8 lamps are not interchangeable. Any mismatch of ballast and lamp power ratings will usually lead to damage of lamp and/or ballast by either over current or hard switching. To solve this problem, automatic lamp detecting methods were presented [1], [2].

There are some literature techniques on lamp detecting methods. One of them using lamp operating voltage[1]. This method can differentiate the lamp power ratings by using the lamp voltage. After ignition, the lamp voltage is collected and used to identify the lamp wattage. However, the striking frequency of the fluorescent lamp can be varied, depending on the lamp temperature, age and manufacturer. Therefore, the lamp voltage after striking(ignition) is also varied. Generally, different lamp types may have overlapping voltage range for example, 32WT8 and 58WT8 lamps operate on the same voltage ranging from 117V to 127V as shown in Fig. 1. The Voltage detection method proposed in [1] may result in misdetection between both lamp. In addition, the voltage can easily be interfered by noise which is always occurred in switching systems. Our previous method[2] fixed the detecting condition by regulating output power at proper rated. By doing this, the power of the lamp is fixed and easier to classify the lamp. Instead of using voltage, this paper uses the operating frequency to classify the lamp. This outcome more accuracy results because the frequency is generated by controller itself (Fig. 5). However, frequency considering is highly depended on the variation of resonant parameters. By changing the value of inductor or capacitor, the controller will changes the operating frequency to regulate the output power. This may results the misclassifying.

This paper proposes an automatic fluorescent lamp detection for electronic ballasts based on the operating frequency and phase shift compensation. A slight deviation of resonant parameters are recognized by considering the phase shift between the inverter output voltage and current. The frequency detection region is then shifted to the appropriate range. Although the system parameter is dependent on the resonant circuit, the error from small variation of resonant parameters is decreased. The proposed algorithm can easily implemented on a 8-bits micro-controller based electronic ballast.

II. BALLAST DESIGN CONSIDERATION

In this work, a typical 2-stages electronic ballast is considered. It consists of a DC-DC converter and a half bridge inverter with resonant circuit. The micro-controller controls the inverter by generating a signal to the MOSFET driver. In Fig. 2, by varying the square wave frequency, the ballast can operate in pre-heat, strike and running stages. The lamp current can also be controlled through frequency variation as shown in Fig. 3 [3]. Fig. 2 shows the block diagram of the electronic ballast and its driving circuit used in this paper.

978-1-4244-4349-9/09/$25.00 ©2009 IEEE

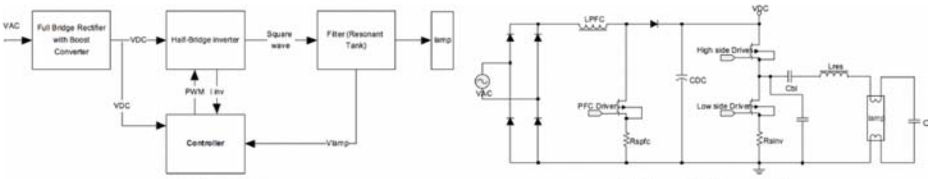

(a) Block Diagram (b) Schematic of power parts

Fig. 2. Block diagram and schematic of electronic ballast using in this paper

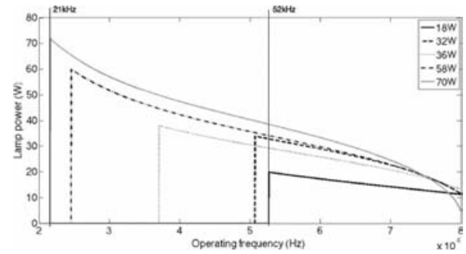

Fig. 3. Operating frequency VS Lamp power

A. Resonant circuit design

First of all, both inductor and capacitor of resonant circuit should be selected. Note that, this paper focuses on driving all of the lamp power ratings in T8 series, which are widely used and easily to purchase. The resonant inductor is calculated using the method from [5]. This method assumes that the resonant circuit with the lamp in configuration will appear to the source as positive resistance. Thus the lamp resistance, negative differential resistance [6], is disappeared from the following equation.

$$L = \frac{V_{DC}^2 \eta}{4 f_{run} \sqrt{2} \pi^2 P_{lamp}} \quad (1)$$

where V_{DC} is the DC supply voltage(V); η is the efficiency of inverter; f_{run} is the running or operating frequency and P_{lamp} is the power using by the lamp.

An operation at a frequency lower than 25kHz would significantly reduce the light efficacy. If the operating frequency is chosen too high, more current will be drawn to the lamp terminals due to the lower capacitor reactance (Xc). The increased current however, turns into power loss at the lamp terminals and the light efficacy would further decrease. In this work, the frequency range of 25kHz to 65 kHz is empirically chosen and substituted in (1) with η = 0.95 and VDC = 400V. The inductances of each lamp wattage are shown in TABLE I. Notice that for the lamp wattage of 32W to 70W, the overlapped inductance is in the range of 1.309mH to 1.556mH while the lamp wattage of 18W to 36W gives the inductance of 2.327mH to 3.025mH. The midpoint inductance between the two ranges is chosen at 1.9mH and used in the design procedure in [5] to determine the operating frequency. The resonant capacitance is calculated by

TABLE I
RESONANCE INDUCTOR CALCULATED USING EQUATION 1

Power rate(W)	L(mH) at f=25kHz	L(mH) at f=65kHz
18	6.050	2.327
32	3.403	1.309
36	3.025	1.163
58	1.878	0.722
70	1.556	0.598

$$C = \frac{I_{ph}^2 L}{(V_{ph} + V_{DC}/\pi)^2 - (V_{DC}/\pi)^2} \quad (2)$$

Where Iph is the preheat current (A); Vph is the peak preheat voltage (V) and L is the resonant inductance obtained from (1). A quick substitution in (2) gives the resonant capacitance of 4.11nF. Due to availability, a typical capacitance of 4.7 nF is chosen. Once the inductance and capacitance are obtained, they are used in computer simulation to validate the operating frequency as shown in Fig. 3. The operating frequency is located in the range of 21kHz to 52kHz where the lowest frequency is slightly lower than the originally selected frequency of 25kHz with no noticeable difference in light efficacy [6].

B. Lamp power regulation

The operating frequency plays an important role since the lamp power is increased as the frequency is reduced. The inverter must operate under appropriate frequency to avoid lamp damages. The current regulation method is used to control the lamp power with in its rating[4]. The average voltage of the R_{sinv} on the low side driver MOSFET in Fig. 2(b) represents the current through the half-bridge driver. This current is provided by the DC-BUS voltage which is regulated by the boost converter. The input power(P_{inv}) is given as,

$$P_{inv} = V_{DC}.I_{inv} \quad (3)$$

With constant DC voltage:

$$P_{inv} \ \alpha \ I_{inv} \quad (4)$$

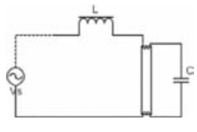

Fig. 4. Simplify version of inverter

Thus,

$$P_{inv} = P_{lamp} + P_{loss} \tag{5}$$

where P_{loss} is the system loss and constant related to P_{lamp}. The power relationship is found as,

$$P_{inv} \ \alpha \ P_{lamp} \ \alpha \ I_{inv} \tag{6}$$

where I_{inv} is the current through the inverter; P_{inv} is the power supplied by V_{DC} through the inverter and $P_{loss}$is the ower loss by lamp filaments and electrical components From (6), controls $V_{R_{sinv}}$ indirectly control P_{lamp}.

The simplify version of inverter [9] as shown in Fig. 4 is used to simulate the results. Lamp power can be calculated as;

$$I_{lamp} = \frac{\sqrt{2}V_S}{Z_0\sqrt{Q_L^2\left[1-\left(\frac{\omega}{\omega_0}\right)^2\right]^2+\left(\frac{\omega}{\omega_0}\right)^2}} \tag{7}$$

$$P_{lamp} = \frac{V_S^2 R_{lamp}}{Z_0^2\left[Q_L^2\left(1-\left(\frac{\omega}{\omega_0}\right)^2\right)^2+\left(\frac{\omega}{\omega_0}\right)^2\right]} \tag{8}$$

where $V_S = \frac{\sqrt{2}}{\pi}V_{DC}$, $\omega_0 = \frac{1}{\sqrt{LC}}$, $Z_0 = \sqrt{\frac{L}{C}}$ and $Q_L = \frac{R_{lamp}}{Z_0}$. From [7] the negative differential resistance of fluorescent is simplified as;

$$R_{lamp} = \frac{V_0 R_S}{V_0 - V_H} \tag{9}$$

where V_0 is the voltage at present condition and R_S and V_H are defined as;

$$R_S = \frac{V_{Max} - V_{min}}{I_{Max} - I_{min}} \tag{10}$$

$$V_H = V_{min} - I_{min}R_S \tag{11}$$

where V_{Max} is lamp voltage at the highest power; V_{min} is the lamp voltage at the lowest power; I_{Max} is the lamp current at the highest power and I_{min} is the lamp current at the lowest power. These parameters were acquired from [8]. To simulate the results, assume the initial R_{lamp} is 1000. Use (7) to calculate the current. Then the new V_0 is calculated using $V = IR$. Using this V_0 to calculate the new R_{lamp}. Recalculate the current and R_lamp until the current is stable. Then the lamp power from this current is calculated. If the lamp power is less than the power command then reduce the frequency and recalculate the lamp power. Repeat these procedures until lamp power is equal to the power command. After that, this frequency and power command is plotted in Fig. 5. Since the high frequency ballast result 10% higher efficacy than magnetic ballast, the fluorescent lamp usually set the output power 2W below its rating as using in this paper.

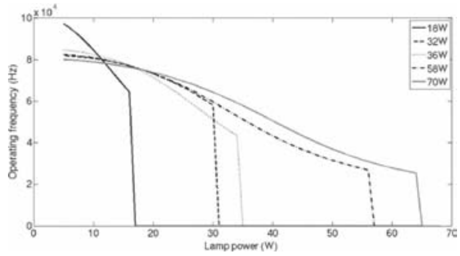

Fig. 5. Simulation output using power regulation command and frequency results

III. Lamp detection algorithm

At preheating process, the inverter is driven at high frequency. Then the micro-controller quickly decreases the driving frequency until the lamp is striked. The striking process is detected via the negative of $\frac{dv}{dt}$. The power command is applied. This applied command is the lowest power rating of lamps to be detected. For example, the 16W power command is used for the group of T8. At the steady state ($P_{out} = P_{command}$), operating frequency is collected. The operating frequency is controlled by power regulating loop; thus, the external frequency measurement is not necessary. , it already knows the frequency itself. None of external frequency measurement is need. This frequency is used to classify the 18W(lowest) power rating lamp from the group due to 10% higher efficacy.

A. The lamp detection by considering the operating frequency

The classification algorithm is as follows;

1) Regulate at the lowest power rating. Ex: 16W for T8 series.
2) Calculate the possibility weights (W_P). From the samples of lamps regulated power at each rate include 16, 30, 34, 56 and 68 W, trapezoidal-shaped possibility weight function (W_P) is setting as shown in (12).
   - If the highest W_P is on the lamp rating related to this power regulated command then STOP. Ex:W_P is the highest on 18W lamp when it is regulated at 16W ($W_{P(18at16)}$ is the highest)
   - If not, then increase to the next power command. Ex: W_P is the highest on 36W lamp when it is regulated at 16W ($W_{P(36at16)}$ is the highest)
3) Step up to the next power command (30, 34, 56 and 68 in sequence) and do step 1) again until the power command reaches the highest value or STOP at step 2).
4) Sum the W_P of each lamp power rating. Ex: $W_{P(36)} = W_{P(36at16)} + W_{P(36at30)} + W_{P(36at34)}$

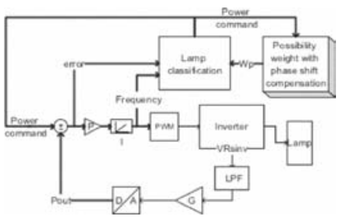

Fig. 6. Lamp detection based on operating frequency and phase shift compensation

5) Run at the maximum of sum W_P in step 4).

$$W_P = \begin{cases} 1, & \overline{x}_f - 0.5sd_f < f < \overline{x}_f + 0.5sd_f; \\ \frac{1}{sd_f}f - \frac{\overline{x}_f - 1.5sd_f}{sd_f}, & \overline{x}_f - 1.5sd_f < f < \overline{x}_f - 0.5sd_f; \\ \frac{-1}{sd_f}f + \frac{\overline{x}_f + 1.5sd_f}{sd_f}, & \overline{x}_f + 0.5sd_f < f < \overline{x}_f + 1.5sd_f; \\ 0, & \text{elsewhere.} \end{cases} \tag{12}$$

The Block diagram of this control scheme is shown in Fig. 6. Operating frequency are acquired from sample lamps to calculate the average ($\overline{x}_f$) and deviation (sd_f) of operating frequency of lamps operating at 16, 30, 34, 56 and 68 W power regulated as shown in (13).

$$\overline{x}_f = \frac{1}{n}\sum_{i=1}^{n} f_i, \; sd_f = \sqrt{\frac{1}{n}\sum_{i=1}^{n}(f_i - \overline{x}_f)^2} \tag{13}$$

For example with a Philips 36W T8 TLD lamp, if the average operating frequency of 36W lamp running at 16W regulated is 54.2 kHz and its standard deviation is 1.084 kHz. The W_P can be calculated as;

$$W_{P(36at16)} = \begin{cases} 1, & 53.66 < f < 54.74 \text{ kHz}; \\ 0.92f - 48.5k, & 48.5 < f < 53.66 \text{ kHz}; \\ -0.92f + 51.5k, & 54.74 < f < 55.83 \text{ kHz}; \\ 0, & \text{elsewhere.} \end{cases} \tag{14}$$

Where the 36W T8 lamp is operated at 16W (Ex:f = 55.8kHz), $W_{P36at16}$ equals 0.32. Using this frequency to calculate another W_P, results $W_{P18at16} = 0$, $W_{P32at16} = 0.32$, $W_{P58at16} = 1$ and $W_{P70at16} = 0.45$. The highest W_P is not on $W_{P18at16}$. Thus, the next power command is 30W regulated and W_P is recalculated again at this level. The calculated results is shown in TABLE II. The algorithm stops at 36W lamp due to the maximum on $W_{P(36at34)}$. The summation of W_P as 2.32 is the highest at 36W so the lamp is detected as 36W which is correct.

B. Phase shift compensation

Change in parameters of resonant circuit affects this algorithm which results misclassification. These variation might occur from the production, temperature and life of each L or C. Fig. 7 and 8 show the change in operating frequency due to the variation of capacitance and reductance in this circuit.

TABLE II
CALCULATED RESULT OF W_P OF UNKNOWN CONNECTED LAMP

Power command / Lamp rating	16W	30W	34W	56W	68W	Sum
18W	0					0
32W	0.32	0				0.32
36W	0.32	1	1			2.32
58W	1	0	0			1
70W	0.45	0	0			0.45

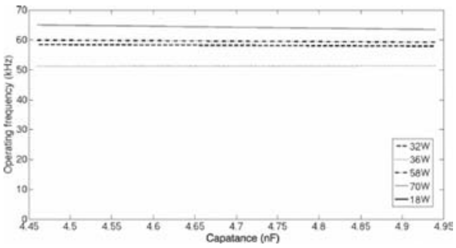

Fig. 7. Relation between capacitance and operating frequency

From Fig. 7, there is a small change in operating frequency because the capacitance is very high compare to a lamp resistance. The variation of inductance affects the operating frequency and consequently the output power as shown in (8).The relations between L and f, L and phase angle (ϕ) and phase angle and f are plotted in Fig. 8, 9 and 10. The relationship between frequency and phase angle due to the variation of L within 10% is almost straight line. Thus, this can be approximate as linear equations (15).

$$\overline{x}'_f = a\phi + b : \phi_{min} < \phi < \phi_{max} \tag{15}$$

$$a = \frac{f_2 - f_1}{\phi_2 - \phi_1}, \; b = f_1 - a\phi_1 \tag{16}$$

By using (15), the $\overline{x}_f$ in (12) is changed to $\overline{x}'_f$ in order to compensate with small change in resonant circuit parameters.

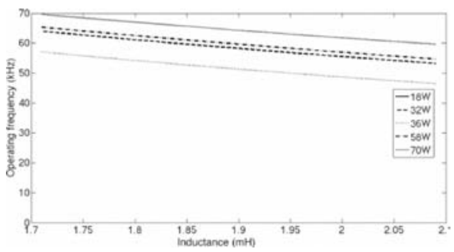

Fig. 8. Relation between inductance and operating frequency

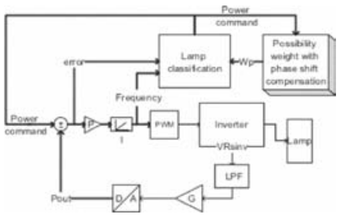

Fig. 6. Lamp detection based on operating frequency and phase shift compensation

5) Run at the maximum of sum W_P in step 4).

$$W_P = \begin{cases} 1, & \overline{x}_f - 0.5sd_f < f < \overline{x}_f + 0.5sd_f; \\ \frac{1}{sd_f} f - \frac{\overline{x}_f - 1.5sd_f}{sd_f}, & \overline{x}_f - 1.5sd_f < f < \overline{x}_f - 0.5sd_f; \\ \frac{-1}{sd_f} f + \frac{\overline{x}_f + 1.5sd_f}{sd_f}, & \overline{x}_f + 0.5sd_f < f < \overline{x}_f + 1.5sd_f; \\ 0, & \text{elsewhere.} \end{cases} \quad (12)$$

The Block diagram of this control scheme is shown in Fig. 6. Operating frequency are acquired from sample lamps to calculate the average ($\overline{x}_f$) and deviation (sd_f) of operating frequency of lamps operating at 16, 30, 34, 56 and 68 W power regulated as shown in (13).

$$\overline{x}_f = \frac{1}{n}\sum_{i=1}^{n} f_i, \; sd_f = \sqrt{\frac{1}{n}\sum_{i=1}^{n}(f_i - \overline{x}_f)^2} \quad (13)$$

For example with a Philips 36W T8 TLD lamp, if the average operating frequency of 36W lamp running at 16W regulated is 54.2 kHz and its standard deviation is 1.084 kHz. The W_P can be calculated as;

$$W_{P(36at16)} = \begin{cases} 1, & 53.66 < f < 54.74 \text{ kHz}; \\ 0.92f - 48.5k, & 48.5 < f < 53.66 \text{ kHz}; \\ -0.92f + 51.5k, & 54.74 < f < 55.83 \text{ kHz}; \\ 0, & \text{elsewhere.} \end{cases} \quad (14)$$

Where the 36W T8 lamp is operated at 16W (Ex:f = 55.8kHz), $W_{P36at16}$ equals 0.32. Using this frequency to calculate another W_P, results $W_{P18at16} = 0$, $W_{P32at16} = 0.32$, $W_{P58at16} = 1$ and $W_{P70at16} = 0.45$. The highest W_P is not on $W_{P18at16}$. Thus, the next power command is 30W regulated and W_P is recalculated again at this level. The calculated results is shown in TABLE II. The algorithm stops at 36W lamp due to the maximum on $W_{P(36at34)}$. The summation of W_P as 2.32 is the highest at 36W so the lamp is detected as 36W which is correct.

B. Phase shift compensation

Change in parameters of resonant circuit affects this algorithm which results misclassification. These variation might occur from the production, temperature and life of each L or C. Fig. 7 and 8 show the change in operating frequency due to the variation of capacitance and reductance in this circuit.

TABLE II
CALCULATED RESULT OF W_P OF UNKNOWN CONNECTED LAMP

Power command / Lamp rating	16W	30W	34W	56W	68W	Sum
18W	0					0
32W	0.32	0				0.32
36W	0.32	1	1			2.32
58W	1	0	0			1
70W	0.45	0	0			0.45

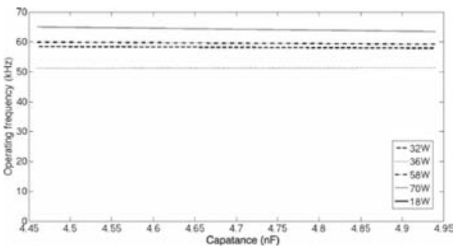

Fig. 7. Relation between capacitance and operating frequency

From Fig. 7, there is a small change in operating frequency because the capacitance is very high compare to a lamp resistance. The variation of inductance affects the operating frequency and consequently the output power as shown in (8).The relations between L and f, L and phase angle (ϕ) and phase angle and f are plotted in Fig. 8, 9 and 10. The relationship between frequency and phase angle due to the variation of L within 10% is almost straight line. Thus, this can be approximate as linear equations (15).

$$\overline{x}'_f = a\phi + b : \phi_{min} < \phi < \phi_{max} \quad (15)$$

$$a = \frac{f_2 - f_1}{\phi_2 - \phi_1}, \; b = f_1 - a\phi_1 \quad (16)$$

By using (15), the $\overline{x}_f$ in (12) is changed to $\overline{x}'_f$ in order to compensate with small change in resonant circuit parameters.

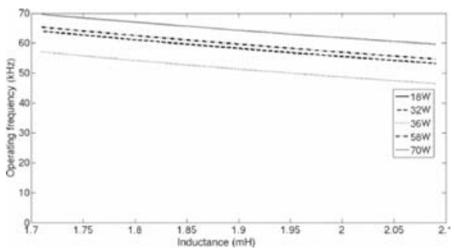

Fig. 8. Relation between inductance and operating frequency

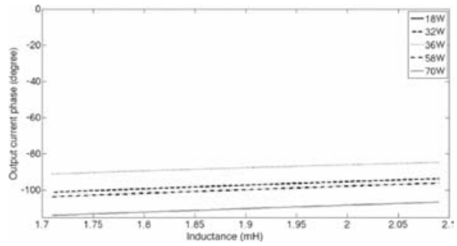

Fig. 9. Relation between inductance and current phase angle

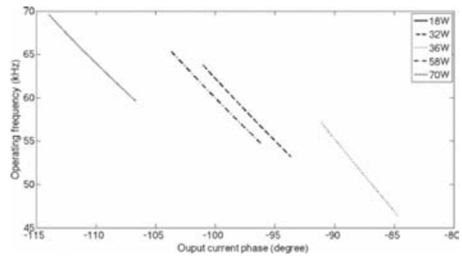

Fig. 10. Relation between operating frequency and current phase angle

This will make the better classification results.

IV. Experimental results

This experiment is divided into 4 groups. The first group uses the plain frequency detection with designed L and C. The second group decreases L by 5%. The third group heat up the lamp to change the resistance. The last group decreases C by 5%.

Using designed resonant inductor and capacitor, the results of the tested lamps with frequency detection is outcome the correct results since the variation of lamp resistance has not much effect on frequency. TABLE III shows the highest W_P at 32W. This is the worst case because the impedance of 32W is very close to that of 58W lamp. The small variation of L makes the big change in operating frequency with results in the misclassification.

By changing L from 1.9 to 1.8 mH causes the operating frequency move from 58.2 to 61.1 kHz when ballast regulates at 30W. This frequency will be considered as 58W lamp which has average operating frequency around 59.62kHz using L 1.9mH. Driving 32W at 56W is danger and will damage lamp and ballast. With the phase shift compensation (15) the new $\overline{x'}_f$ is 61.12kHz (ϕ=-99.25). This process makes the recognition result to the right 32W lamp (TABLE V). The "or" in TABLE IV means ϕ is over ϕ_{Max} or under ϕ_{min}. It blocks the algorithm not to detect.

With the rising of lamp temperature it has an effect on lamp resistance and will change the current phase angle too. With the phase angle change, this algorithm will move the $\overline{x}_f$ to $\overline{x'}_f$ as shown in (15). Fig. 11 shows the relation between ϕ and f when lamp resistance is varied. This graph shows the same slope direction as the change of L but with difference slope values. From the result the change in phase angle, it does not much affect the frequency calculated by phase shift compensation.

By heating up the lamp, the operating frequency increases to 58.5kHz and ϕ is -97.67. This phase shift make the new $\overline{x}_f$ move to 58.84kHz. The result is shown in TABLE VI. It also results the correct 32W.

The last test deals with changing C to 4.5nF. It results

TABLE III
Calculated results of W_P for an unknown lamp

Power command / Lamp rating	16W	30W	34W	56W	68W	Sum
18W	0					0
32W	1	1				2
36W	0	0				0
58W	1	0.44				1.44
70W	0.94	0				0.94

TABLE IV
Phase shift compensation for 30W regulated, L=1.8mH

Rating	a	b	ϕ_{min}	ϕ_{Max}	$\overline{x'}_f$
32W	-1.4328	-81.0834	-99.26	-95.33	61.12
36W	-1.6652	-94.6468	-89.38	-86.06	70.62(or)
58W	-1.4054	-80.5046	-101.76	-97.8	58.98
70W	-17.4	-1884.8	-112.17	-108.32	-157.85(or)

TABLE V
Calculated results of W_P of 32W lamp with L=1.8mH

Power command / Lamp rating	16W	30W	34W	56W	68W	Sum
18W	0(or)					0
32W	0.22	1				1.22
36W	0(or)	0(or)				0
58W	0	0				0
70W	0(or)	0(or)				0

TABLE VI
Phase shift compensation for 30W regulated, R=624.2Ω

Rating	a	b	ϕ_{min}	ϕ_{Max}	$\overline{x'}_f$
32W	-1.4328	-81.0834	-99.26	-95.33	58.84
36W	-1.6652	-94.6468	-89.38	-86.06	67.98(or)
58W	-1.4054	-80.5046	-101.76	-97.8	56.75
70W	-17.4	-1884.8	-112.17	-108.32	-185.52(or)

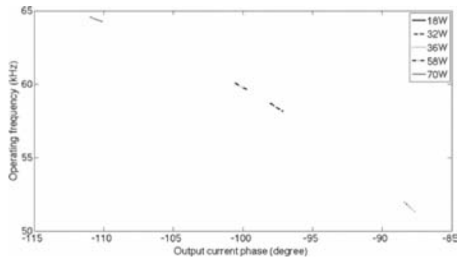

Fig. 11. Relation between operating frequency and current phase angle

TABLE VII
PHASE SHIFT COMPENSATION FOR 30W REGULATED, C=$4.5nF$

Rating	a	b	ϕ_{min}	ϕ_{Max}	$\overline{x'}_f$
32W	-1.4328	-81.0834	-99.26	-95.33	55.92
36W	-1.6652	-94.6468	-89.38	-86.06	64.58(or)
58W	-1.4054	-80.5046	-101.76	-97.8	53.88(or)
70W	-17.4	-1884.8	-112.17	-108.32	-221.01(or)

in frequency changing to 58.4kHz and ϕ is -95.6. The $\overline{x'}_f$ moves to 55.92kHz. The result is shown in TABLE VI. By recalculates the W_P, It also results the correct 32W.

Fig. 12 shows the operation process result of this proposed algorithm applied with 36W lamp. The oscilloscope is setup with 0.5A/div in channel 1 ,200V/div in channel 2 and 800ms/div for time. The recognition process take approximately 2.8 seconds after striking or 4 seconds from startup. The algorithm has 3 step of lamp regulated consist of 16W, 30W and 34W. This process will take longer that in case of higher lamp rate. The maximum classification time is with 70W lamp rating is less than 6 seconds from startup.

From the detection results with another tested lamp outcome the correct answer with L variation is less than 5% compare to not more than 1% with only frequency detection. With the variation of lamp resistance or capacitance is different. The tolerance of changing them is significantly dropped. This algorithm allows R and C to be varied with in 5%. Compare to the previous methods the previous one has higher tolerance for both C and R values shifting by 10-15%. But for the L it has only 1% tolerance. And comparing to the voltage consideration method, this frequency and phase consideration method can classify the lamp that has very close impedance like 58w and 32w in the tolerance region.

V. CONCLUSION

An automatic lamp detection method by considering the frequency and phase shift has been tested for T8 fluorescent lamps. The results show the correct classification; especially, for the lamp that has very close impedance like 58W and 32W lamps. But the very weak point of this method is such a frequency is much depended on resonant parameters. This

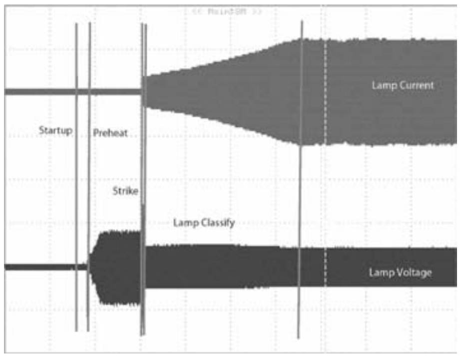

Fig. 12. The tested lamp output waveform running with this proposed algorithm

becomes a low tolerance of resonant circuit parameters especially the inductor. With the proposed phase compensation, the tolerance of inductance varied to 5%. This is in exchange with the lower tolerance with capacitance and lamp resistance variation dropped down to around 5%. Although this does not affect the normal condition lamps, the end of life and the near end of life lamps are affected. An unpredictable result occurred for such this kind of lamp. Thus, the end of life protection should be applied in order to shutdown the ballast when connected to the end of life lamp.

ACKNOWLEDGMENT

The authors would like to thank DYNO Electric Co.,Ltd, Thailand for the sample lamps and the other essential stuffs.

REFERENCES

[1] L. Lee, S. Hui, and H. Chung. "An automatic lamp detection technique for electronic ballasts.", *Applied Power Electronics Conference and Exposition, 2005, Twentieth Annual IEEE*, 1:575–581 Vol. 1.
[2] P. Navaratana, S. Naetiladdanon, and A. Sangswang. "Automatic fluorescent lamp detection technique for electronic ballasts.", *IEEE International Conference on Robotics and Biomimetics*, 2009.
[3] F. Teng, C. Liu, K. Wei, and Z. Zhang. "Mixed mode control for dimming electronic ballast.", *Power Electronics and Motion Control Conference, 2004. The 4th International*, 2:831–835 Vol.2.
[4] R.-L. Lin and Y.-T. Chen. "Electronic ballast for fluorescent lamps with phase-locked loop control scheme.", *IEEE Transactions on Power Electronics*, 21(1):254–262, 2006.
[5] T. Ribarich and J. Ribarich. "A new procedure for high-frequency electronic ballast design.", *IEEE Transactions on Industry Applications*, 37(1):262–267, 2001.
[6] l. John, E. Kaufman, and J. F. Christensen. *IES Lighting Handbook*. Illuminating Engineering Society, 1984.
[7] T.-F. Wu, J.-C. Hung, and T.-H. Yu. "A pspice model for fluorescent lamps operated at high frequencies.", *IEEE 21st International Conference on Industrial Electronics, Control, and Instrumentation, 1995*, 1:359–364 vol.1.
[8] I. R. Corporation. Ir ballast designer version 4.1.7. PC Software, 2006.
[9] A. Ng, W.-H. Ki, P. Mok, and J. Sin. "Lamp modeling for design of dimmable electronic ballasts.", *Power Electronics Specialists Conference, 2000 IEEE 31st Annual*, 3:1358–1362 vol.3.

3. P. Navaratana, S. Naetiladdanon, and A. Sangswang, 2011, “Multi-rating Electronic Ballast for Fluorescent Lamps Based on Operating Frequency Determination”, **IEEJ Transactions on Industry Applications**, Vol.131, No.10.

Paper

Multi-rating Electronic Ballast for Fluorescent Lamps based on Operating Frequency Determination

Piyasawat Navaratana Na Ayudhya* Non-member
Sumate Naetiladdanon** Non-member
Anawach Sangswang*** Non-member

This paper presents an electronic ballast system with lamp rating detection capability. From the experimentally obtained operating frequency of the lamps, a possibility weight is constructed to help facilitate the lamp classification. The proposed detection algorithm employs a multi-step lamp power regulation algorithm where decision making is based on the sensed frequency and the possibility weight. Simulation and experimental results show that the proposed detection method can successfully detect the targeted lamp power rating and deliver the desired power to the lamp.

Keywords: ballast, fluorescent lamps, automatic detection, frequency determination

1. Introduction

Fluorescent lamps are commonly used in lighting applications because they consume less power than alternative lamps. Unlike incandescent lamps, fluorescent lamps always require a ballast to stabilize the lamp at the required operating point by limiting the discharge current [(1)(2)]. Simple magnetic ballasts that operate at the line frequency have many drawbacks, such as low efficiency, low input power factor and bulky size. However, electronic ballasts that employ transistors to boost line-frequency to high-frequency improve the lamp efficacy and system efficiency [(3)]. If the lamp is operated at a frequency higher than 20 kHz, instead of a line frequency of 50-60 Hz, the result is an increased light output (lumens) of 10-20%. The electronic ballast is often implemented as a series-parallel-loaded resonant inverter. This implementation can both ignite the lamp and supply the lamp as a current source at constant frequency [(4)~(6)]. The use of a power factor correction (PFC) AC-DC stage, specifically a boost rectifier operating in discontinuous conduction mode (DCM) with constant frequency and constant duty cycle, can achieve an input power factor close to unity. Moreover, modern electronic ballasts are implemented with microprocessor circuits, allowing control strategy implementation for energy savings and lamp protection features [(7)].

Commercially available lamps, such as 18W, 32W and 36W T8 lamps, must be used with electronic ballasts specifically designed for each lamp power rating. A mismatch between ballast and lamp ratings usually results in damage to both the lamp and the ballast circuit, caused by over-current or hard switching [(8)(9)]. With a large number of different ratings of fluorescent lamps, an equally large stock of specifically rated electronic ballasts is required. The multi-rating fluorescent ballast is a solution to eliminate this problem. The controller of the multi-rating ballast must regulate and deliver the correct power to a lamp of unknown rating. Thus, the lamp rating detection algorithm must be accurate and sufficiently fast. The voltage detection method can differentiate between lamp power ratings by using the operating lamp voltage [(10)(11)]. However, the lamp voltage after striking (ignition) varies with the lamp temperature, age, and manufacturer. Thus, different lamp ratings may have overlapping voltage ranges. For example, 32WT8 and 58WT8 lamps operate at the same voltage, ranging from 117 V to 127 V, which can result in misidentification of the lamp. In addition, noise can interfere with the voltage, and adding a filter may increase the cost of the system.

This paper presents a multi-rating electronic ballast for fluorescent lamps based on operating frequency de-

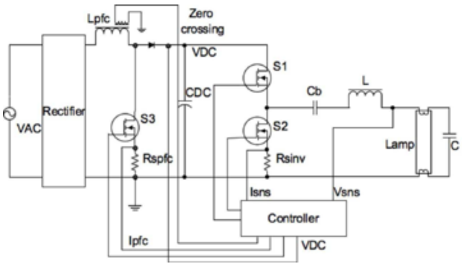

Fig. 1. Schematic of electronic ballast using in this paper

* King Mongkut's University of Technology Thonburi (KMUTT), Thailand, piyasawat.nav@kmutt.ac.th
** KMUTT, sumate.nae@kmutt.ac.th
*** KMUTT, Anawach.San@kmutt.ac.th

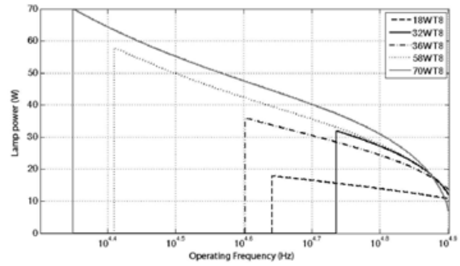

Fig. 2. Operating frequency VS Lamp power

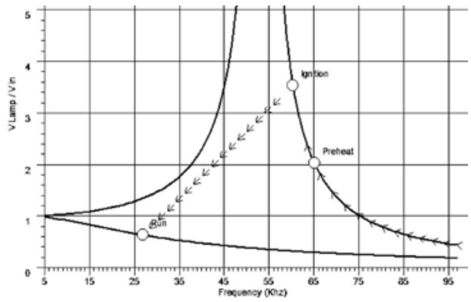

Fig. 3. Operating frequency vs. voltage gain (before and after striking)

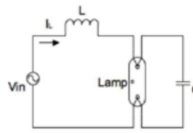

Fig. 4. Simplified resonant inverter for electronic ballast

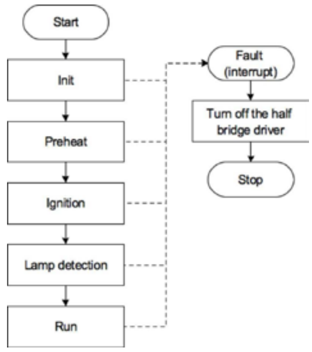

Fig. 5. Flowchart of the mult-rating electronic ballast operation

termination. The paper includes the configuration and the controller design of a multi-rating electronic ballast. We propose a lamp rating detection algorithm, composed of multi-step lamp power regulation and the trapezoidal possibility weight determination [12] based on a given set of lamp operating frequency data. Finally, we present numerical and experimental results. A hardware prototype of the electronic ballast is carried out on an 8 bits micro-controller.

2. Multi-rating Electronic Ballast Configuration

The two-stage electronic ballast consists of a PFC boost rectifier and a half-bridge resonant inverter as shown in Fig. 1. By varying the inverter frequency, the ballast operates in pre-heat, strike, and running stages. The lamp current can be controlled through frequency variation as shown in Fig. 2 [13] [14].

Before ignition, the fluorescent lamp resistance is assumed to be infinite. By operating with frequency higher than the circuit resonant frequency, the current flows through the lamp filaments via the series capacitor. In this stage, the filaments are heated while the lamp voltage is not high enough to be ignited. After one second of preheating, the frequency is decreased to increase the output voltage gain until the lamp voltage is high enough to strike the lamp. Note that the relationship between the ballasts voltage gain and frequency is shown in Fig. 3, obtained from the equivalent resistance of the lamp at steady-state condition using IR ballast designer software [15].

Initially, the resonant circuit is in the high quality factor mode (High-Q). Once the lamp has been ignited, the lamp resistance decreases and exhibits a negative differential resistance behavior. This results in lamp voltage reduction and changes the resonant circuit condition to the low quality factor condition (Low-Q). At this stage, the lamp rating must be detected accurately. After this stage, the controller will command the switch signals to operate the ballast at proper frequency for the lamp.

2.1 Half-bridge resonant inverter By assuming that the resonant capacitor (C) is only used for lamp preheating and striking while the resonant inductor (L) is for limiting the lamp current, the values of L and C must be chosen to ensure the optimal power transfer of the low-Q RCL circuit. The resonant inverter input power (P_{inv}) is [16] [17],

$$P_{in} = V_{in} I_L = \frac{P_{lamp}}{\eta} \tag{1}$$

By using the simplified version of resonant inverter that shown in Fig. 4. The input voltage (V_{in}) is the fundamental component of the square wave produced by the inverter [24]. This square wave is toggle between 0V and V_{DC}.

$$V_{in} = \frac{\sqrt{2}V_{DC}}{\pi} \tag{2}$$

$$\frac{P_{lamp}}{\eta} = V_{in} I_L = \frac{\sqrt{2}V_{DC}}{\pi} I_L \tag{3}$$

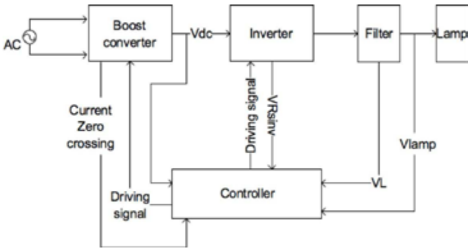

Fig. 6. Controller block diagram

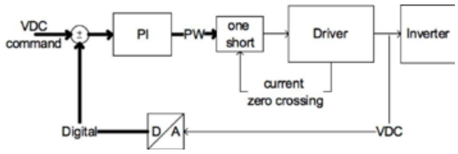

Fig. 7. DC bus voltage control

Where P_{lamp} is the power dissipated at the lamp; V_{DC} is the DC bus voltage, and η is the inverter efficiency. It is assumed that the inductor and lamp voltages are the same. The inductor current can be calculated by using a half of the DC bus voltage which results in,

$$I_L = \frac{V_{DC}}{4\omega L} \tag{4}$$

Thus:

$$P_{in} = \frac{\sqrt{2}V_{DC}}{\pi}\frac{V_{DC}}{4\omega L} = \frac{V_{DC}^2}{4\sqrt{2}\pi^2 f_{run} L} \tag{5}$$

From (3) and (5) , the resonant inductance is:

$$L = \frac{V_{DC}^2\eta}{4f_{run}\sqrt{2}\pi^2 P_{lamp}} \tag{6}$$

where f_{run} is the running or operating frequency. The controller is divided into two parts: the boost rectifier (DC bus voltage control), and the resonant inverter (lamp power control). These are shown in Fig. 7 and 8, respectively.

During preheat, the resistance of the lamp is infinite and the filament resistance is negligible. This results in an LC series circuit. Using the impedance across the capacitor, the peak preheat voltage V_{ph} is given as:

$$V_{ph} = \frac{I_{ph}}{2\pi f C} \tag{7}$$

where I_{ph} is the preheat lamp current and f is the preheat frequency. The transfer function is

$$V_{ph} = \frac{2V_{in}}{\pi\left(|1-4\pi^2 f^2 LC|\right)} \tag{8}$$

To preheat the lamp filament with the desired current while the lamp voltage is kept below V_{ph}, the resonant capacitance can be calculated from (8) as,

$$C = \frac{I_{ph}^2 L}{(V_{ph}+V_{DC}/\pi)^2 - (V_{DC}/\pi)^2} \tag{9}$$

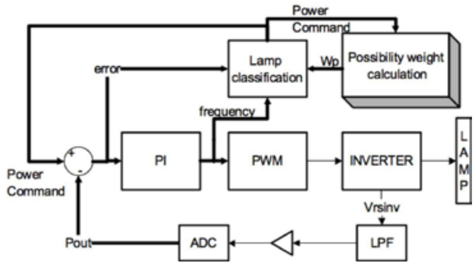

Fig. 8. Lamp power control with rating detection

2.2 PFC boost rectifier The PFC boost converter parameters are obtained by assuming an operation in the critical-conduction mode. With this control method, the PFC boost inductance is obtained from [17] [18]

$$L_{PFC} = \frac{8\times 10^{-6}\eta V_{AC(rms)}\left(V_{DC}-\sqrt{2}V_{AC(rms)}\right)}{2\sqrt{2}P_{OUT}} \tag{10}$$

where η is the target efficiency of the converter; $V_{AC(rms)}$ is the minimum input RMS voltage and P_{OUT} is output power.

2.3 Preheating condition Although the multi-rating ballast has an advantage on that it can operate more than one lamp power ratings, the preheat condition is taken into account. According to [21], the filaments must be operated at temperatures between $700°C$ and $1000°C$, to avoid a premature wear of the emissive coating which will reduce the average life of the lamp. Since it is difficult to measure this temperature, there are recommendations and standards regarding correlated parameters, such as the voltage across the filaments and their equivalent resistances. Under appropriate temperature, the resistance of the filament should be in the range of 4.25 to 6.25 times of its resistance at room temperature [21] [22]. To increase the filament temperature, an electrical current is applied to the filament with the following relationship [19].

$$R_{hc}\left(i_{ph(rms)},t\right) = 1 + r_1\left(e^{\left(\frac{i_{ph(rms)}}{r_2}\right)} - 1\right)t \tag{11}$$

Where R_{hc} is the resistance ratio between hot resistance (R_c) and cold resistance(R_h)
$i_{ph(rms)}$ is the filament current (A) during preheating
t is the preheating time (s)
r_1 and r_2 are the constants of the lamp

Note that for T8 series r_1 and r_2 are given as $0.112\,s^{-1}$ and $0.155\,A$, respectively. In addition, the suitable preheating time should be in the range of 0.5 and 1.5 s. The minimum current is obtained as 467 mA using the R_{hc} value of 4.25 and the preheating time of 1.5 s from (11). Similarly, with the R_{hc} value of 6.25 and the preheating time of 0.5 s, the maximum current is given as 705.5 mA. As long as the $i_{ph(rms)}$ is in between the men-

Table 1. Average running frequency of ballast at various lamp power ratings

Average of operating frequency at power command	16W (kHz)	30W (kHz)	34W (kHz)	56W (kHz)	68W (kHz)
T8-18	49.54	-	-	-	-
T8-32	76.26	55.44	-	-	-
T8-36	75.88	48.25	40.59	-	-
T8-58	76.26	57.16	50.09	25.21	-
T8-70	75.79	62.49	56.82	28.73	21.75

Table 2. Standard deviation of running frequency of ballast at various lamp power ratings

S.D. of operating frequency at power command	16W (kHz)	30W (kHz)	34W (kHz)	56W (kHz)	68W (kHz)
T8-18	1.7	-	-	-	-
T8-32	0.004	0.816	-	-	-
T8-36	0.036	1.022	1.210	-	-
T8-58	0.002	0.288	0.444	0.476	-
T8-70	0.010	0.160	0.234	0.360	0.270

tioned range, there will be no damage for all T8 series lamps. If the lamp is turned off and turned back on while the filament temperature is still higher than the room temperature, a power control loop must be included to protect the filament

3. Electronic Ballast Controller Design

The operation of the electronic ballast system can be described as five stages: initialization, pre-heat, lamp detection, run, and stop. The flowchart of these operations is illustrated in Fig. 5. The block diagram of controller is shown in Fig. 6.

3.1 Initialization state During the initial phase, the controller sets the PWM frequency at 100 kHz and keeps it steady for 200 ms. This feature has been implemented to charge the blocking capacitor.

3.2 Preheat state The controller raises the frequency by one step every time the measured current is greater than the desired value, and lowers the frequency if the current is lower than the desired value. This state takes approximately 0.5 to 1 second depending on the current command value [19].

3.3 Ignition state The controller decreases the frequency (increases the voltage) to ignite the lamp. Since the voltage across the lamp will significantly decrease after ignition because the current begins to flow through the lamp then, the voltage change is used as ignition indication. After detecting the ignition, the controller moves to the next phase.

3.4 Stop state If abnormal conditions occur, the software will automatically switch into the safety state that is designed to turn off the half bridge driver. Abnormal conditions may arise due to lamp bulb removal, lamp failure to ignite, over-current or over-voltage, or a rectifying effect (end of life).

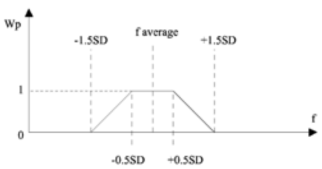

Fig. 9. Trapezoidal possibility weight (W_P) VS running frequency

3.5 Run state During this phase, the controller measures the current required to deliver a given power to the lamp. The measured value is compared with a preset power command value, and consequently the software tries to correct any discrepancy. As mentioned above, the lamp power can be controlled by varying the operating frequency. The lamp power decreases when the supplied frequency increases, as shown in Fig. 2. The appropriate frequency must be generated to ensure that the connected lamp is not overdriven. The current regulation method is used to control the lamp power at its rating [20]. The average voltage across the series resistor on the low side of the driver MOSFET (V_{Rsinv}) represents the inverter current (I_{inv}). P_{inv}, P_{lamp}, and I_{inv} are related as:

$$P_{inv} \ \alpha \ P_{lamp} \ \alpha \ I_{inv} \tag{12}$$

From (12), the lamp power can be controlled through V_{Rsinv}. Note that the required inverter power will be about 1-2 W less than the lamp rating for the same lumen output, due to the high frequency of operation.

3.6 Lamp detection state The lamp rating detection algorithm is composed of multi-step lamp power regulation and the trapezoidal possibility weight determination based on the lamp operating frequency. After ignition, the multi-step lamp power regulation is started with the lowest power command. For example, the 16W power command is used for the T8 series lamps. In the power control loop, the operating frequency is determined and collected in the controller. This frequency is used to classify the 18W (lowest) from the group. If the measured frequency is within the valid range, then no further decision is necessary and the controller proceeds to the running state. However, due to the variation between lamp manufacturers, bulb age, and temperature, the running frequency is not necessarily constant. We experimentally verified that the operating frequency varies during our lamp power regulation experiment.

Plenty of T8 lamps are operated at 16W, 30W, 34W , 56W and 68W to acquire the running frequencies. These frequencies are used in order to define the possibility weight function. Table 1 and 2 present the average and standard deviation of running frequency at 16 to 68 W of power regulation. A dash(-) symbol is a prohibited power command. By simplifying the Gaussian distribution, the trapezoidal possibility weight (W_P) based on the operating frequency can be calculated from

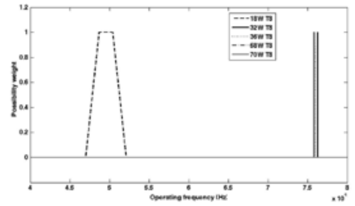

Fig. 10. Possibility weight (W_P) VS operating frequency of T8 lamps at 16W power regulation

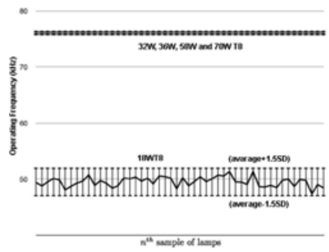

Fig. 11. Operating frequency at 16W power regulation of n^{th} lamp sample in the possibility weight region

$$W_P = \begin{cases} 1; \bar{f}-0.5sd, f, \bar{f}+0.5sd \\ \frac{1}{sd}f - \frac{\bar{f}-1.5sd}{sd}; \bar{f}-1.5sd, f, \bar{f}-0.5sd \\ \frac{-1}{sd}f + \frac{\bar{f}+1.5sd}{sd}; \bar{f}+0.5sd, f, \bar{f}+1.5sd \end{cases} \tag{13}$$

Where

$$\bar{f} = \frac{1}{n}\sum_{i=1}^{n} f_i, sd = \sqrt{\frac{1}{n}\sum_{i=1}^{n}(f_i-\bar{f})^2} \tag{14}$$

and n=number of samples, f_i = frequency of sample i.

The relation between the probability weight and the running frequency is illustrated in Fig. 9. For example, if the average operating frequency of a 36 W lamp running at 16 W is 75.88 kHz, and its standard deviation is 36 Hz, then $W_{P(36Wat16W)}$ is

$$W_{P(36at16)} = \begin{cases} 1; 48.69kHz, f, 50.39kHz \\ 0.588f-46.99; 46.99Hz, f, 48.69kHz \\ 0.588f+50.39; 50.39kHz, f, 52.09kHz \end{cases} \tag{15}$$

where f = measure lamp operating frequency (kHz).

Fig. 10 and 11 shows the possibility weight and operating frequency of T8 series lamps at 16 W power regulation. The operating frequency of 18 W lamp is significantly far from others resulting in high accuracy of 18W lamp detection. However, the possibility weight of 58W lamp is overlapped by that of 32W lamp causing inaccurate detection in this state. When the 30 W power regulation is applied with the 32 W, 36 W, 58 W and 70 W T8 lamps, there is no overlapping in the possibility weight of T8 lamps as shown in Fig 12 and

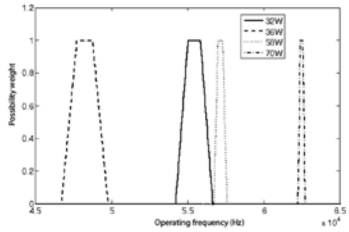

Fig. 12. Possibility weight (W_P) VS operating frequency of T8 lamps at 30W power regulation

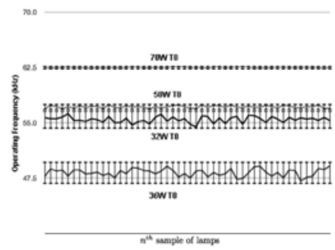

Fig. 13. Operating frequency at 30W power regulation of n^{th} lamp sample in the possibility weight region

13 where the 32 W lamp can be accurately detected.

From the reason above, both the multi-step lamp power regulation and possibility weight determination are applied together and the lamp rating detection algorithm can be described as follows:

(1) Regulate at the lowest power command. Example: 16W for T8 series.

(2) Calculate the probability weight for all lamp ratings. If the highest W_P is obtained at the lamp rating that equals the power command, the lamp rating equals the power regulated, then go to step 4.

(3) If the delivered power is still below the lamp rating, step up to the next power command (30, 34, 56 and 68 W) and repeat step 1) and 2) again until the power command reaches the highest value of the series then go to step 4.

(4) Summarize the total W_P of each lamp rating for each power regulation. The lamp rating is determined from the total highest W_P.

The flowchart of the detection algorithm is illustrated in Fig. 14.

3.7 Discussions on Aging Effect Regarding to the lamp aging, this might cause an increase in filament resistance, sputtering and filament damage respectively. The lamp discharge characteristics also change as well. After striking, the lamp with sputtering or filament damage will be shut off by the designed protection as previously stated. However, the aging effect from an increased filament resistance and lamp discharge char-

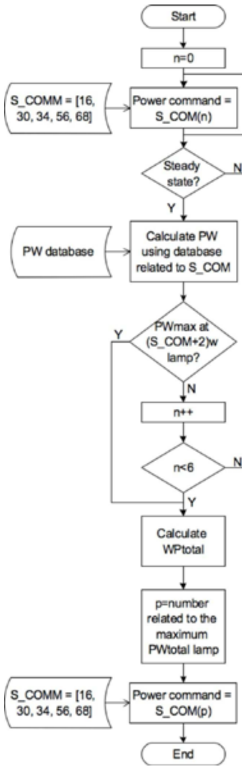

Fig. 14. Flowchart of the lamp rating detection algorithm

acteristics might cause the inaccurate detection. For example; the overlapped operating frequency of 32WT8 and 58WT8 might occur during the 30 W power regulation. In our designed ballast, the 18W, 32W and 36W T8 lamps, which are mostly used in our country, are selected. The operating frequencies of these lamps are quite far from each other causing the high accurate detection. Moreover, the cost of ballast can be reduced for not using the unnecessary high power components.

4. Numerical calculation Results

The simplified resonant inverter is used in the simulation [24]. The controllable ac voltage source is connected through the resonant inductor and capacitor as a low-pass filter, with the fluorescent lamp as a resistive load (R_{lamp}) as shown in Fig. 4. Using an operating frequency range from 25 kHz to 65 kHz, as described in [2], and assuming that η_{inv} is 0.95 and V_{DC} is 400 V, the resonant inductance can be calculated by (6) which is given as 1.9 mH. With I_{ph} as 0.6 A and V_{ph} as 300 V, the substitution of the resonant inductance in (9) yields the resonant capacitance of $4.11nF$. Because of commercial availability, a capacitance of 4.7 nF is chosen. During the running stage, the lamp acts as a negative differential resistor [25]~[28], which can be calculated as:

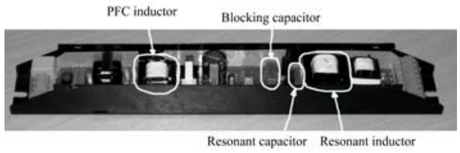

Fig. 15. A prototype of the multi-rating ballast

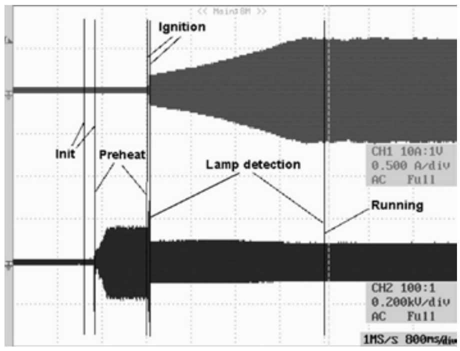

Fig. 16. The 36WT8 lamp current and voltage waveforms. Channel 1 is lamp current. Channel 2 is lamp voltage.

$$R_{lamp} = \frac{V_0 R_S}{V_0 - V_H} \tag{16}$$

where V_0 is the voltage at present condition and R_S and V_H are defined as;

$$R_S = \frac{V_{Max} - V_{min}}{I_{Max} - I_{min}} \tag{17}$$

$$V_H = V_{min} - I_{min} R_S \tag{18}$$

where V_{max} is the lamp voltage at the highest power, V_{min} is the lamp voltage at the lowest power, I_{max} is the lamp current at the highest power, and I_{min} is the lamp current at the lowest power. Specifications for V_{max}, V_{min}, I_{max}, and I_{min} can be obtained from the lamp manufacturers. Because the higher-order harmonics only account for a small percentage of the input, the voltage and current waveforms appearing at the lamp are assumed to be sinusoidal. Considering only the fundamental component, lamp power (P_{Lamp}) can be calculated as:

$$P_{lamp} = \left| \frac{-\frac{jV_{in}}{\omega C R_{lamp}}}{\left(j\omega L - \frac{j}{\omega C_{bl}}\right)\left(R_{lamp} - \frac{j}{\omega C}\right) - \frac{jR_{lamp}}{\omega C}} \right|^2 \tag{19}$$

Starting with an initial operating frequency, the lamp power is calculated. If P_{lamp} is less than the power

Table 3. Simulation result of $W_P$for the 32 W T8 lamp

Power command / Lamp rating	16W	30W	34W	56W	68W	Sum
18W	0	-	-	-	-	0
32W	1	0.2	-	-	-	1.2
36W	0	0	-	-	-	0
58W	1	0	-	-	-	1
70W	0	0	-	-	-	0

Table 4. Experimental results of W_P for 58W lamp

Power command / Lamp rating	16W	30W	34W	56W	68W	Sum
18W	0	-	-	-	-	0
32W	1	0	-	-	-	1
36W	0	0	0	-	-	0
58W	1	1	1	1	-	3
70W	0	0	0	0	-	0

command, the frequency is decreased and the lamp voltage, current, and resistance are recalculated at the new power level. The calculation is then iteratively repeated until the P_{lamp} is sufficiently close to the power command and the running frequency is obtained. The simulation result for the probability weight calculation for the 32W T8 lamp is shown in Table 3. Starting at the 16W power command, the running frequency is 76.26 kHz and W_P at 16 W is calculated. The highest $W_P$is not at $WP_{18Wat16W}$, thus the 30W power command is regulated and W_P at 30 W is recalculated. The algorithm stops at 30W power command due to the maximum on $WP_{32Wat30W}$. The summation of WP_{32W} is 1.2, which is the maximum, and the lamp is detected as a 32W rated lamp.

5. Experiment Results

A hardware prototype of the electronic ballast, shown in Fig. 15, was built. The values for the resonant inductance and capacitance match those used in the simulation. The PFC boost inductance and the DC bus capacitance are 0.94 mH and 22 μF, respectively. A 100 nF blocking capacitor is used. Fig. 16 shows the ballast operation with the 36W lamps.

In the preheat state, the controller maintains the lamp current and voltage at 600 mA and 300 V, respectively. After striking, the lamp power is regulated according to the lamp rating detection algorithm. All tested lamps have been successfully detected at their ratings. The startup process, including lamp detection, takes approximately 3 to 40 seconds. The sample of detection results for a 58W T8 lamp is shown in Table 4.

The voltage detection is the commonly used method in detecting ballasts rating [10] [11]. With different power ratings, the lamp resistances may be different and the lamp peak voltages after strikes may be used to classify the power ratings. However, this may not be the case for T8 series because the lamp peak voltages of different ratings can and have been found to be in the same range. In Fig. 17, the lamp voltages are obtained from 50 samples of each of the T8 series lamp rating with the total number of 250 lamps. The voltages after strikes of the 32W and 58W lamps are located in the ranges of 162 V to 177 V and 166 V to 177 V, respectively. The detection result is very likely to be incorrect for both lamp ratings. This method yields the result of detection rate as 86%.

Table 5. Detecting results of T8 lamp at 16W, 30W, 34W, 56W and 68W power regulation state

Lamp rating	18W	32W	36W	58W	70W
16W power regulation					
% Detection rates	100	90	90	20	36
% Type I error	0	10	10	80	64
% Type II error	0	2	0	32	0
30W power regulation					
% Detection rates	-	100	100	100	98
% Type I error	-	0	0	0	2
% Type II error	-	0	0	0	0
34W power regulation					
% Detection rates	-	-	100	100	100
% Type I error	-	-	0	0	0
% Type II error	-	-	0	0	0
56W power regulation					
% Detection rates	-	-	-	100	100
% Type I error	-	-	-	0	0
% Type II error	-	-	-	0	0
68W power regulation					
% Detection rates	-	-	-	-	100
% Type I error	-	-	-	-	0
% Type II error	-	-	-	-	0

To evaluate this proposed method, hundreds of arbitrarily chosen fluorescent lamps with varied age are tested with proposed ballast. The operating frequencies of tested lamps at 16W and 30W power regulation are shown in Fig. 11 and 13, respectively. At 30W power regulation, the operating frequencies of all lamps are in the areas of their possibility weight. Thus, the proposed method can distinguish between 32W and 58W lamps. Note that some lamps with low possibility weight might have the chance of type I error (the false positive - the error of rejecting lamp when it is actually at rating) as well as the type II error (the false negative - the error of failing to reject a lamp when it is in fact not at rating). Even though the 16W power regulation state returns 100%-accuracy 18W lamps detection, this state returns detection errors for the other ratings. Table 5 shows the lamp detection rate, type I error rate and type II error rate of T8 lamps at various power regulations.

The proposed frequency detection, on the other hand, uses the frequency command for lamp power regulation to detect the lamp power. This frequency command is the same frequency command that is used to regulate the lamp power in order to avoid overdriven condition. Together with the proposed possibility weight functions,

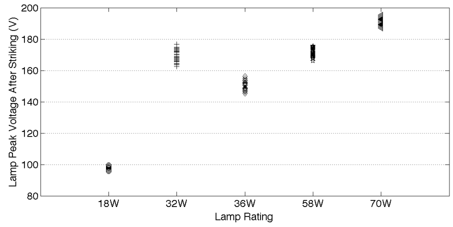

Fig. 17. Relationship between lamp voltages and ratings after strikes

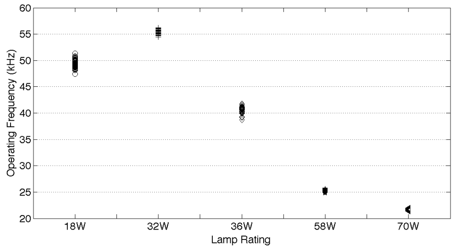

Fig. 18. Relationship between lamp frequencies and ratings from power regulation

the operating frequencies of each lamp rating are obtained from the multi-stage power regulation starting from the lowest rating available as shown in Fig. 18. With the same set of 250 lamps used in obtaining the results in Fig. 17, the operating frequency range of each rating is located apart from each other. Clearly, the frequency detection method does not suffer from overlapping range of the detection parameter. The detection results of the proposed method are evidently more accurate. It is worth noting that if a delay of 10s is added before obtaining the operating frequency, 100% detection accuracy may be achieved since the lamp resistance is allowed to reach its stable state.

The important advantage of implementing the proposed frequency detection method is that the frequency command to be used in the detection process is sent out from the controller. Unlike the voltage detection, the detecting parameter does not need to go through sensing circuitry and the analog-to-digital conversion process. Therefore, it is not subjected to external noise which can worsen the detection results.

From table 5, the lamp detection rate, type I error rate and type II error rate are calculated as:

$$D.R. = \frac{N_{Correct}}{N_{Lamp}} \times 100 \tag{20}$$

where D.R. is detection rate, $N_{Correct}$ is number of the accurately detected lamps and N_{Lamp} is number of tested lamp.

$$TypeI = \frac{N_{Reject}}{N_{Lamp}} \times 100 \tag{21}$$

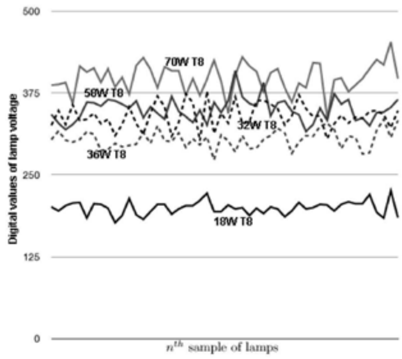

Fig. 19. Peak voltage of n^{th} sample of lamps after ignition using the micro-controller analog to digital converter

Table 6. Voltage detecting method (V.D.) VS Proposed frequency detecting method results

Lamp rating	18W	32W	36W	58W	70W
V.D. Method					
% Detection rates	100	60	100	70	100
% Type I error	0	40	0	30	0
% Type II error	0	30	0	40	0
Proposed method					
Lamp rating	18W	32W	36W	58W	70W
% Detection rates	100	100	100	100	100
% Type I error	0	0	0	0	0
% Type II error	0	0	0	0	0

where N_{Reject} is number of lamps that are rejected when it is actually at its rating.

$$TypeII = \frac{N_{WrongAccept}}{N_{Lamp}} \times 100 \tag{22}$$

where $N_{WrongAccept}$ is number of lamps that are accepted when it is not at its rating.

Because of the overlapped possibility weight of the 32 W and 58 W lamp, the high type I and type II error of 58W lamps are occurred during 16W power regulation. Even the low accuracy occurs in 16W power regulation state, the next power regulation state results in the high detection accuracy implying the right rating will be detected at the final decision. Therefore, this algorithm results in a 100% detection rate of all tested lamps. For the testing with very old lamps, the inaccurate detection is occurred but the protection algorithm stops the ballast operation due to the rectifying effect.

Comparing the proposed detection with the voltage detection method, the experiment for measuring lamp voltages after ignition are carried out as shown in Fig. 17. Using this method, the 70W and 18W lamps are easily detected but the detection between 32W and 58W lamps is not possible. The main reason is that the lamp voltage after ignition varies with the lamp temperature, age, and manufacturer. Moreover, the use of A/D converter in micro-controller will cause the noise amplification as shown in Fig. 19. The noisy switching environment will worsen the detection accuracy. With the proposed method, the frequency is generating by the micro-controller itself which is not interfered by noise. And the multi-step power regulation constrains the lamp operating condition during the detection as well. The Detection results of the proposed method and the voltage detecting method are shown in Table 6.

6. Conclusion

A multi-rating electronic ballast for fluorescent lamps based on operating frequency determination has been presented. The detection algorithm is based on the probability weight distribution of the lamp operating frequency, and multi-step lamp power regulation. The proposed algorithm has shown great accuracy in detecting the targeted lamp power rating compared with the commonly used voltage detection method. In some cases, aging lamps may result in misclassification of the lamps therefore, a protection circuit must be implemented with the ballast. With the proposed detection algorithm, the multi-rating ballast will help eliminate concerns about matching the ballast circuit with the designated lamp power rating.

References

(1) L. Davies, H. Ruff, and W. Scott, "Fluorescent lamps," *Electrical Engineers - Part II: Power Engineering, Journal of the Institution of*, vol. 89, pp. 447–465, October 1942.

(2) l. John, E. Kaufman, and J. F. Christensen, *IES Lighting Handbook*. Illuminating Engineering Society, 1984.

(3) M. Kazimierczuk and W. Szaraniec, "Electronic ballast for fluorescent lamps," *IEEE Transactions on Power Electronics*, vol. 8, pp. 386–395, Oct 1993.

(4) M. Matsuo, T. Suetsugu, S. Mori, and I. Sasase, "Class de current-source parallel resonant inverter," *Industrial Electronics, IEEE Transactions on*, vol. 46, pp. 242–248, Apr 1999.

(5) J. Cosby, M.C. and R. Nelms, "A resonant inverter for electronic ballast applications," *Industrial Electronics, IEEE Transactions on*, vol. 41, pp. 418–425, Aug 1994.

(6) C. Liu, F. Teng, C. Hu, and Z. Zhang, "Lclc resonant converter for multiple lamp operation ballast," *Applied Power Electronics Conference and Exposition, 2003. APEC '03. Eighteenth Annual IEEE*, vol. 2, pp. 1209–1213 vol.2, Feb. 2003.

(7) J. Alonso, J. Cardesin, Calleja, Rico-Secades, and J. Garcia, "A fluorescent lamp electronic ballast for railway applications based on low-cost microcontroller," *IEEE Transactions on Industry Applications*, vol. 41, pp. 1391–1400, Sept.-Oct. 2005.

(8) R.-L. Lin and Y.-T. Chen, "Electronic ballast for fluorescent lamps with phase-locked loop control scheme," *IEEE Transactions on Power Electronics*, vol. 21, pp. 254–262, Jan. 2006.

(9) Y. Ji, R. Davis, C. O'Rourke, and E. Chui, "Compatibility testing of fluorescent lamp and ballast systems," *Industry Applications, IEEE Transactions on*, vol. 35, pp. 1271–1276, Nov/Dec 1999.

(10) L. Lee, S. Hui, and H. Chung, "An automatic lamp detection technique for electronic ballasts," *Twentieth Annual IEEE Applied Power Electronics Conference and Exposition, 2005. APEC 2005*, vol. 1, pp. 575–581 Vol. 1, March 2005.

(11) L.-M. Lee and S. Hui, "Automatic lamp detection and operation for warm-start tubular fluorescent lamps," *IEEE Transactions on Power Electronics*, vol. 24, pp. 2933 –2941, dec. 2009.

(12) S.-M. Chen, Y.-K. Ko, Y.-C. Chang, and J.-S. Pan, "Weighted fuzzy interpolative reasoning based on weighted increment transformation and weighted ratio transformation techniques," *Fuzzy Systems, IEEE Transactions on*, vol. 17, pp. 1412–1427, Dec. 2009.

(13) T.-F. Wu, Y.-C. Liu, and Y.-J. Wu, "High-efficiency low-stress electronic dimming ballast for multiple fluorescent lamps," *Power Electronics, IEEE Transactions on*, vol. 14, pp. 160–167, Jan 1999.

(14) T.-F. Wu and T.-H. Yu, "An electronic dimming ballast with bifrequency and fuzzy logic control," *Industry Applications, IEEE Transactions on*, vol. 36, pp. 1308–1317, Sep/Oct 2000.

(15) I. R. Corporation, "I.R. ballast designer version 4.1.7." PC Software, 2006.

(16) T. Ribarich and J. Ribarich, "A new procedure for high-frequency electronic ballast design," *IEEE Transactions on Industry Applications*, vol. 37, pp. 262–267, Jan/Feb 2001.

(17) S. S. M. Chan, H. S.-H. Chung, and Y.-S. Lee, "Design and implementation of dimmable electronic ballast based on integrated inductor," *Power Electronics, IEEE Transactions on*, vol. 22, pp. 291–300, Jan. 2007.

(18) H. Sartori, H. Hey, and J. Pinheiro, "An optimum design of pfc boost converters," in *EPE '09. 13th European Conference on Power Electronics and Applications, 2009.*, pp. 1–10, Sept. 2009.

(19) F. Wakabayashi, M. de Brito, C. Ferreira, and C. Canesin, "Setting the preheating and steady-state operation of electronic ballasts, considering electrodes of hot-cathode fluorescent lamps," *Power Electronics, IEEE Transactions on*, vol. 22, pp. 899–911, May 2007.

(20) D. Klien, "A sensing and regulation concept for high end dimming ballasts," in *38th IAS Annual Meeting. Conference Record of the Industry Applications Conference, 2003.*, vol. 2, pp. 785–790 vol.2, Oct. 2003.

(21) Y. Ji, R. Davis, C. O'Rourke, and E. Chui, "Compatibility testing of fluorescent lamp and ballast systems," *IEEE Transactions on Industry Applications*, vol. 35, pp. 1271–1276, Nov/Dec 1999.

(22) *American National Standard for Ballasts for Fluorescent Lamps: Specifications*, ANSI C82.1-1985, 1985.

(23) P. Tam, S. Lee, S. Hui, and H.-H. Chung, "Practical evaluation of dimming control methods for electronic ballasts," *Power Electronics, IEEE Transactions on*, vol. 21, pp. 1769–1775, Nov. 2006.

(24) Z. Li, P. Mok, W.-H. Ki, and J. Sin, "A simple method to design resonant circuits of electronic ballast for fluorescent lamps," *ISCAS '97., Proceedings of 1997 IEEE International Symposium on Circuits and Systems.*, vol. 3, pp. 1744–1747 vol.3, Jun 1997.

(25) A. Ng, W.-H. Ki, P. Mok, and J. Sin, "Lamp modeling for design of dimmable electronic ballasts," *2000 IEEE 31st Annual Power Electronics Specialists Conference, 2000. PESC 00.*, vol. 3, pp. 1358–1362 vol.3, 2000.

(26) S. Glozman and S. Ben-Yaakov, "Dynamic interaction analysis of hf ballasts and fluorescent lamps based on envelope simulation," *Industry Applications, IEEE Transactions on*, vol. 37, pp. 1531–1536, Sep/Oct 2001.

(27) T.-F. Wu, J.-C. Hung, and T.-H. Yu, "A pspice model for fluorescent lamps operated at high frequencies," *21st International Conference on Industrial Electronics, Control, and Instrumentation, 1995., Proceedings of the 1995 IEEE IECON*, vol. 1, pp. 359–364 vol.1, Nov 1995.

(28) M. Sun and B. Hesterman, "Pspice high-frequency dynamic fluorescent lamp model," *Power Electronics, IEEE Transactions on*, vol. 13, pp. 261–272, Mar 1998.

Acknowledgment
This work was supported by the Higher Education Research Promotion and National Research University Project of Thailand , Office of the Higher Education Commission.

Piyasawat Navaratana Na Ayudhya (Non-member) was born in Bangkok, Thailand, on April 8, 1976. He received the B.E. and M.E. degrees in electronic and telecommunication engineering from King Mongkut's University of Technology Thonburi (KMUTT), Bangkok, Thailand, in 1997 and 2000, respectively. Since 2000, he has been a Lecturer in the Electrical Engineering Department, King Mongkut's University of Technology Thonburi, teaching digital techniques and micorcontroller system. Since 2004, he has also been a consultant of DYNO electric Co.,Ltd., Nakornpatom, Thailand. His research interests include electronic ballast, battery charger, switching power supplies, digital signal processing and machine intelligence.

Sumate Naetiladdanon (Non-member) received the B.Eng. degree from Chulalongkorn University, Bangkok, Thailand, in 1995, the M.Sc. degree from Rensselaer Polytechnic Institute, NY, USA., in 1999, and the Ph.D. degree from Osaka University, Japan in 2006. He is currently a Lecturer in the Department of Electrical Engineering of King Monkuts University of Technology Thonburi (KMUTT). His research interests are in the areas of power electronics for power quality improvement and renewable energy.

Anawach Sangswang (Non-member) received the B.Eng. degree from King Mongkuts University of Technology Thonburi (KMUTT), Bangkok, Thailand, in 1995, and the M.S. and Ph.D. degrees from Drexel University, Philadelphia, PA, in 1999 and 2003, respectively. He is currently a Lecturer in the Department of Electrical Engineering, KMUTT. His research interests include stochastic modeling and digital control of power electronic converters. His recent work has been in the application of PV gridconnected systems and power distribution systems.

CURRICULUM VITAE

NAME	Mr. Piyasawat Navaratana Na Ayudhya
DATE OF BIRTH	8 April 1976
EDUCATION RECORD	
BACHELOR'S DEGREE	Bachelor of Engineering (Electronics and Telecommunication Engineering) King Mongkut's University of Technology Thonburi, 1998
MASTER'S DEGREE	Master of Engineering (Electrical Engineering) King Mongkut's University of Technology Thonburi, 2001
DOCTORAL'S DEGREE	Doctor of Philosophy (Electrical and Computer Engineering) King Mongkut's University of Technology Thonburi, 2011
EMPLOYMENT RECORD	Lecturer King Mongkut's University of Technology Thonburi, 2001
SCHOLARSHIP	The University Development Commission (UDC), Office of the Higher Education Commission.
FUNDING	The Higher Education Research Promotion and National Research University Project of Thailand, Office of the Higher Education Commission.
PUBLICATIONS	P. Navaratana, S. Naetiladdanon, and A. Sangsawang, 2008, "Automatic Fluorescent Lamp Detection Technique for Electronic Ballasts", **IEEE International Conference on Robotics and Biomimetics**, Feb., pp. 1047–1052. P. Navaratana, S. Naetiladdanon, and A. Sangswang, 2009, "Automatic Fluorescent Lamp Detection for Electronic Ballasts Based on Operating Frequency and Phase Shift Compensation", **IEEE International Symposium on Industrial Electronics**, July, pp. 53–58. P. Navaratana, S. Naetiladdanon, and A. Sangswang, 2011, "Multi-rating Electronic Ballast for Fluorescent Lamps Based on Operating Frequency Determination", **IEEJ Transactions on Industry Applications**, Vol.131, No.10.